

## Durham E-Theses

---

### *Decompacting a Late Holocene sea-level record from Loch Laxford, northwest Scotland.*

CULLEN, BENJAMIN,JOHN

#### How to cite:

---

CULLEN, BENJAMIN,JOHN (2013) *Decompacting a Late Holocene sea-level record from Loch Laxford, northwest Scotland.*, Durham theses, Durham University. Available at Durham E-Theses Online:  
<http://etheses.dur.ac.uk/7325/>

#### Use policy

---

The full-text may be used and/or reproduced, and given to third parties in any format or medium, without prior permission or charge, for personal research or study, educational, or not-for-profit purposes provided that:

- a full bibliographic reference is made to the original source
- a [link](#) is made to the metadata record in Durham E-Theses
- the full-text is not changed in any way

The full-text must not be sold in any format or medium without the formal permission of the copyright holders.

Please consult the [full Durham E-Theses policy](#) for further details.

---

Academic Support Office, Durham University, University Office, Old Elvet, Durham DH1 3HP  
e-mail: [e-theses.admin@dur.ac.uk](mailto:e-theses.admin@dur.ac.uk) Tel: +44 0191 334 6107  
<http://etheses.dur.ac.uk>

# **Decompacting a Late Holocene sea-level record from Loch Laxford, northwest Scotland.**

Benjamin John Cullen

Geography – Masters by Research

Durham University - 2012

Title Page .....	i
Table of Figures .....	v
Table of Tables.....	ix
Acknowledgements .....	x
Abstract .....	xi
Declaration .....	xii
Chapter 1 Introduction .....	1
1.1 Introduction.....	1
1.2 Aim and Objectives .....	2
Chapter 2 Sea Level Change and Sediment Compaction .....	3
2.1 Sea-Level Change.....	3
2.2 Errors in Sea-Level Reconstruction.....	5
2.3 Sediment Compaction .....	7
2.4 Decompaction Approaches .....	9
2.5 Geotechnical Theory .....	12
2.6 Organic Materials .....	19
2.7 Implications of BR1 for Sea-Level Studies .....	20
2.8 Research Context.....	22
2.9 Assumptions and Development of BR1.....	23
2.10 Summary .....	23
Chapter 3 Field Site & Methods .....	25
3.1 Field Site .....	25
3.2 Methods.....	35
3.3 Summary .....	46
Chapter 4 Results .....	48
4.1 Introduction.....	48
4.2 Contemporary Surface .....	48
4.3 Contemporary Physical Properties.....	50



4.4 Contemporary Geotechnical Properties .....	52
4.5 Key Compression Properties of Surface Materials.....	58
4.6 Core Sediments.....	63
4.7 Core Physical Properties .....	63
4.8 Core Geotechnical Properties .....	65
4.9 Summary .....	66
Chapter 5 Model Development & Compression Modelling .....	67
5.1 Model Development .....	67
5.2 Compression Modelling.....	72
5.2.5 Summary .....	81
Chapter 6 Lower Marsh Erosion and Compression .....	83
6.1 Introduction.....	83
6.2 Evidence of an erosive event .....	83
6.3 Sediment Compaction .....	84
6.5 Summary .....	87
Chapter 7 Discussion: Implications and Future Research .....	88
7.1 Introduction.....	88
7.2 New Regression Models .....	88
7.3 Sediment Compression Modelling.....	89
7.4 Identification of Erosive Events .....	90
7.5 Summary .....	92
Chapter 8 Conclusions.....	93
References.....	95
Appendix 1 Methods .....	103
1.1 Moisture Content and LOI .....	103
1.2 Specific Gravity .....	103
1.3 Void Ratio.....	104
Appendix 2 Results Summary.....	105
Appendix 3 Compression Properties against Elevation .....	107

3.1 Introduction.....	107
3.2 Specific Gravity ( $G_s$ ).....	107
3.3 Void Ratio at 1 kPa ( $e_1$ ).....	107
3.4 Recompression Index ( $C_r$ ).....	107
3.5 Compression Index ( $C_c$ ).....	107
3.6 Yield Stress ( $\sigma'_y$ ).....	107
3.7 Summary .....	108
Appendix 4 Effects of Variable Loading .....	109
4.1 Introduction.....	109
4.2 Yield Stress ( $\sigma'_y$ ).....	109
4.3 Void Ratio at 1 kPa ( $e_1$ ).....	109
4.4 Recompression Index ( $C_r$ ).....	109
4.5 Compression Index ( $C_c$ ).....	110
4.6 Summary .....	110

## Table of Figures

2.1	Examples of salt marsh reconstructions from the last 2000 years (Source: Kemp <i>et al.</i> , 2011).	4
2.2	The potential effects of sediment compaction upon a stratigraphic succession and the subsequent effects upon a sea-level reconstruction upon SLIPs. Figure adapted from Brain (2006).	7
2.3	Logarithmic time displacement curve for sediment with an applied load within an oedometer.	13
2.4	Image of an oedometer used for testing and a schematic drawing describes the cell which encloses the sample	15
2.5	$e \log \sigma'$ plot used for compression models. Figure adapted from Brain <i>et al.</i> (2011; 2012).	16
2.6	A summary of the methodological steps of BR1.	21
2.7	Example runs from BR1. Source Brain <i>et al.</i> (2012).	22
3.1	Location map of Loch Laxford.	26
3.2	The lower salt marsh / sand flat cliff observed at Loch Laxford.	28
3.3	An extensive creek network is present across much of Loch Laxford.	28
3.4	Vegetation observed across the whole marsh at Loch Laxford.	28
3.5	Stratigraphy from multiple cores at Loch Laxford. Source Barlow <i>et al.</i> (unpublished data).	29
3.6	Age-model for the middle marsh core (LA-11-03). Source Barlow <i>et al.</i> (unpublished data).	30

3.7	Age-model for the middle marsh core (LA-10-2C). Source Barlow <i>et al.</i> (unpublished data).	31
3.8	Probable marsh development at Loch Laxford.	32
3.9	The location in relation to Loch Laxford and relative sea-level history of nearby Coigach. Figure adapted from Shennan and Horton (2002).	33
3.10	The relative sea-level history of Loch Laxford and long term tide gauge data from Aberdeen. Source Barlow <i>et al.</i> (unpublished data)	35
3.11	Example of Class 1 sediment sample collection.	36
3.12	Geonor H-60 hand-held shear vane tester.	37
3.13	Testing strategy undertaken to obtain downcore bulk density.	38
3.14	Example of a full sample collected within the oedometer ring.	40
3.15	Variable root content within samples collected at different locations within the marsh.	41
3.16	The potential effects of oedometer loading with and without root content.	42
3.17	Presence of root material within the marsh environment.	43
3.18	Root removal and then subsequent 'repair' for oedometer samples.	44
3.19	A continuously curved time-displacement curve.	44
4.1	Variations in LOI against elevation (m OD) are displayed from both this thesis and Barlow <i>et al.</i> (unpublished data).	49

4.2	Variations in moisture content against elevation (m OD) from both this thesis and Barlow <i>et al.</i> (unpublished data).	49
4.3	Variations in particle size against elevation (m OD).	50
4.4	Variations in bulk density against elevation (m OD).	52
4.5	Variations in initial void ratio against elevation (m OD).	53
4.6	Variations in hand shear strength (kPa) against elevation (m OD).	53
4.7	Cumulative displacement of LA-11-GC9-1+2 following the application of various loads.	54
4.8	Cumulative displacement of LA-11-GC16-1, 2+3 following the application of various loads.	55
4.9	Time-displacement curve of LA-11-GC16-1. 45 min loading of 2.7 kPa load.	56
4.10	Time displacement curve of LA-11-GC5-1. 1 min loading of 3.7 kPa load.	57
4.11	Compression behaviour of all samples	58
4.12	The key compression variables against their primary controlling variables, or proxies thereof.	60
4.13	Summary of physical and geotechnical properties from the middle marsh core (LA-10-2C).	61
4.14	Summary of physical and geotechnical properties from the lower marsh core (LA-11-03).	62
5.1	PDL curve of using the linear and power regression model for $C_r$ .	73
5.2	Bulk density and effective stress profiles from the linear and power regression models for $C_r$ .	74
5.3	Modelled outputs using the linear regression models.	76
5.4	The effects of a variable initial load is demonstrated by applying a range of values between 0.0001 – 0.1 kPa.	77

5.5	Void ratio from modelled and measured data and their residuals.	78
5.6	Bulk density from modelled and measured data and the residuals.	78
5.7	Effective stress from modelled and measured data and their residuals.	78
5.8	Modelled void ratio against measured data.	79
5.9	Modelled bulk density against measured data.	79
5.10	Modelled effective stress against measured data.	79
5.11	RSL record from Barlow <i>et al.</i> (unpublished data) and the decompacted RSL curve.	82
6.1	Variations in PMSE (measured by Barlow <i>et al.</i> (unpublished data)) against void ratio from both the middle (LA-10-2C) and lower (LA-11-03) marsh core.	84
6.2	Hypothetical PDL curves based upon the assumed lower marsh erosive event considered in Figure 3.8.	86
7.1	Variations in yield stress against shear strength.	88

## Appendix

A3.1	Variations in LOI and the compression properties measured within the intertidal zone against elevation (m OD).	108
A4.1	Compression properties ( $e_1$ , $\sigma'_y$ , $C_r$ and $C_c$ ) are plotted against their controlling variables (LOI and SWLI) to assess the effect of a variable loading approach.	110

## **Table of Tables**

2.1	Summary of the main errors involved in the calculation of SLIPs. Table adapted from Engelhart and Horton (in press).	6
3.1	Relative water levels (m OD) for Loch Laxford (Admiralty Tide Tables, 2001).	25
4.1	Conventional methods used for testing.	38
4.2	Sample identification codes.	40
4.3	Pre-25 kPa stress loading strategies used for each sample.	46
5.1	British Standards (2002) descriptions of sample lithology.	51
5.2	British Standards (2002) description of core lithology.	63

## **Appendix**

A2.1	Summary of physical properties.	105
A2.2	Summary of geotechnical properties.	106

## **Acknowledgements**

Firstly, I would like to thank my supervisors, Matt Brain and Antony Long who have both been incredibly helpful and supportive throughout this year in the field, the laboratory, in our regular meetings and their comments on my work. Without their help this project would not have been possible.

Thanks must also go to Dr. Natasha Barlow for putting up with my constant requests for 'more data' and always being willing to discuss ideas. This thesis has been possible due to the much larger 'North Atlantic sea-level changes and climate in the last 500 years' project (PIs Profs. Antony Long and Roland Gehrels) which has given me the opportunity to use huge resources of data which would simply have not been available within this project otherwise.

This research would not have been possible without the excellent assistance in the field for the two field trips from Antony, Matt, Tasha, Tim Dowson and Martin Black. Both trips yielded a large number of high quality samples that allowed a lot of exploratory testing. Thanks must also go to the Sea-Level 500 project for funding the first trip and Nick Rosser for arranging financial support for the second. Thanks also to Dougal Lindsay, Ian Morrison and the Scottish National Heritage for providing access to the site for both fieldtrips.

This work has also been greatly aided by the technical help of the laboratory staff. In particular, Neil Tunstall, Chris Longley, Alison Clark and Frank Davies have been incredibly helpful during the time I spent in the laboratory.

This year has been made much easier with the friends I have made in Durham from both the postgraduate community (in no order: Bertie, Ed, Chris, Chris, Laura, Louise, Mattie, Martin, Rachel, Tim and Will), college and also the rest of the geography department.

I would also like to thank my grandparents who have funded this year for me. Without their help I would not have had any way of undertaking this research.

Last, but not least, I would like to thank my family for putting up with me when I haven't been able to talk about anything other than 'squashing soil'! Their support and love throughout this year has helped me immeasurably in completing this thesis.



## Abstract

This thesis assesses the degree to which sediment compression affects a Late Holocene sea-level reconstruction from Loch Laxford, northwest Scotland. The reconstruction is based on analysis of a short sediment core (~0.7 m) that records a progressive increase in organic content up-core with loss on ignition rising from 5% at the base to ~60% at the surface. The core is decompacted using site-specific geotechnical data and a modified version of a previously published compaction model. Compression properties at the site, measured using geotechnical laboratory tests upon contemporary surface samples have significant correlations with key physical properties and environmental parameters. These data are combined to reconstruct compression properties downcore. Model predictions of bulk density, void ratio and effective stress downcore closely match those observed *in situ* ( $r^2 = 0.80$ ,  $r^2 = 0.78$  and  $r^2 = 0.98$  respectively), providing confidence in model accuracy. Modelled decompaction of the core produces estimates of post-depositional lowering (PDL, m), providing quantification of the degree to which sea level index points developed from the sample core have been lowered since their formation. A maximum PDL value of  $0.013 \pm 0.005$  m ( $2\sigma$  error) is identified between 0.35 and 0.45 m below ground level. Compaction therefore has minimal effect on reconstructed sea level at Loch Laxford and can be ruled out as a key control on the relative sea-level history at Loch Laxford.

The research also assesses the potential for geotechnical methods, particularly downcore void ratio, to identify erosive breaks in sediment successions that are not evident in routine litho- or bio-stratigraphic analysis. This allows a first-order assessment of the suitability of cores for high resolution sea-level studies without the need for the development of expensive age-depth models and time-consuming laboratory analyses.

## **Declaration**

I confirm that no part of the material presented in this thesis has previously been submitted for a degree in this or any other university. In all cases the work of others, where relevant has been fully acknowledged.

The copyright of this thesis rests with the author. No quotation from it should be published without the author's prior written consent and information derived from it should be acknowledged.

Ben Cullen, 2012.

## Chapter 1 Introduction

### 1.1 Introduction

In their Fourth Assessment Report, the IPCC (Bindoff *et al.*, 2007) predicted that sea level will rise by 0.18 - 0.59 m by the year 2100. These ranges in predictions reflect different greenhouse gas emission scenarios and are globally averaged values of future sea-level change. Gehrels and Long (2008) suggest that in order to more accurately predict future local to regional sea-level change, a combined approach is required that considers both modelled and geological data that reflect local site conditions as opposed to global averages.

Geological and observational data are crucial in order to validate and calibrate sea-level models; the errors involved in both are important to enable an understanding of future change (Gehrels and Long, 2008). Errors associated with sea-level predictions arise from the age and elevation of sea-level index points (SLIPs) (Shennan and Horton, 2002). They are generally well understood and their effect can be displayed graphically by using error bars or boxes (Shennan, 1980; 1982; 1986; Kidson, 1986; Shennan and Horton, 2002). However, compaction is an error in salt marsh reconstructions of sea level that has not been resolved and remains a factor which affects the prediction of future sea-level change and, for example, the calibration and validation of geophysical models (Peltier *et al.*, 2002; Brooks *et al.*, 2008; Brain *et al.*, 2011).

Compaction is defined by Allen (2000) as a set of processes which cause a sediment column to reduce in volume as a result of its self-weight and burial (Allen, 1999). When organic matter is present there is also the potential for biological and chemical decay (Allen, 2000). Sediment compaction is an important process to consider in salt marsh stratigraphic studies of sea level, where it can cause the lowering of sea-level markers, thus creating potential overestimates and errors in the rate of sea-level rise (Allen, 2000; Shennan *et al.*, 2000a; Brain *et al.*, 2012). Compaction has been observed in the field (Cahoon *et al.*, 1995) and has been modelled through a variety of techniques (e.g. Allen, 1999; Paul and Barras, 1998; Pizzuto and Schwendt, 1997; Brain *et al.*, 2011; 2012). Despite compaction being recognised as a process which can cause significant errors in sea-level reconstructions there has, until recently, been a limited understanding of the

process with regard to the controlling variables in salt marsh sediments and, hence, its effects (Brain *et al.*, 2011; 2012).

Brain *et al.* (2011; 2012) have taken a geotechnical approach to modelling compaction within the intertidal zone (LOI < 40%). (The Brain *et al.* (2012) model is henceforth referred to as BR1.) The results have shown that previous geotechnical modelling techniques are not applicable in the intertidal zone due to the specific nature of the sediments as well as their variability in sediment structure (Brain *et al.*, 2011).

Using modelled stratigraphic sequences, Brain *et al.* (2012) suggest that compaction can contribute to reconstructed accelerations in sea-level rise obtained from salt marsh records. They also suggest that short, regressive sediment successions are affected minimally by the effects of sediment compaction. However, at present BR1 is limited by a lack of geotechnical data that describe highly organic materials (LOI > 40%) and has not yet been applied to empirical stratigraphic data. This thesis addresses the above two issues.

## **1.2 Aim and Objectives**

The main aim of this research project is to decompact a Late Holocene sea-level record from salt marsh data using geotechnical methods and theory. In order to achieve this aim, the specific objectives are:

- To develop a sampling and laboratory strategy to quantify the compression behaviour of intertidal sediments of highly organic sediments.
- To develop regression models for the compression properties required for BR1.
- To assess the effect of sediment compaction upon a sea-level record from the last 2000 years.
- To address the implications that findings could have for future sea-level research.

## Chapter 2 Sea Level Change and Sediment Compaction

### 2.1 Sea-Level Change

Coastal areas are some of the most populated in the world and therefore management of these coastal areas is required to adapt to rising sea-level (Adger *et al.*, 2005; Gehrels and Long, 2008). To predict future sea-level changes and successfully manage the coastal environment, understanding the magnitude and timing of rises and falls in sea level, particularly in the recent past (< 500 years), is critical in the context of longer-term (Late Holocene) sea-level change (Gehrels and Long, 2008). An increased understanding of Late Holocene sea-level variability provides insight into the interrelationship between the cryosphere, ocean and climate system enabling greater precision with future modelled predictions of sea level (Rahmstorf, 2007; Horton *et al.*, 2009; Kemp *et al.*, 2011).

Satellite observations suggest a rapid increase in the rate of sea-level rise between 1993 and 2003 (3.1 mm/yr from the 20<sup>th</sup> century rate of 1.7 mm/yr) (Cazenave and Nerem, 2004). However, satellite observations have only been collected for a short period of time (~20 years) and may only describe a short-term trend (Bindoff *et al.* 2007; Gehrels and Long, 2008). Tide gauge data is also limited as there are few tide gauge records older than 100 years and the majority are concentrated in northwest Europe (Douglas, 1992; Church and White, 2006; Holgate, 2007; Woodworth *et al.*, 2009). Most geological reconstructions of sea level are not continuous to present and often lack the required resolution to observe small changes in sea level (Horton *et al.*, 2009).

More recently salt marsh sediments have enabled high-resolution sea-level studies which can 'bridge the gap' between instrumental and geological data (e.g. Gehrels *et al.*, 2005; 2006; 2008; 2012; Leorri *et al.*, 2008; Kemp *et al.*, 2009; 2011). These salt marsh reconstructions of sea level have documented a marked increase in the rate of sea-level rise from ~0 - 1 mm/yr to 2 - 3 mm/yr (Figure 2.1) in the late 19<sup>th</sup> or early 20<sup>th</sup> Century (~1820 - 1920 AD) in both the Northern and Southern Hemisphere (Donnelly *et al.*, 2004; Gehrels *et al.*, 2002; 2005; 2006; 2008; 2012; Leorri *et al.*, 2008; Kemp *et al.*, 2009; 2011). Kemp *et al.* (2011) suggest this rise in sea level may be a result of increased temperature due to natural and anthropogenic effects and similar relationships have been identified in global temperature records (e.g. Mann *et al.*, 2003; Mann and Jones, 2003).

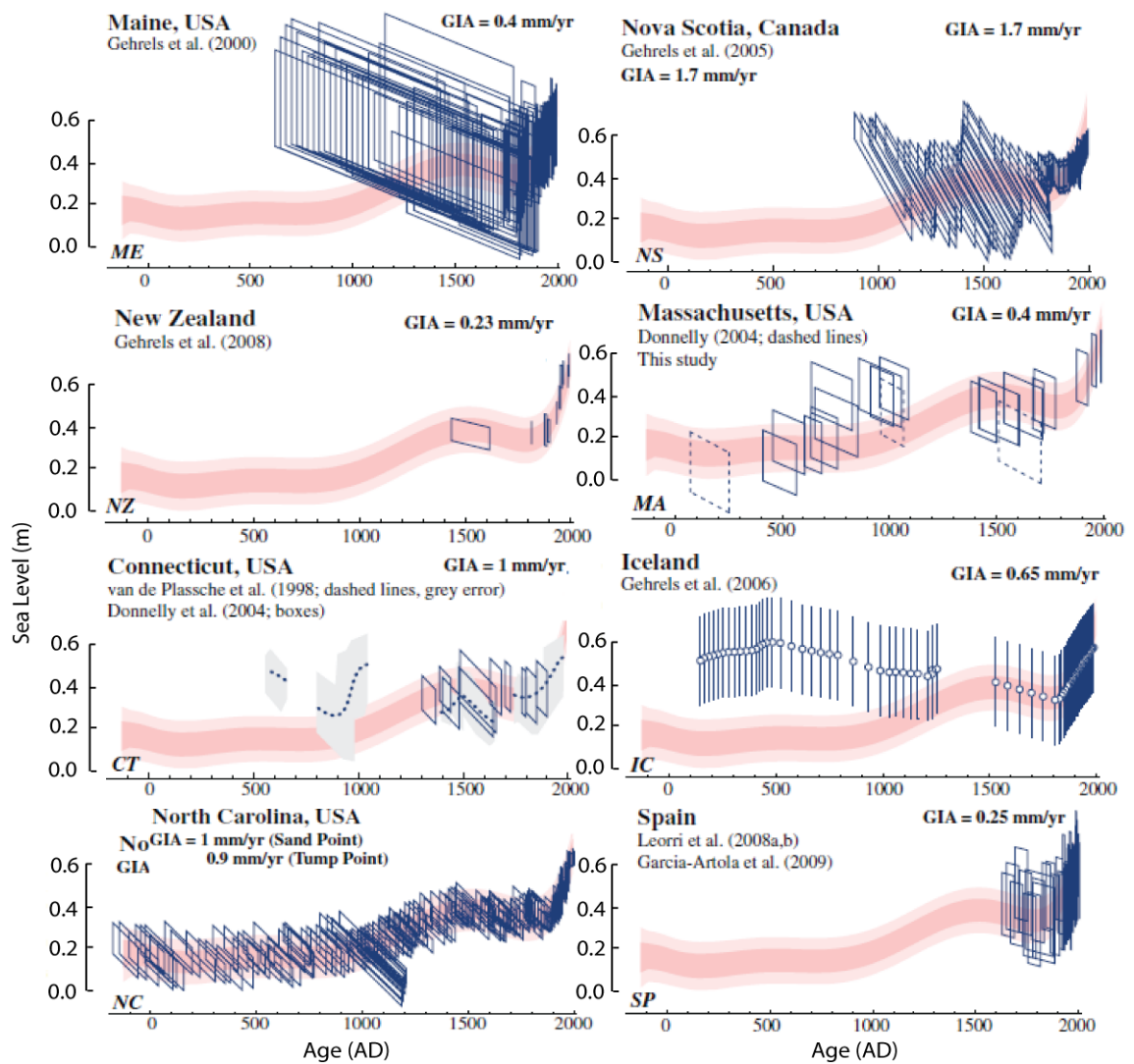


**Figure 2.1** Examples of salt marsh reconstructions from the last 2000 years (Source: Kemp *et al.*, 2011). The pink line displays the North Carolina record from Kemp *et al.* (2011) and blue boxes describe the detrended sea-level record from each location which accounts for the local glacio-isostatic-adjustment (GIA) at each site allowing each site to be directly compared. Error bars are displayed by the blue boxes/lines. Horizontal boxes represent errors in the age of the SLIP. Vertical lines/boxes represent errors in the sea-level measurement. For more details on the errors bars displayed see Kemp *et al.* (2011).

However, recent modelling work by Kopp *et al.* (2010) has suggested that for a meltwater signal to be observable a significant amount of melt is required for the mass loss signal to exceed the ‘dynamic sea-level’ changes (Gregory *et al.*, 2001) created by thermosteric effects and changes in circulation. This is particularly evident in locations in Oceania (Kopp *et al.* 2010; e.g. Gehrels *et al.*, 2008; 2011). It could therefore be inferred that there is another cause for these sea-level inflections that arises from the effects of local processes, be they oceanographic (e.g. Sallenger *et al.*, 2012) or site specific relating to the nature of the sedimentary succession under consideration (Brain *et al.*, 2012).

## 2.2 Errors in Sea-Level Reconstruction

Over time salt marshes accumulate sediment and can create a continuous record which can be used to reconstruct former sea level (Allen, 2000; Gehrels *et al.*, 2011). Tooley (1982) suggested that the lithostratigraphy of salt marshes can be used to determine trends in sea-level, whether transgressive or regressive sequences. However, more recently, biostratigraphic indicators have been used (e.g. Shennan, 1982; Tooley, 1985; Reed, 1995) particularly in conjunction with statistical techniques such as transfer functions (Edwards and Horton, 2000; Horton and Edwards, 2006; Gehrels *et al.*, 2008; 2012; Kemp *et al.*, 2009; 2011). Common biostratigraphic indicators are foraminifera (Scott and Medioli, 1978; e.g. Gehrels *et al.*, 2005; 2008; 2012) and diatoms (Devoy, 1979; e.g. Horton *et al.*, 2006; Gehrels *et al.*, 2001; Long *et al.*, 2010). Species of these microfossils are found at specific heights in the tidal frame meaning that the altitude of former sea levels can be identified based upon their relative abundances (Gehrels, 2000; Gehrels *et al.*, 2001). Using transfer functions, microfossils can be used to establish high precision and resolution reconstructions with vertical errors as low as  $\pm 0.05$  m in microtidal locations (Southall *et al.*, 2006; Callard *et al.*, 2011).

Reconstructing sea-level change from salt marsh stratigraphies frequently uses the SLIP method (Shennan, 1986; Tooley, 1978) which fixes relative sea level (RSL) in space and time. A SLIP requires information pertaining to its location, indicative meaning, altitude, tendency and age. SLIPs are, however, prone to errors relating to levelling, their indicative meaning/range or transfer function, tidal range changes, dating and compaction (Table 2.1).

**Table 2.1** Summary of the main errors involved in the calculation of SLIPs. MTL = Mean tide level and HAT = highest astronomical tide. Table adapted from Engelhart and Horton (in press).

Source of error	Example	Magnitude	References
Altitude	High precision surveying (e.g. total station)	$\pm 0.05$ m	Shennan (1986)
	Position in tidal frame estimated salt marsh vegetation Surface height is (HAT-MTL)/2	$\pm((\text{HAT}-\text{MTL})/2)$	Engelhart and Horton (in press)
	Offshore coring related to MTL	$\pm$ Tidal range	Shennan (1989)
Benchmark	Levelling of benchmark to OD	$\pm 0.15$ m	Shennan (1982)
Extrusion of sample	Angle of borehole	$\pm 1\%$ overburden	Törnqvist <i>et al.</i> (2008)
	Sampling error	$\pm 0.01$ m	Shennan (1986)
	Compaction due to corer	$\pm 0.01$ m (Russian corer)	Shennan (1986)
Sample	Thickness of sample	$\pm$ Half of sample thickness	Shennan (1986)
Tidal levels	Sample equidistant to two tide gauge when calculating relative water levels	$\pm$ Difference in tidal datum's between gauges	Shennan (1986)

Whilst errors can be accounted for through standard techniques (e.g. Shennan, 1980; 1982; 1986) and modelling (e.g. Shennan *et al.*, 2000b; Shennan and Andrews, 2000), sediment compaction is an exception and a better understanding of the process is required (Brain *et al.* 2011).



### 2.3 Sediment Compaction

Allen (1999; 2000) refers to sediment compaction as a set of processes which causes a sediment column to reduce in volume as a result of its self-weight as well as chemical and biological processes (e.g. biodegradation and oxidation). It therefore encompasses all processes causing the rearrangement of sediment structure, leading to a reduction in the volume of a deposited sediment succession (Allen, 2000). Compaction can cause a distortion of stratigraphic successions (van Asselen *et al.*, 2009) causing the potential lowering of SLIPs from their original depositional elevation (Edwards, 2006) (Figure 2.2).

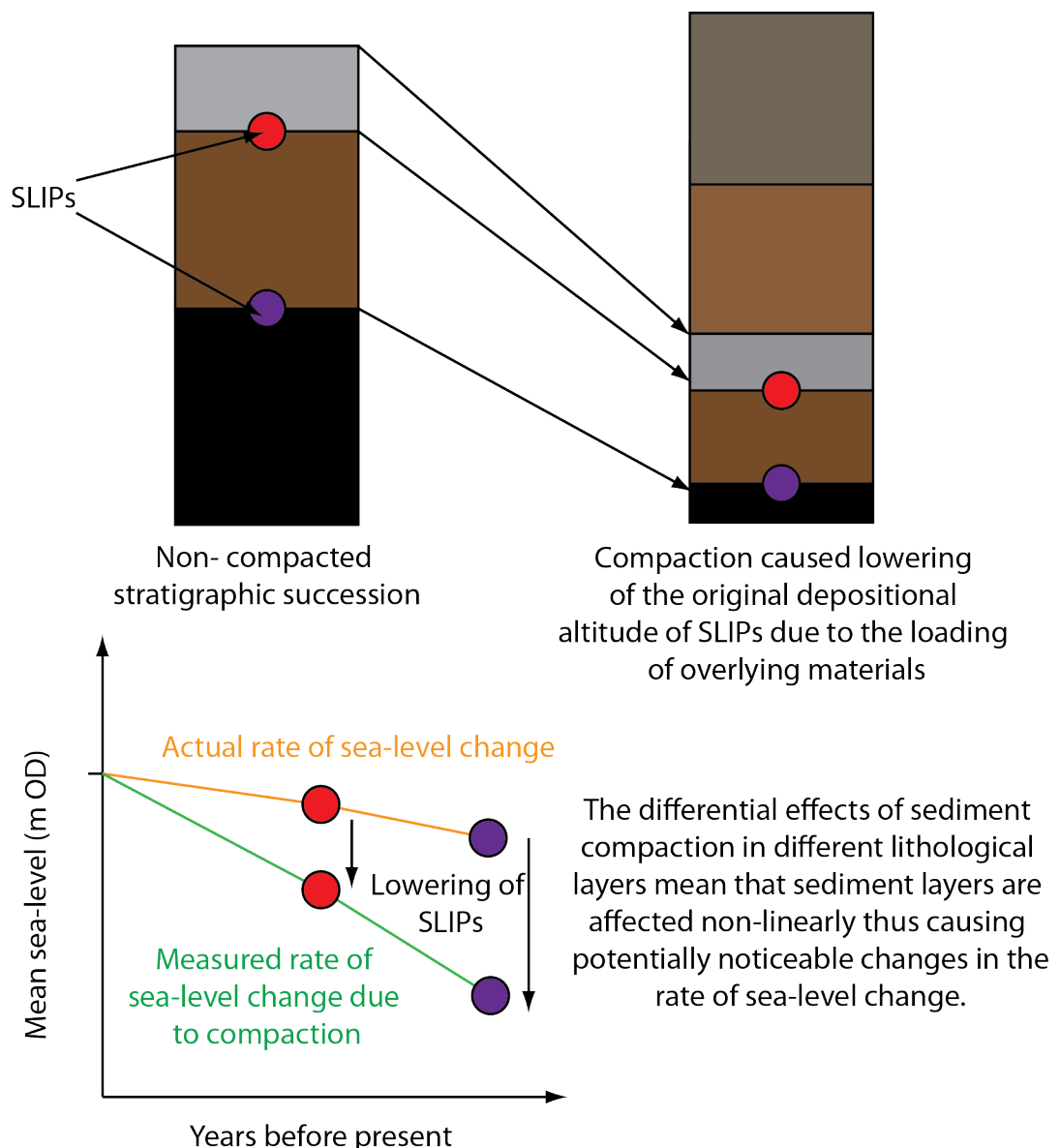


**Figure 2.2** The potential effects of sediment compaction upon a stratigraphic succession and the subsequent effects upon a sea-level reconstruction upon SLIPs. Figure adapted from Brain (2006).

Direct observations of sediment compaction have been made in the field by Cahoon *et al.* (1995) who reported that salt marshes in Louisiana, Florida and

North Carolina were subsidising by between 4.5 - 49 mm over a two year period. Some of the first attempts to address the issue of sediment compaction in the intertidal zone were undertaken in the early 1960s (Kaye and Barghoorn, 1964; Bloom, 1964). Kaye and Barghoorn (1964) found elliptical tree trunks within lithological units which they assumed to be initially circular, and their apparent deformation could offer information pertaining to the magnitude of compaction which had taken place. This technique is severely limited by the differences in relative compressibility between organogenic materials and tree trunks and the slip that could occur between the two; issues that were recognised by the authors (Kaye and Barghoorn, 1964). Bloom (1964) used a combination of basal peats and samples from the top of a peat layer and used a comparative approach, discussed in Section 2.4.2, to find that a peat bed has been compacted by between 13 - 44% of its original thickness in Hammock River marsh, Connecticut.

However, until recently, a lack of detailed understanding has prevented compaction being quantified with sufficient accuracy and precision. Shennan and Horton (2002) suggest that organic peats can compact by as much as 90%, though this is unlikely over Holocene timescales and instead describes a maximum compaction potential (Greensmith and Tucker, 1986). However, even over shorter timescales the magnitude of compaction can be considerable. Törnqvist *et al.* (2008) compared uncompacted basal peats in the Mississippi delta to stratigraphic cores and identified a millennial scale compaction rate of 5 mm/yr, which on shorter timescales could be as much as 10 mm/yr (Törnqvist *et al.*, 2008). Horton and Shennan (2009) undertook a similar approach with 363 SLIPs since the Last Glacial Maximum along the east coast of the British Isles and found an average compaction rate of  $0.4 \pm 0.3$  mm/yr. This could lead to overestimations of sea-level records by 0.1 - 0.4 mm/yr (Horton and Shennan, 2009), potentially causing overestimations of sea-level changes by as much as double the actual rate (Shennan *et al.*, 2011; Shennan *et al.*, 2000a).

The implications of such an overprediction are significant, particularly upon short term sea-level records such as the 19<sup>th</sup>/20<sup>th</sup> Century inflection, where the magnitude of sea-level change is much less than those that occurred in the early- to mid- Holocene (e.g. Donnelly *et al.*, 2004; Gehrels *et al.*, 2005; 2006; 2008; 2012; Leorri *et al.*, 2008; Kemp *et al.*, 2009; 2011). Brain *et al.* (2012) highlight that sediment compression (the reduction in volume of a sediment column due to loading by overlying sediments; Van Asselen *et al.*, 2009) could, in favourable

conditions, contribute as much as 0.1 - 0.4 mm/yr to the acceleration in sea-level change. Prior to BR1 there have been multiple methods for decompacting sediment successions; these have broadly suffered from a lack of theoretical knowledge of the geotechnical properties of intertidal sediments, and so have largely been inappropriate for sea-level studies. Some of these approaches are considered below.

## **2.4 Decompaction Approaches**

Thin basal peats are relatively resistant to sediment compaction as they lie upon incompressible Pleistocene sediments and cannot be lowered significantly from their initial depositional elevations (Jelgersma, 1961; Shennan and Horton, 2002). Basal peats have been used in order to try and minimise the effects of sediment compaction in sea-level studies by either using only basal peats in sea-level reconstructions (e.g. Donnelly *et al.* 2004), by comparing the relationship between intercalated and basal peats to approximate the degree of compaction (e.g. Gehrels, 1999) or by assessing the broader scale implications of sediment compaction (e.g. Shennan and Horton, 2002, Horton and Shennan, 2009). However, Shennan and Horton (2002) highlight that by only using compaction-free basal peats, the current database of SLIPs would be significantly limited and would tend to ignore many of the methodological advances which have allowed high-resolution sea-level records to be obtained from salt marsh sediments. Furthermore basal peats are not always available in locations where sea-level reconstructions are undertaken and so an approach is required which is capable of decompacting non-basal stratigraphic successions (Brain *et al.*, 2011; 2012).

### **2.4.1 Empirical Approaches**

There have been several examples of empirical approaches used to decompact sediment successions. As mentioned previously, Cahoon *et al.* (1995) used a Sediment-Erosion-Table (SET) at three salt marshes in order to observe the magnitude of sediment compaction which had occurred. SETs were installed upon incompressible substrates and measured elevation changes of the marsh. Vertical accretion was measured with marker horizons (Cahoon *et al.*, 1995). The difference between the two was attributed to sediment compaction.

There have also been several attempts (e.g. Gehrels *et al.*, 2006; 2012; Kemp *et al.*, 2009) to link either increasing downcore bulk density to downcore compaction or constant bulk density to a lack of compaction. Gehrels *et al.* (2012) suggest that

they can correct the elevation of salt marsh sediments by correcting the density of materials to the density observed at the surface for that particular lithology. They do this by stretching material slices so the bulk density is the same as the assumed surface density.

#### **2.4.2 Comparative Approaches**

Comparative approaches where the elevation of basal and intercalated peats have been used in order to account for the process of sediment compaction (e.g. Haslett *et al.*, 1998) have been used in a variety of locations. Haslett *et al.* (1998) compared the altitudes of basal peats with a similar intercalated peat, which they assume to have accumulated in a uniform manner and have had an upper surface with the same altitude. They observe compaction of up to 2.22 m of peats overlain by denser clays.

Edwards (2006) collected five new SLIPs from the Llanrhidian marshes, southwest Wales and used these data alongside the work of other authors (Housley, 1988; Somerset County Council, 1992; Godwin and Willis, 1961; Heyworth and Kidson, 1982; Smith and Morgan, 1989; Haslett *et al.*, 1998; 2001) from Southwest England to assess the impact of sediment compaction. Shennan and Horton (2002) suggest that geological sea-level data from Southwest England is relatively scarce, but where good coverage is identified, modelled predictions of sea level lie in the upper elevations of SLIPs. Shennan *et al.* (2002) argue that many of the offsets between geological and modelled data could be attributed to, and thus removed, if the process of compaction is considered. Edwards (2006) correlate the residuals between modelled and geological data to overburden and underlying material thicknesses and are able to reduce the scatter of SLIPs. It is therefore suggested that compaction could be a factor in causing the observed offset in modelled and geological data, with compaction rates as high as 0.7 - 1.0 mm/yr being possible for the last 4000 years. It must, however, be recognised that a decompaction approach will, by definition, reduce the observed offset between modelled and geological data (Edwards, 2006) and therefore it is a first order approach for decompaction.

#### **2.4.3 Problems with Previous Decompaction Approaches**

An issue that is consistent through all of the methods described is that they offer little benefit in terms of building an understanding of the process of sediment compaction. Generally, work has sought to calculate the magnitude to which

sediment compaction may have distorted sea-level records. This is useful, in that it allows records to be decompacted in favourable conditions with the presence of basal peats or a significant number of SLIPs. However, they do not allow the prediction of compaction at other locations as the observed magnitude and rates of compaction cannot reliably be extrapolated to sites where stratigraphic and environmental settings vary (Brain *et al.*, 2011).

Another limitation with the methods described above is the need to extrapolate data from a specific time period to provide useful information. This is particularly predominant for the case of Cahoon *et al.* (1995), who are able to generate information for two years of sediment compaction, but offers little information to rates of compaction which are of interest to Late Holocene sea-level scientists. Basal peat analysis can predict changes in magnitude over longer (millennial) time periods, but over shorter (centennial) time periods they are of limited detail without a high resolution set of radiocarbon dates (Törnqvist *et al.*, 2008).

Other problems are attributed to the cost of application. The cost of collecting either a high resolution set of radiocarbon dates, installing a SET upon a marsh for an extended period of time or collecting a large number of SLIPs for the statistical analysis of Edwards (2006) is prohibitive and, as suggested above, of limited benefit for generating an increased understanding of the process of sediment compaction across appropriate timescales.

An increased understanding of sediment compaction is crucial for identifying sites which are affected minimally by the process and also for applying methods to try and account for the process. The method of Gehrels *et al.* (2012) is an example of an attempt to account for sediment compaction without a process based understanding of compaction. The work of Brain *et al.* (2012) has highlighted that post-depositional lowering (PDL) is not solely related to the *in situ* conditions of a particular layer, but is rather a cumulative effect of all underlying layers. So although their method attempts to account for sediment compaction, it does not do so in a way that suitably quantifies the degree of post-depositional lowering of SLIPs.

There is a need to develop a method that can decompact sediment successions over short time periods without the need for expensive data collection, that can be applied in locations where basal peats are not present. One way to this is to

develop a detailed, processes-based understanding of sediment compaction in intertidal sediments. Geotechnical theory offers the potential to do this.

## 2.5 Geotechnical Theory

Geotechnical theory has been used to develop various compaction models in sea-level studies throughout the past 15 years. Decompaction models previously developed (Pizzuto and Schwendt, 1997; Paul and Barras, 1998; Brain *et al.*, 2012) have each varied in their approach, ease of application and in some cases their accuracy and validity.

A geotechnical approach to modelling sediment compaction uses the concept of effective stress (Terzaghi, 1936), defined as:

$$\sigma' = \sigma - u \quad (2.1)$$

where  $\sigma'$  is the effective stress,  $\sigma$  is the total stress and  $u$  is the pore water pressure. Deposition occurs upon a marsh with materials of bulk density,  $\rho$  (g/cm<sup>3</sup>). The unit weight of a sediment layer can be calculated as follows:

$$\gamma = \rho g \quad (2.2)$$

where  $\gamma$  (kN/m<sup>3</sup>) is the unit weight and  $g$  is the gravitational constant (9.81 m/s<sup>2</sup>). The total stress experienced at a particular depth can then be calculated from:

$$\sigma = \gamma z \quad (2.3)$$

where  $\sigma$  is the total stress (kPa) and  $z$  is the depth (m) of the bottom of the layer below the ground surface. Pore water pressure,  $u$ , is calculated as follows:

$$u = \gamma_w z \quad (2.4)$$

where  $\gamma_w$  is the unit weight of water (9.81 kN/m<sup>3</sup>) and  $z$  is the depth (m) below ground level of the material. These equations make up the base for a mechanical understanding of compaction.

### 2.5.1 Assumptions of Geotechnical Approaches

In using the above equations, several assumptions are made regarding the nature of a stratigraphic succession and the nature by which it compresses. Principally it is assumed that a stratigraphic succession is saturated, meaning there is no air within any of the pore spaces (voids) (Head, 1988). Furthermore, sediment particles and water are assumed to be incompressible and therefore retain their

volume when a stress is applied (Head, 1988; Powrie, 2004). Therefore, a change in volume is caused by the readjustment of the soil structure causing water to escape from pore spaces due to increased effective stress (Head, 1988; Powrie, 2004). The speed at which this can occur is controlled by the permeability and length of drainage of the sediment and, therefore, this process of deformation is time dependent (Powrie, 2004). The different stages of sediment compaction observed are initial compression, primary consolidation and secondary compression (Head, 1988) (Figure 2.3). The process by which volumetric deformation takes place due to the expulsion of pore water fluid is termed primary consolidation (Head, 1988). Prior to primary consolidation there is a near instantaneous period of initial compression, where any small pockets of gas are expelled and contact surfaces are compressed (Head, 1988) (Figure 2.3). Following primary consolidation, a stage of secondary compression, also known as creep, begins to occur. Creep refers to the continued rearrangement of particles despite excess pore water pressures having dissipated (Head, 1988). Whilst this describes the stages of primary consolidation and secondary compression as being separate processes, it is likely that both occur at the same time, particularly with the presence of organic material, until pore water pressures dissipate where creep becomes the dominant process (Van Asselen *et al.*, 2009).

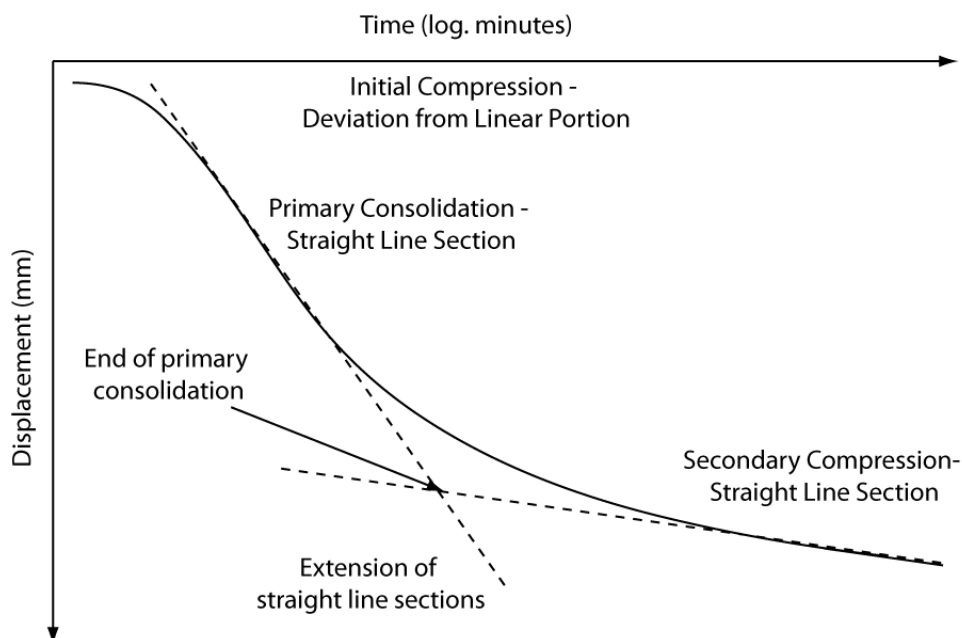


**Figure 2.3** Logarithmic time displacement curve for sediment with an applied load within an oedometer.

### 2.5.2 Compression

Sediment compression is perhaps the best understood compaction process in low energy intertidal sediment, since it can be replicated and modelled in the laboratory (Brain *et al.* 2011). A compression based approach to decompacting sediments is considered to be generally appropriate to a burial depth of approximately 3000 m (Skempton, 1970) which has subsequently been validated by further testing of terrestrial (Gutierrez and Wangen, 2005; Nygard *et al.*, 2004) and intertidal (Brain *et al.*, 2011; 2012) sediments. A compression based model refers to volumetric reduction which takes place until the point whereby pore water pressure is dissipated.

Gibson (1958) suggests that due to the slow deposition rates of most natural sediments, pore water pressures are likely to dissipate during an annual cycle meaning they are fully compressed during this time. This assumption has been debated in the past by Tovey and Paul (2002) who suggest that the coupling of porosity and permeability mean that pore pressures cannot dissipate when a sediment succession length is greater than ~5 m; however, the majority of Holocene intertidal successions are shorter than this. Mesri *et al.* (1997) further highlight that organic peat layers, common to intertidal sediments (Allen, 2000), have a high permeability and thus primary consolidation is completed quickly. Brain (2006) also investigated the time dependency of compaction properties of materials from Cowpen Marsh, northwest England and found that for predominantly minerogenic materials (LOI < 40%) primary consolidation is dominant and thus models do not require a time-dependent creep component.



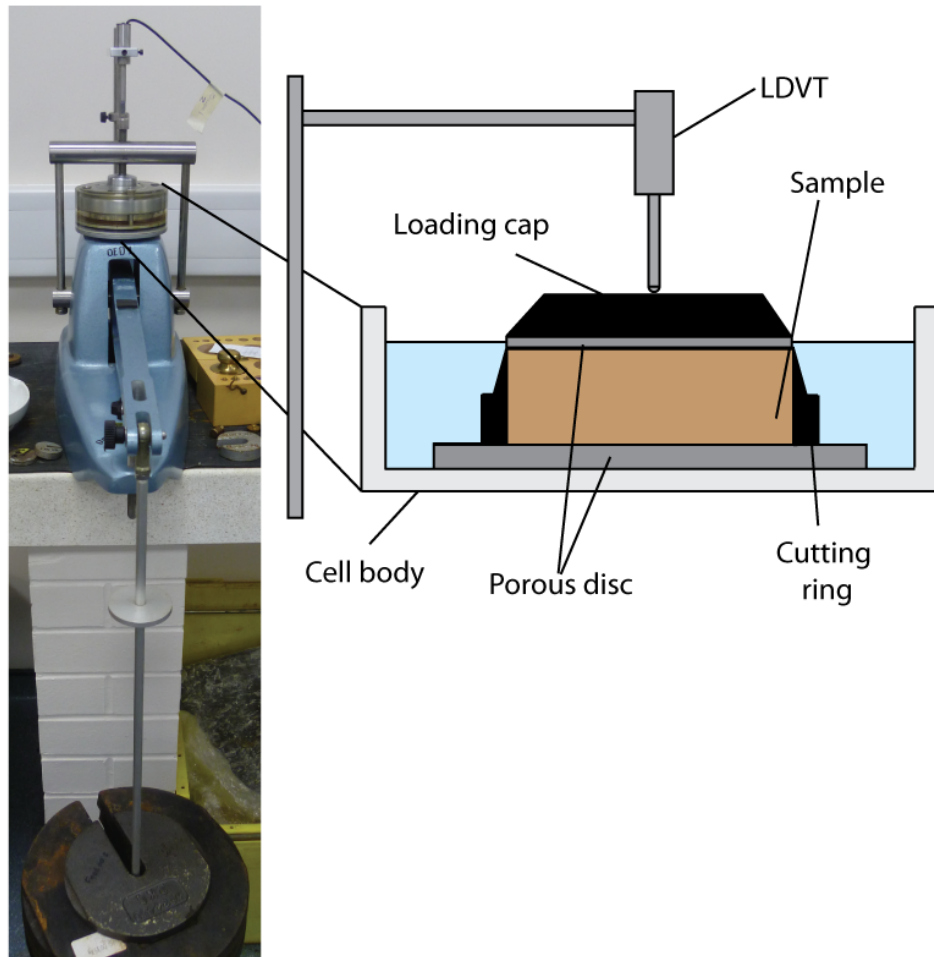
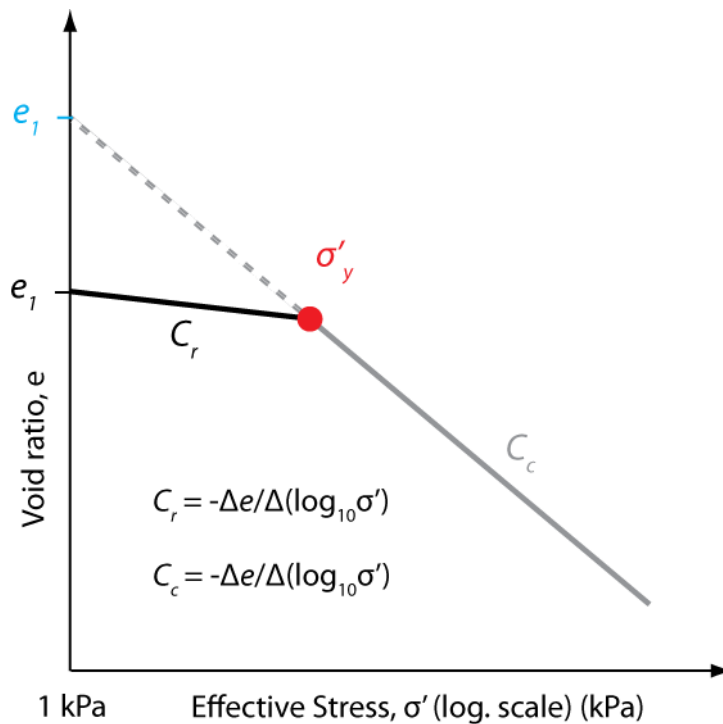


**Figure 2.4** Image of an oedometer used for testing and a schematic drawing describes the cell which encloses the sample. Weights are loaded onto the hanger which applies a load to the sample and is measured by the LDVT.

An oedometer test can be used to assess the one-dimensional compression properties of a material (Figure 2.4). Although oedometer testing does not exactly replicate the complex three dimensional effects observed *in situ* (Davis and Poulos, 1965), it does provide a good estimation for the amount of PDL, and thus information, pertaining to sediment compressibility (Head, 1988). The test is carried out within a rigid metal ring of approximately 75 mm in diameter and 19 mm in height, with porous discs on the top and bottom to allow drainage of pore water (Head, 1988; see Figure 2.4). Vertical compressive loads are then applied to the sediment and the amount of settlement is measured using a linear variable differential transformer (LDVT). The loads are generally applied in a 2:1 loading ratio, whereby loads are doubled, for 24-hour periods; this type of testing is the conventional loading approach (Head, 1988). Head (1988) does however highlight that the oedometer testing of organic material may require specific loading conditions in order to minimise the effects of secondary compression. This is important in order to develop an understanding of the compression behaviour of organic intertidal sediments.

### 2.5.3 Virgin Compression Models

The most frequently used compaction model in UK intertidal settings is the Paul and Barras (1998) model, or variations thereof (e.g. Massey *et al.*, 2006). The Paul and Barras (1998) model is referred to as a Virgin Compression Model (VCM) (Brain *et al.* 2011). A VCM is run by extrapolating a plot of void ratio against effective stress ( $e \log \sigma'$ ) (Figure 2.5), back to a reference intercept value of commonly 1 kPa (e.g. Smith, 1985). The gradient of this line is termed the compression index,  $C_c$ .



Brain *et al.* (2011; 2012)  
framework

VCM

$e_1$  Void Ratio at 1 kPa

$C_r$  Recompression Index

$C_c$  Compression Index

$e_1$  Void Ratio at 1 kPa -  
no overconsolidation

- - - Virgin Compression Line

$\sigma'_y$  Yield Stress

**Figure 2.5**  $e \log \sigma'$  plot used for compression models. A VCM model and the Brain *et al.* (2011; 2012) framework (see Section 2.5.4) are outlined. Figure adapted from Brain *et al.* (2011; 2012).

Therefore the model is simple to run as all that is required are the compression index ( $C_c$ ), the gradient of the void ratio against effective stress (logarithmic scale) curve, and a void ratio value at a particular layers depositional surface. Both these values can be determined via oedometer testing, but more commonly, are

estimated from relationships with physical properties of the sediments. This is an important aspect of developing a decompaction model as the collection of high quality materials from depth is often not possible (Brain, 2006). Paul and Barras (1998) estimate the void ratio of materials and use the liquid limit to estimate  $C_c$  (Skempton, 1944). The model assumes that materials under consideration have not been subjected to effective stresses greater than those they are presently under. When this is the case a material is referred to as being normally consolidated and the  $e \log \sigma'$  curve is referred to as a virgin compression curve (Powrie, 2004; Head, 1988). Furthermore, it is assumed that materials have no variability within the same lithology and thus a deterministic approach is appropriate (Brain *et al.* 2011).

### **2.5.3.1 Limitations**

Despite their use, there has been little testing of the validity of assumptions that are used to implement a VCM prior to Brain *et al.* (2011). Firstly, using the liquid limit to estimate the compression index ( $C_c$ ) (Skempton, 1944; Paul and Barras, 1998) is potentially a problematic approach within the intertidal zone. Liquid limit testing was not developed for peaty or granular materials but for clays. Whilst corrections are available for peats they are for freshwater peats and such relationships are poorly quantified in intertidal sediments (Brain, 2006). Furthermore the liquid limit method is semi-quantitative and is very much dependent upon user skill and experience in carrying out the test (BS, 1990). Brain *et al.* (2011) have also shown sediments that form at identical elevations within the intertidal zone have variable structure and compression behaviour, suggesting a deterministic modelling approach is not valid. Brain *et al.* (2011) highlight that effective stresses can increase without an increase in total stress due to the drying out of surface materials. Hawkins (1984) demonstrates that sediments in Avonmouth, Severn Estuary show decreases in sediment saturation by up to 56% following four hours of exposure, suggesting that materials are not always fully saturated. Capillary suction stresses cause the pore water pressure to decrease at a rate of 9.81 kPa/m above the groundwater level (Powrie, 2004; Brain, 2006), therefore causing an increase in effective stress without an increase in total stress. Soils are not fully elastic (Powrie, 2004; Head, 1988) and as a result they do not fully recover to their original form when subjected to a load, but instead retain the structural conditions experienced during previous loading conditions. These materials thus become more resistant to compression at effective stresses lower

than the maximum experienced previously (Head, 1988; Powrie, 2004; Brain *et al.*, 2011; 2012). When this process occurs the materials are termed overconsolidated (Head, 1988; Powrie, 2004; Brain *et al.*, 2011). This implies that VCMs are not valid in all intertidal sediments as they overestimate compression at effective stresses less than the yield stress and that the variability in structure prevents a deterministic modelling approach (Brain *et al.*, 2011).

#### **2.5.4 BR1**

Brain *et al.* (2011; 2012) advocate the use of a modified version of the  $e \log \sigma'$  framework used for VCMs (Figure 2.5). They argue that primary consolidation is still the main control upon compression behaviour, despite the overconsolidated nature of the materials. Fluctuating effective stresses create overconsolidated materials which have more stable structures at lower effective stresses, causing reduced rates of creep (Brain, 2006). Furthermore, as effective stresses do not remain stable they inhibit the creep process (Brain, 2006). BR1 requires four model parameters; the recompression index ( $C_r$ ), compression index ( $C_c$ ), void ratio at 1 kPa ( $e_1$ ) and the yield stress ( $\sigma'_y$ ).  $C_r$  describes a state of reduced compressibility and  $\sigma'_y$  is the compressive yield stress (kPa) at which soil stiffness decreases, indicating a transition from a low compressibility to high compressibility phase as materials change from  $C_r$  to  $C_c$ .

Brain *et al.* (2012) further develop the above framework by undertaking the same geotechnical testing from a range of locations across two extra UK salt marshes – Thornham Marsh and Roudsea Marsh as well as further testing at Cowpen Marsh. They found that the four parameters required for the framework are all related to the elevation of samples within the intertidal frame at the three sites tested. They also found that  $C_r$ ,  $C_c$  and  $e_1$  covary with LOI (LOI < 40%) (Brain *et al.*, 2012), which is to be expected due to the porous nature of organic soil structures (Delaune *et al.*, 1994). Increased organic content resulting from vascular plant growth creates more open and porous structures which are prone to compression, allowing prediction of  $e_1$ ,  $C_r$  and  $C_c$  (Brain *et al.*, 2012). At lower elevations within a salt marsh increased sedimentation rates are caused by denser suspension, thus creating materials with greater density and lower organic contents (Been and Sills, 1981; Sills, 1998; Brain *et al.*, 2012). Therefore with increased elevation, materials are less dense owing to their reduced flooding frequency. Materials with greater density are more resistant to compression due to the reduced void space

compared to their reduced density organic counterparts (Burland, 1990; Price *et al.*, 2005; Skempton, 1970; Brain *et al.*, 2012).

The  $\sigma'_y$  of samples are found to display a complex but statistically significant relationship with SWLI (Horton and Edwards, 2006), which is defined as:

$$\frac{\text{Alt}_{ab} - \text{MLWST}_b}{\text{MHWST}_b - \text{MLWST}_b} \times 100 \quad (2.5)$$

where  $\text{Alt}_{ab}$  is the altitude of sample a at site b,  $\text{MLWST}_b$  is the mean low water spring tide at site b and  $\text{MHWST}_b$  is the mean high water spring tide at site b. Increasing  $\sigma'_y$  occurs at elevations between the tidal flat and low marsh zones due to reduced flooding frequency and duration, causing increased desiccation with greater elevation (Brain *et al.*, 2012). A peak followed by a decline in values of  $\sigma'_y$  in the high marsh is observed due to the presence of above ground biomass (AGB). AGB limits direct subaerial exposure and so prevents surface moisture loss in the higher marsh and thus can prevent desiccation (Brain *et al.*, 2012). Desiccation results in an increase in effective stress, causing overconsolidation and an increased resistance to compression (Greensmith and Tucker, 1971).

At present, BR1 does not have empirical data for materials with a LOI > 40%. It is important to consider the potential compaction behaviour of organic materials prior to modelling their behaviour within the intertidal zone.

## 2.6 Organic Materials

Salt marsh sediments are commonly made up of alternating peat and silt layers (Allen, 2000), therefore the compaction behaviour of organic peat layers need consideration. The main difference between organic and minerogenic materials are primarily a result of the difference in their sediment structure and composition. Organic materials and peats have very low densities and are primarily made up of compressible organic matter (Head, 1988; Hobbs, 1986) and thus the soil skeleton of these materials can deform resulting in a highly compressible material (Mesri and Ajlouni, 2007).

One of the primary issues associated with organic materials when measuring their compression behaviour is their susceptibility to be affected by the process of creep (Mesri *et al.*, 1997). It is recognised that the degree of secondary compression increases with organic content because the secondary compression index,  $C_\alpha$ , is closely related to how compressible a material is (Mesri *et al.*, 1997). It has also been found that the amount of secondary compression increases with an

increased load (Hobbs, 1986; Head, 1988). As a result, secondary compression is a non-linear process that can potentially cause variation in the compression behaviour of organic, intertidal sediments. There have been multiple models developed for freshwater clays and peats by either developing a consolidation model (Berry and Poskitt, 1972), or to describe creep processes (Garlanger, 1972; Bjerrum, 1967; Den Haan, 1996); however, as described in Section 2.5.3.1, models designed for freshwater environments are not necessarily applicable within the dynamic intertidal zone.

One method has previously been developed to account for the time dependency of materials in the intertidal zone. Pizzuto and Schwendt (1997) use the understanding of mechanical compaction and included a time function by using the finite strain theory (Gibson *et al.*, 1967; 1981). In doing so, they not only consider  $e \log \sigma'$  but also how this changes over time due to consolidation processes. The model itself is coded in FORTRAN and called 'SQUISH3' and is applied to coastal deposits in Wolfe Glade, Delaware. Inputs were obtained via oedometer tests for subtidal units. The presence of woody fragments in organic materials meant tests could not be run for these as they prevented the downward motion of the oedometer during loading. Instead, material properties were varied until the compacted layers from SQUISH3 were of equal thickness to those measured in the core. Calculated void ratios were comparable to those in the core and the relative sea-level history of the region was consistent with the decompacted age-depth relationship of the core (Pizzuto and Schwendt, 1997). The lack of empirical data, calibration techniques and requirement for local data, limits the models applicability to other marshes. Furthermore, SQUISH3 is a VCM and as such assumes that materials are not overconsolidated and, as explained in Section 2.5.3.1, this is not applicable within the intertidal zone.

At present there is no method for addressing the time-dependent process of creep within the intertidal zone. Whilst this is true, it is likely that with overconsolidated intertidal materials creating more stable sediment structures, materials are more resistant to the effects of creep and thus a compression based model, such as that developed by Brain *et al.* (2012), is appropriate given suitable laboratory testing for organic materials.

## **2.7 Implications of BR1 for Sea-Level Studies**

BR1 is described in Figure 2.6. The model is used to decompact synthetic stratigraphic successions. The synthetic successions are split into 0.02 m thick layers where each layer is given a Palaeo Marsh Surface Elevation (PMSE) and loss on ignition value based upon typical values at Cowpen Marsh. They further assign an age and sea level to each layer with an inflection at 1880 AD and a pre-inflection rate of sea-level rise of 0.2 mm/yr and post inflection rate of 1.5 mm/yr.

Synthetic successions were varied in length (0.5 to 3 m) and in type (transgressive, regressive and stable lithostratigraphic sequences) to reflect real-world stratigraphies that document the Late Holocene sea-level inflection (Figure 2.7). Brain *et al.* (2012) found that thicker (2 to 3 m) and transgressive sequences are more prone to the effects of sediment compression. In spite of this, they highlight that sediment compression is unlikely to be the sole cause of the acceleration in sea-level reconstructions observed in salt marsh deposits (Brain *et al.*, 2012).

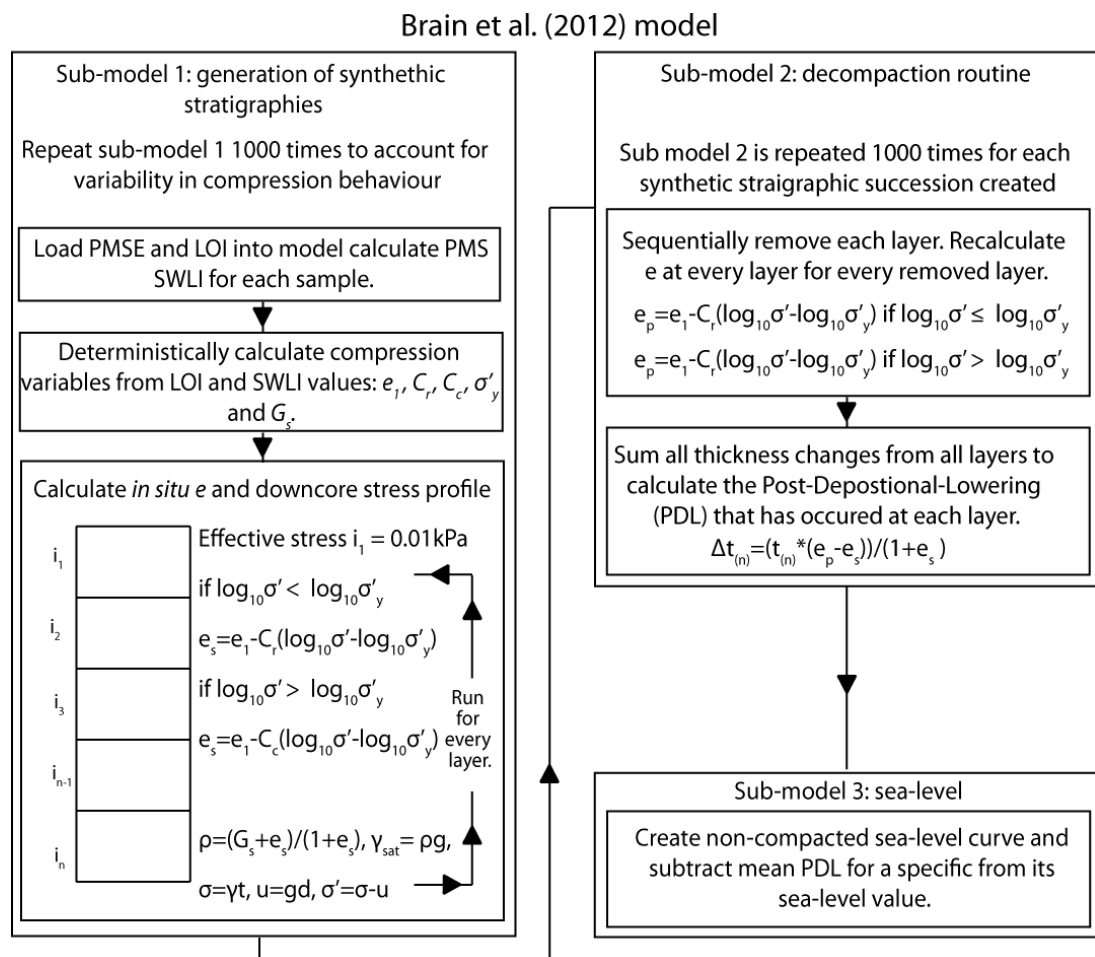


**Figure 2.6** A summary of the methodological steps of BR1.

The findings of Brain *et al.* (2012) helped to develop recommendations for site selection to minimise the effects of sediment compression. Short, regressive sediment successions are preferred as they have smaller effective stresses and a

reduced potential for lowering of near-surface SLIPs. However, these model-based findings have yet to be fully validated in real-world settings.

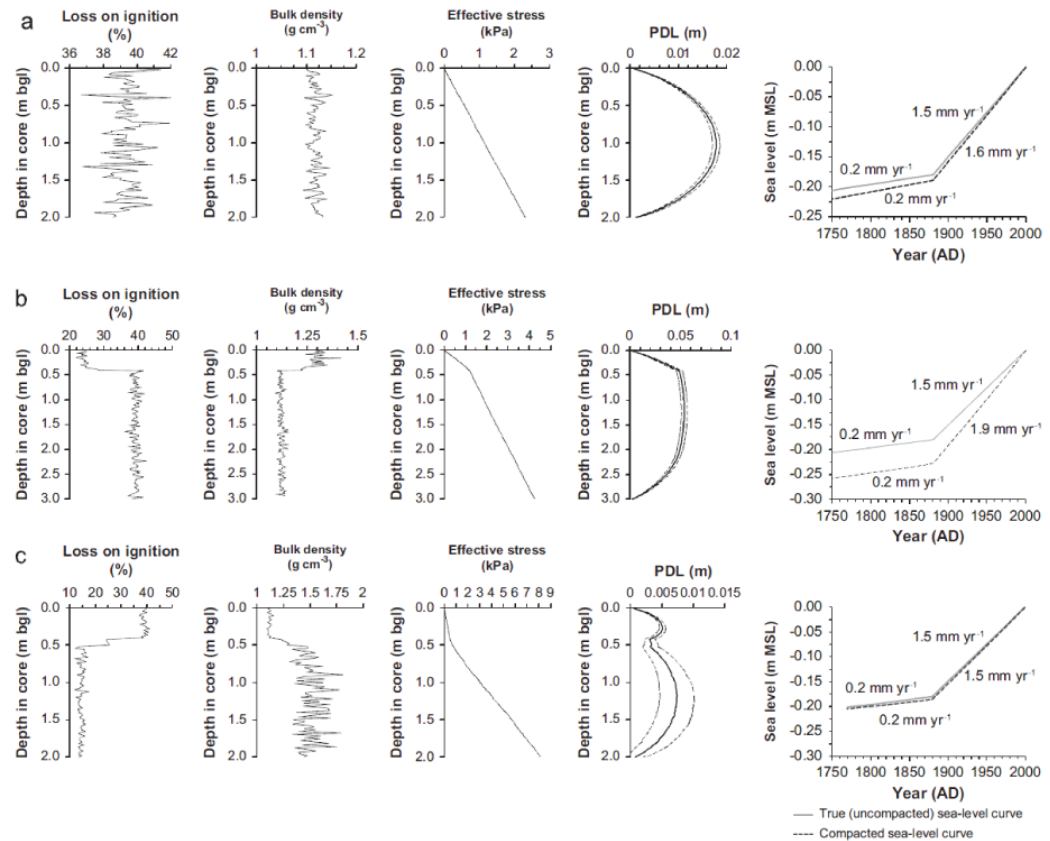


**Figure 2.7** Example runs from BR1 showing (a) a 2 m uniform succession, (b) a 3 m transgressive succession and (c) a 2 m regressive succession. The effect upon the rate of sea-level change is shown for each sediment succession. Shorter regressive sediment successions (c) minimise sediment compression. Source Brain *et al.* (2012).

## 2.8 Research Context

As part of a NERC research project "North Atlantic sea-level variability during the last 500 years" (PIs Professor Roland Gehrels (Plymouth University) and Professor Antony Long (Durham University)), a detailed investigation of a number of salt marshes in the North Atlantic is underway. One of these sites is located at Loch Laxford, northwest Scotland, and contains a c. 2000 year record of sedimentation and sea-level change, that is one of the longest late Holocene records from the UK. This MSc project contributes to the wider NERC project by seeking to decompact the Loch Laxford salt marsh record using state-of-the-art methods in geotechnical testing and an appropriately modified version of BR1 based on local site conditions and observations. A core has been collected from the site which is ~0.7 m long and is a gradual regressive succession. Therefore, Loch Laxford offers a site which empirical and modelling studies suggest will have



been affected minimally by sediment compression. Hence, this site provides a good location for assessing the findings of the findings Brain *et al.* (2012).

## **2.9 Assumptions and Development of BR1**

An assumption of BR1 is that deposition is continuous and no erosive breaks are observed. A completely continuous deposition rate with no erosive breaks is rare in Holocene salt marshes, where erosion can occur that will potentially complicate the effects of sediment compaction. Whilst the stratigraphic successions modelled by Brain *et al.* (2012) are varied to reflect key study sites that document the 19<sup>th</sup>/20<sup>th</sup> Century inflection with transgressive, regressive and uniform sequences, they do not directly consider the effects of erosional phases. An issue with the presence of erosive phases is that they can be difficult to identify, particularly when there is no clear evidence shown in the litho- or biostratigraphy. A method for detecting such phases is important for future sea-level work and subsequent decompaction procedures.

Furthermore, Brain *et al.* (2012) recognise that very low effective stresses ( $< 3$  kPa) are not applied to the materials tested in conventional loading scenarios using oedometer compression tests. They highlight that if yield stresses occur at values  $< 3$  kPa then materials will demonstrate a high compressibility phase of compression ( $C_c$ ). This can cause increased PDL compared to the low compressibility, overconsolidated phase resulting from higher yield stresses.

This thesis intends to develop the regression models used within BR1 for highly organic materials. In order to fully understand the compressibility of highly organic materials it is crucial to gather geotechnical compression data from these materials using appropriate methods.

## **2.10 Summary**

Sediment compaction is a process which has the potential to cause significant errors in sea-level reconstructions (Shennan and Horton, 2002). The importance of generating an understanding of sediment compaction is crucial, particularly if the process has caused the over exaggeration of trends in sea-level records over the past ~500 years. However, until recently there has been a relatively limited understanding of compression behaviour within the intertidal zone (Brain *et al.*, 2011; 2012). Brain *et al.* (2012) have used geotechnical theory to develop a process-based understanding of sediment compaction and in doing so have been able to assess the implications of the process upon Late Holocene sea-level

records. However, application of BR1 is limited at present by a paucity of empirical data that describe the compression behaviour of materials with organic contents above ~40%. This thesis therefore offers the opportunity to produce an understanding of the compression behaviour of organic materials within the intertidal zone to apply BR1 more widely. Finally, in conjunction with the work of Barlow *et al.* (unpublished data), there is an opportunity to perform the first decompaction of geological empirical data with BR1.

## Chapter 3 Field Site & Methods

### 3.1 Field Site

#### 3.1.1 Introduction

This chapter provides an introduction to the study site of this thesis: Loch Laxford, northwest Scotland. Loch Laxford is the northernmost major sea loch on the western coast of Scotland (Figure 3.1). It consists of two smaller lochs, Loch Dùghaill and Loch a' Chadh-Fi (Figure 3.1) (Bates *et al.*, 2004). At the head of the loch there is a small sheltered inlet, Tràigh Bad na Bàighe, which is protected by a bedrock outcrop from the prevailing wind and waves that enter the outermost part of the Loch. The inlet has a predominantly sand covered tidal flat and a vegetated "embayment-type" salt marsh (Allen, 2000) to the north, which is best developed between areas of protruding bedrock (Figure 3.1).

The tidal regime at Loch Laxford is macrotidal (mean spring range = 4.2 m) and semi diurnal (Table 3.1).

**Table 3.1** Relative water levels (m OD) for Loch Laxford (Admiralty Tide Tables, 2001).

Mean low water spring tide (MLWST)	Mean low water neap tide (MLWNT)	Mean sea level (MSL)	Mean high water neap tide (MHWNT)	Mean high water spring tide (MHWST)
-1.80	-0.60	0.25	1.00	2.40

Data presented within this chapter of the marsh stratigraphy (Figure 3.5), age-depth models (Figures 3.6 and 3.7) and relative sea-level reconstructions (Figure 3.10) have been collected as part of the 'North Atlantic sea-level change and climate in the last 500 years' project by Barlow *et al.* (unpublished data pers. comm.) who have kindly made the data available for use within this thesis. Work undertaken by Barlow *et al.* is presented within this chapter and here after is presented as marsh stratigraphy, age-depth models and RSL data respectively.

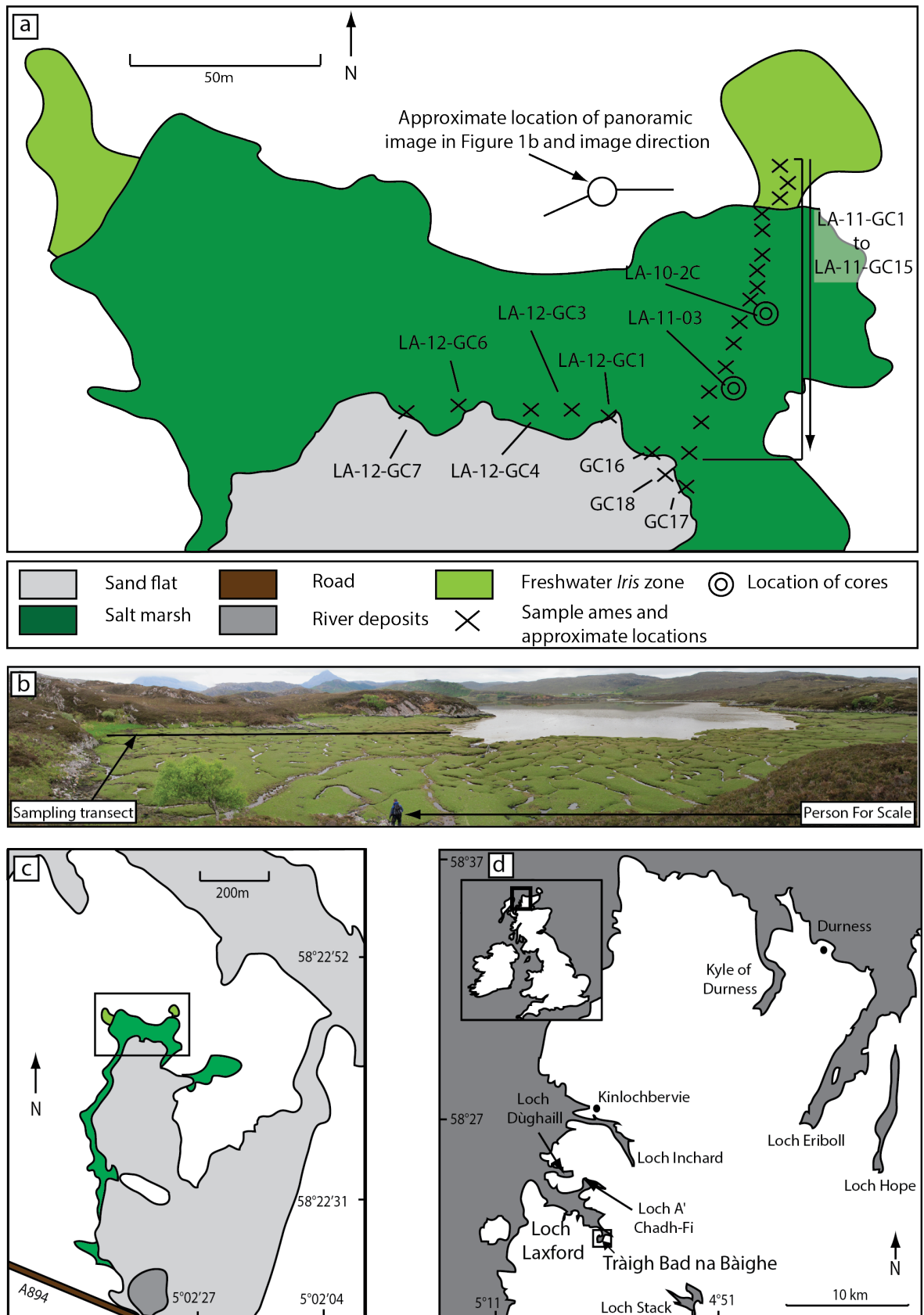


**Figure 3.1** (a) The salt marsh used at Loch Laxford and sampling locations of samples collected. Surface samples are used to develop the regression models used for BR1. Cores LA-10-2C and LA-11-03 are those to be decompacted within this thesis. (b) Panoramic image of the salt marsh – the location of the photo is noted in (a). (c) Tràigh Bad na Bàighe inlet. (d) Location of Loch Laxford in context with the Northwest of Scotland.

### 3.1.2 Marsh Environment

The salt marsh at Loch Laxford abuts the sand flat environment by a small cliff of approximately 0.10 to 0.40 m elevation (Figure 3.2).

The sand flat occurs at elevations below 1.26 m OD (Ordnance Datum Newlyn) and the marsh environment exists between ~1.30 to 2.54 m OD. A freshwater environment is found above the salt marsh and is covered by a zone of *Iris*, before upland heather communities are dominant above. The marsh has an extensive creek network (Figure 3.1b and 3.3) and pooling is evident (Figure 3.3). Drainage of the marsh occurs out the Tràigh Bad na Bàighe inlet. Marsh vegetation does not display clear zonation as often observed within the intertidal zone, and no clear high marsh environment is observed (Figure 3.1b). Instead the marsh is predominantly covered by a presently unknown species (Figure 3.4).

Stratigraphic analysis of the site (Figure 3.5) displays two broad areas: firstly in the higher marsh (>1.80 m OD) with a ~ 0.50 m thick, dark brown peat with increased fibrosity upcore overlying sandy materials and secondly in the lower marsh (<1.80 m OD), displaying a thinner peat overlying a mix of sands and silts. Cores collected either lay upon the uncompressible Lewisian Complex, the bedrock at the site, or coring was prevented by sandy material.



**Figure 3.2** The lower salt marsh / sand flat cliff observed at Loch Laxford.



**Figure 3.3** An extensive creek network is present across much of Loch Laxford. This causes the pooling of water across the marsh.



**Figure 3.4** Vegetation observed across the whole marsh at Loch Laxford. A one penny coin is displayed for scale.



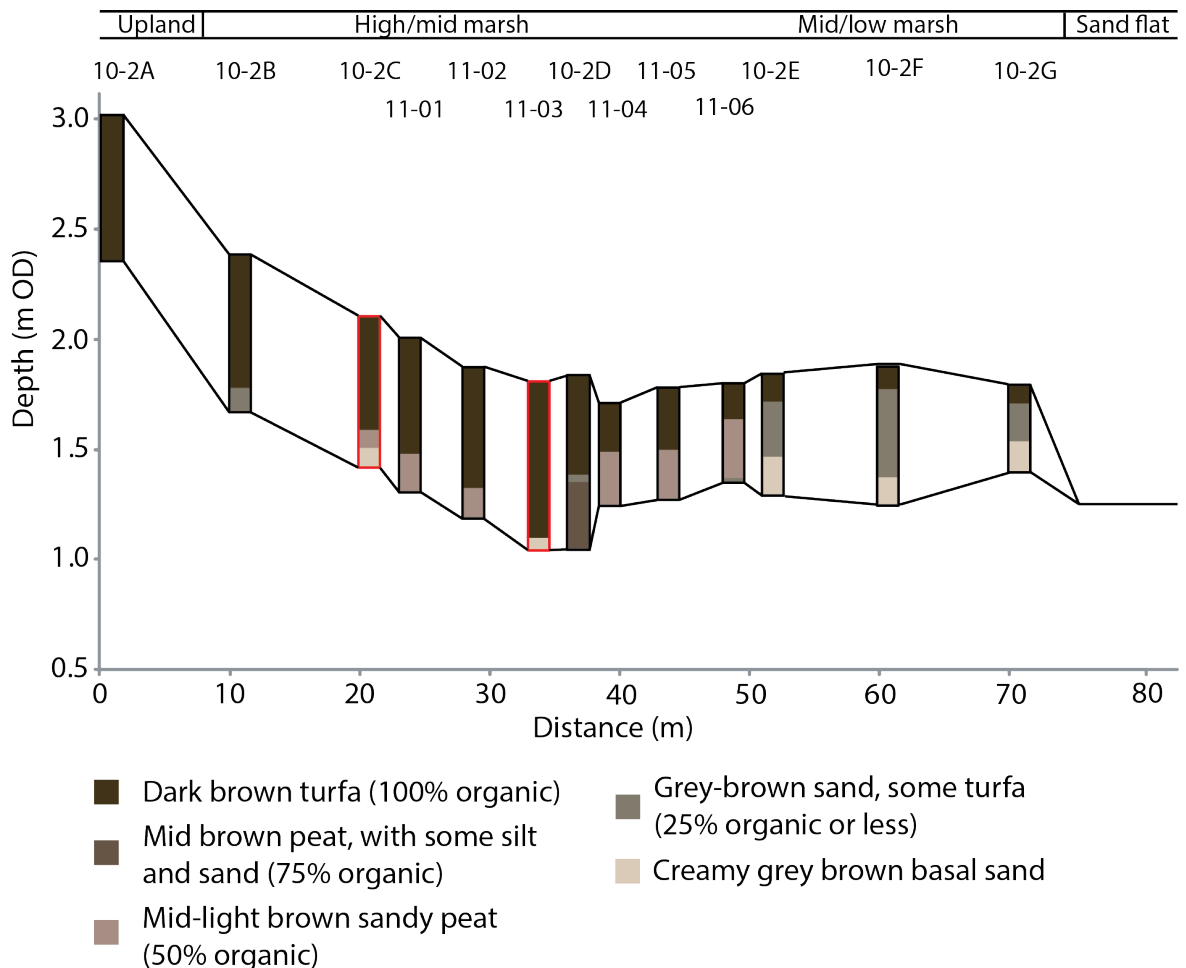


**Figure 3.5** Stratigraphy from multiple cores at Loch Laxford. Cores from the middle (LA-10-2C) and lower (LA-11-03) marsh used for subsequent sea-level studies are highlighted in red. Source Barlow *et al.* (unpublished data).

Cores below an elevation of 1.80 m OD display a more complex stratigraphy, with increased sand content below the upper 0.50 to 0.10 m in cores between 10-2G and 10-2D. It is possible that the development of the marsh below 1.80 m OD is a natural development, however, with the potential for the variable stratigraphy to represent an erosive event detailed analysis has not been undertaken on cores below LA-11-03, above which the stratigraphy displays a clear regressive succession. Biostratigraphic analysis of the middle (LA-10-2C) and lower marsh (LA-11-03) cores corroborate this by showing no evidence for an erosive break in either.

### 3.1.3 Radiometric dating

The stratigraphic analysis is complemented with a suite of radiometric dating upon two seemingly uneroded cores from the middle (LA-10-2C) and lower (LA-11-03) marsh (see Figure 3.5). A combination of AMS  $^{14}\text{C}$ ,  $^{137}\text{Cs}$  and  $^{210}\text{Pb}$  have been used to develop age models for both cores using OxCal (Bronk Ramsey, 2009) (Figures 3.6 and 3.7).

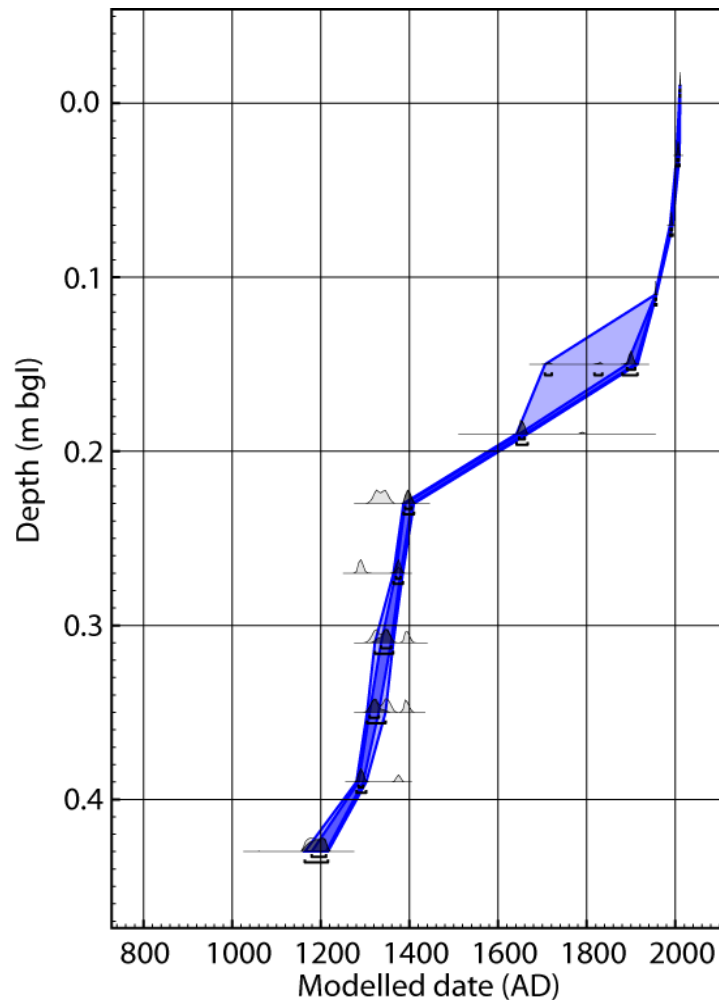


**Figure 3.6** Age-model for the lower marsh core (LA-11-03). The dark blue line represents one sigma error and lighter blue two sigma error. Source Barlow *et al.* (unpublished data).

The lower (LA-11-03) marsh core displays evidence for an erosive phase in the age model despite no obvious indication of such in the bio- or litho-stratigraphy (see Section 3.3). Deposition prior to the erosive event was rapid  $\sim 1.5$  mm/yr before a sudden reduction in rate, attributed to erosion, and finally deposition is rapid again upon recovery,  $\sim 1.3$  mm/yr.



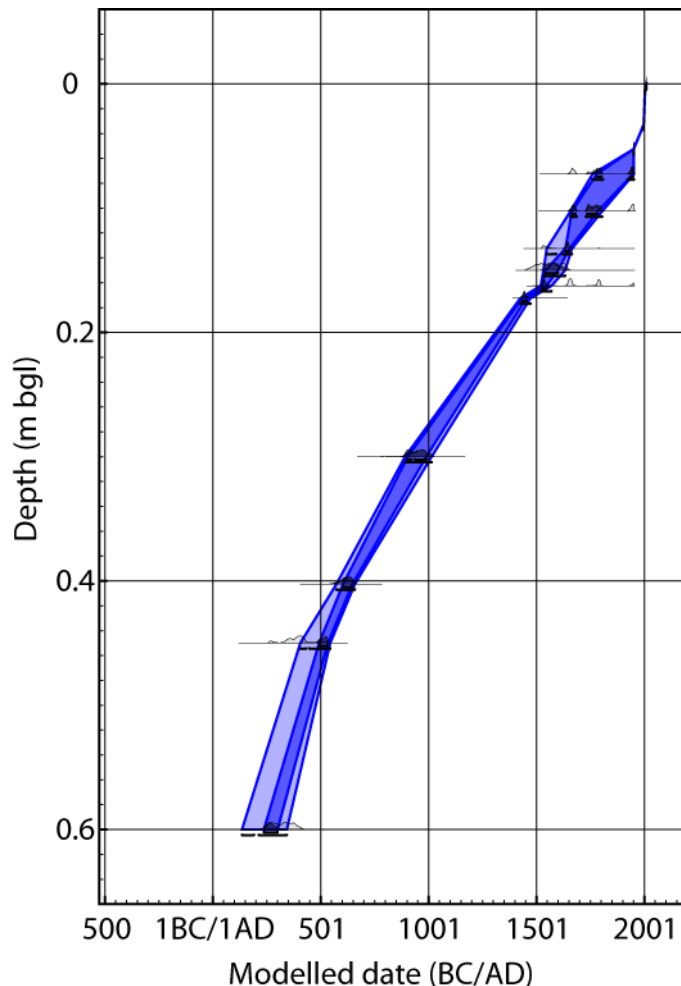


**Figure 3.7** Age-model for the middle marsh core (LA-10-2C). The dark blue line represents one sigma error and lighter blue two sigma error. Source Barlow *et al.* (unpublished data).

The middle (LA-10-2C) marsh core has an approximately linear deposition rate over the last 1500 years of  $\sim 0.3$  mm/yr, indicating that the erosive event referred to in Section 3.3 is not recorded within this succession. The deposition rate increases to  $\sim 0.8$  mm/yr in the most recent 100 years. The deposition rate between 200 to 500 AD is  $\sim 0.5$  mm/yr.

### 3.1.4 Marsh Development

It is considered that an erosive event affected the lower marsh of Loch Laxford between 1400 – 1800 AD (accurately constraining the age of the erosive event from the hiatus in deposition is difficult due to the age model being distorted by the erosive event itself). However, the middle marsh core does not display the same hiatus in radiometric dating. A conceptual model of marsh development is presented in Figure 3.8.

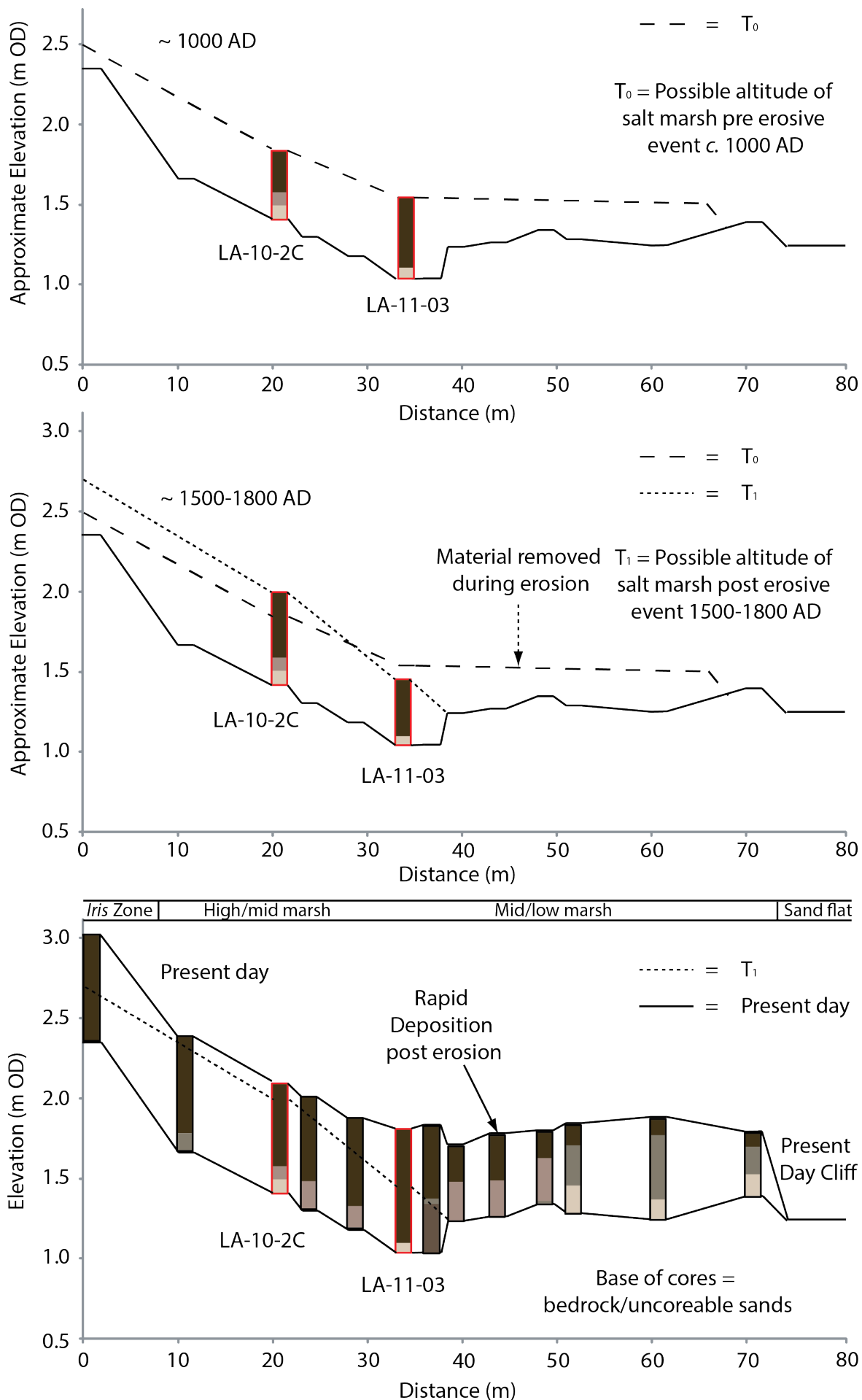


**Figure 3.8** Probable marsh development at Loch Laxford Cores analysed (LA-10-2C and LA-11-03) are highlighted in red.

Prior to the erosive event it is considered that the marsh resembled that of the present day. The stratigraphy outlined in Figure 3.5 suggests that material in the lower marsh cores (those below LA-11-03) display evidence for an erosive break. However, this is not the case in the lower marsh core (LA-11-03) dated; thus it is likely that the lower marsh core was in the transition zone between an eroded lower marsh and unaffected upper/middle marsh explaining the erosive hiatus in the chronostratigraphy that is not evident in the lithostratigraphy. The stratigraphy suggests that the middle marsh core is not affected by the erosive event and subsequent dating corroborates this. Deposition is rapid in the lower marsh after the erosive event, which is also observed in the age model prior to the erosive event, suggesting that the marsh has recovered to its previous setting. The middle marsh core displays an increased rate of deposition within the past 100 years, which is likely due to the recovery of the lower marsh altering the availability of material for deposition or changing salt marsh hydrodynamics affecting flooding frequency and duration (Allen, 2000).

### 3.1.5 Sea-level History

The nearest Holocene record of relative sea-level is obtained from a series of SLIPs and modelled data from Coigach (Figure 3.9) (Shennan *et al.*, 2000a; Shennan and Horton, 2002). Modelled relative sea-level history shows a complex pattern over the last 15 kyr (Figure 3.9) resulting from the interaction between eustatic, isostatic and local sea-level change. Within the past 10 kyr sea level has risen from ~10 m below present to ~3 m above present 3 kyr ago and has slowly been falling since.

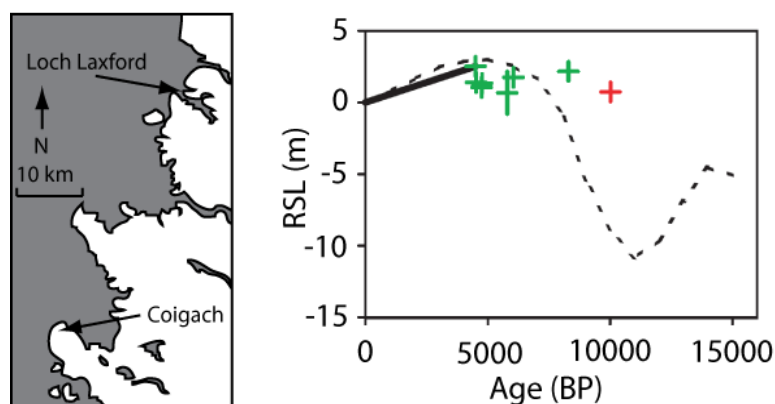


**Figure 3.9** The location in relation to Loch Laxford and relative sea-level history of nearby Coigach. Green SLIPs are intercalated index points and red are limiting dates. Figure adapted from Shennan and Horton (2002).

Bradley *et al.* (2011) have modelled the current rates of sea-level change around the British coast and predict that at present sea-level is falling at Loch Laxford by between 0.6 – 0 mm/yr.

### **3.1.6 Barlow *et al.* (unpublished data) relative sea-level history**

RSL change has been reconstructed at Loch Laxford using diatoms as a proxy for palaeo marsh surface elevation (PMSE). Preparation of diatom samples from the two cores at 0.01 - 0.02 m intervals followed standard laboratory techniques (Palmer and Abbot, 1986), with a minimum of 250 valves counted in each sample. The fossil diatom assemblages were calibrated using both local and regional modern diatom training sets and transfer functions. The local modern dataset comprised 49 samples from the tidal flat – marsh – upland transition from Loch Laxford, and the regional 215 samples from nine sites including Loch Laxford, along the western and northern coasts of Scotland (unpublished data). To allow for tidal range differences between sites in the regional dataset, the elevation of each sample in the regional training set is converted to SWLI. Two weighted averaging partial least squares (two component) transfer function models were developed in the software package C2 (Juggins, 2003), which were applied to each fossil assemblage to produce an estimate of PMSE with a bootstrapping devised root mean squared error of prediction value for each fossil sample. Two different transfer functions were used to account for the change in marsh hydrodynamics or environment as the present day marsh surface did not fully represent assemblages observed downcore. The middle marsh core (LA-10-2C) used the local transfer function for the upper 0.05 m and the lower marsh core (LA-11-03) for the top 0.10 m (which in both cores is approximately the last 100 years). The regional transfer function was applied to the remainder of both cores to produce estimates of PMSE. These values were converted to RSL by subtracting the model estimate of PMSE (m OD) from the depth of the sample (m OD) for both the middle marsh (LA-10-2C) and lower marsh (LA-11-03) core (Figure 3.10).

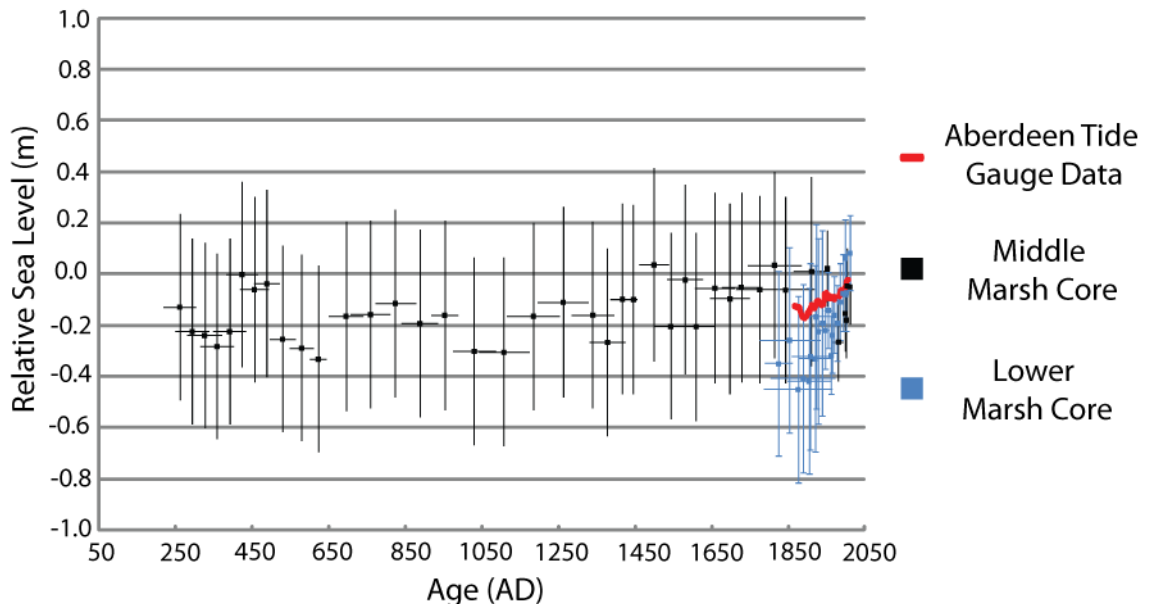


**Figure 3.10** The relative sea-level history of Loch Laxford and long term tide gauge data from Aberdeen. Source Barlow *et al.* (unpublished data).

The sea-level history is approximately constant within the last 1800 years; it is difficult to observe shorter term trends within the record due to the relatively large error bars. The nearest long term tide gauge data is from Aberdeen and displays a net increase in RSL of  $\sim 0.1$  m over the last  $\sim 150$  years (Figure 3.10). This tide gauge data fits within the error bars of the reconstructed sea level.

## 3.2 Methods

### 3.2.1 Introduction

This chapter section outlines the field and laboratory techniques, and methods used to collect appropriate data to address the issue of sediment compaction in salt marsh deposits at Loch Laxford.

### 3.2.2 Field methods

Sampling locations were levelled to a benchmark of known elevation (m OD) with a levelling staff and Quick Set Level. Altitudes are expressed with respect to OD and have a typical precision of  $\pm 0.005$  m.

High quality geotechnical samples were collected using containers of ~0.15 m diameter and ~0.3 m height, which were pushed into the ground to collect materials from the upper layer of the marsh. Samples were high quality, undisturbed ('Class 1') sediment samples (BS, 1999) (Figure 3.11). Samples were collected at ~0.10 m elevation intervals from the freshwater *Iris* zone to the sand flat, as described in Section 3.11 (Figure 3.1), and further samples were collected from the edge of the marsh. Disturbed sediment samples (~100 g) were collected from immediately around the sample (< 0.03 m distance) from the surface to provide sufficient material for subsequent testing.



**Figure 3.11** Example of Class 1 sediment sample collection.

Disturbance to samples was minimised by collecting samples using containers with bevelled edges to facilitate the ease of insertion into the ground surface. The surrounding marsh material was carefully removed before using a knife to cut any excess material away from the container and bottom of the sample. Materials with high organic contents are susceptible to disturbance during collection due to their initial porous structure, low shear strengths and high water content (Hobbs, 1986). In order to minimise disturbance and prevent shearing of the materials collected, a sharp knife was used to aid entry of the sampling containers into the ground.

Hand shear vane measurements were also taken at the same elevation as samples to measure *in situ* shear strength of surface materials. A Geonor H-60 Hand-Held Vane Tester (Figure 3.12) was used with both the 20 x 40 mm and 25.4 x 50.8 mm vanes, which cover the shear strength ranges of 0 – 100 kPa and 0 – 200 kPa respectively. For testing, the vane was pushed into the ground, slowly

rotated (~30 seconds per full rotation) and upon failure the torque (N m) was recorded. Ten measurements were taken at every sampling location to ensure a representative recording was obtained. Upon return from the field a calibration correction was applied to change the torque readings into hand shear strengths (kPa).



**Figure 3.12** Geonor H-60 hand-held shear vane tester. Testing was carried out by placing the bladed vane (left) into the ground, turning the handle and upon the sediment failure the torque measurement was recorded.

The two sediment cores used for the sea-level reconstructions were recollected with a large diameter open gouge corer. A description of lithology was recorded using the British Standards (2002) method.

After collecting surface and fossil materials, samples were immediately stored in air-tight bags or wrapped with cling film to prevent moisture loss (Brain *et al.*, 2011; 2012). Containers used to collect surface samples prevented stress relief and prevented deformation of core material (Brain *et al.*, 2011; 2012). Upon return from the field, materials were placed in a refrigerator to prevent bacterial decomposition (Brain *et al.*, 2011; 2012).

### **3.2.3 Laboratory methods**

Standard laboratory tests were undertaken using conventional methods and are referred to below in Table 3.2 and Appendix 1.



**Table 3.2** Conventional methods used for testing.

Property	Method/Source
Moisture Content, $w$	Oven dried at 110°C for 24 hours to remove moisture. BS 1337 (1990).
Loss-On-Ignition, LOI	Furnace at 550°C for four hours to combust non-carbonate organic. Heiri <i>et al.</i> (2001).
Specific Gravity, $G_s$	Small pycnometer method, BS 1377 (1990)
Void Ratio, $e$	Height of solids method. Head (1980)

### 3.2.3.1 Bulk density

The field bulk density of fossil core material (henceforth referred to as bulk density) was calculated by first cutting the cores into 0.01 m slices, before a sampler of known area (4.91 cm<sup>2</sup>) with a sharp bevelled edge was used to cut specific sections of the material (Figure 3.13).



**Figure 3.13** Sediment cores were cut into individual 0.01 m slices before using the cutter to remove a section of known volume to calculate bulk density.

These materials were weighed and bulk density (BD) calculated with equation (3.1):

$$\square\square \times \square \quad (3.1)$$

where  $m$  is the mass of the material,  $a$  is the cross-sectional area of the material and  $h$  is the height of the material. The materials used for calculation of bulk density were also used for calculation of moisture content, LOI and void ratio.



### 3.2.3.2 Particle Size Analysis (PSA)

For PSA between 1 and 10 g of material was used, depending upon the moisture and organic contents of the sample. Samples were initially digested in 20 ml of 20% hydrogen peroxide ( $\text{H}_2\text{O}_2$ ) in a water bath for a minimum of 24 hours to remove organic content. However, for the majority of samples, 100% hydrogen peroxide was required, and at times needed to be left for up to 2 weeks with hydrogen peroxide being replenished when no further gas was evolved from the sediment. Following the digestion of hydrogen peroxide, materials were washed with distilled water, centrifuged at 4,000 rpm for 4 minutes and supernatant liquid decanted. This process was repeated twice to ensure all hydrogen peroxide was removed. Finally, 20 ml of distilled water was added to the sample with 2 ml of aqueous sodium hexametaphosphate (3.3 wt %) buffered with sodium carbonate (0.7 wt %) to ensure the separation of flocculated particles. The sample was then analysed using a Coulter LS 230 laser granulometer with Polarisation Intensity Differential Scattering (PIDS). The Coulter provides highly reproducible grain size distributions between the 0.04 – 2000  $\mu\text{m}$  range. Data was then analysed using the Gradistat program (Blott and Pye, 2001).

### 3.2.3.3 Oedometer testing

Oedometers prevent horizontal strain, and thus create  $K_0$  conditions.  $K_0$  conditions are defined by the ratio of vertical and horizontal effective stresses acting upon a soil when no lateral strain is occurring (Chang *et al.*, 1977). Natural, undisturbed sedimentary systems are assumed to undergo negligible horizontal strain (Powrie, 2004) due to the vertical loading of sediment and thus an oedometer can mimic these conditions (Brain, 2006). Fixed ring, front loading oedometers were used (See Figure 2.4).

Sediment samples were placed within a cutting ring of 19 mm height and 75 mm diameter (Head, 1988). The consolidation ring prevents any lateral movement of the sample, and with porous plates being placed both above and below the sample water is able to drain from the sample in two directions (Head, 1988). Load is applied to the material by adding weight to a loading lever arm. Displacement was measured using a Linear Variable Differential Transformer (LVDT) and recorded digitally.

Samples collected for use within this thesis are identified using the system detailed in Table 3.3.

**Table 3.3** Sample identification codes.

<b>Code used</b>	LA	11 or 12 (depending upon year of collection)	1 to 18 inclusive (see Figure 3.1)	1-3 (see text for more details)
<b>Information</b>	Loch Laxford	Year	Sample number/location	Sample number within sample related to depth

Multiple samples were collected from several sampled containers to assess the implications of variable root content. Sub-surface samples were collected from 0.01 m below the sample above. Surface samples were cut cleanly at the base to ensure sub-sampling was possible.

Sample preparation for oedometer testing began by removing surface flora with scissors. The ring was lowered to collect a full sample (Figure 3.14) and exterior material was removed when it was no longer supporting the interior material (Head, 1988). A sharp knife was used to separate the sample from the remaining material and create flat surfaces on both sides.



**Figure 3.14** Example of a full sample collected within the oedometer ring.

Variable root content was present in different samples as shown in Figure 3.15; this greatly affected the time taken to prepare samples. Samples in which roots were woody and thick relative to the oedometer ring were not tested (Figure 3.15c).



**Figure 3.15** Variable root content within samples collected at different locations within the marsh. (a) shows a common root matrix observed within all locations within the marsh. (b) shows vertical roots which can potentially act as ‘pillars’ within the sediment sample. (c) shows substantial root content observed within the freshwater environment. Freshwater root content made up ~50% of the sample collected and as such were not tested.

Substantial root content has the potential to alter the compression behaviour of samples by acting as relatively high strength ‘pillars’ within an oedometer sample (Figure 3.16). Head (1988) suggests that samples with hard woody material should be avoided, as they could cause a marked reduction in compressibility and potentially cause the jamming of the loading cap. Head (1988) suggests that if these woody samples require testing then the woody material should be removed before being replaced by the surrounding material and ensuring that any holes are filled to prevent large voids in the sample.

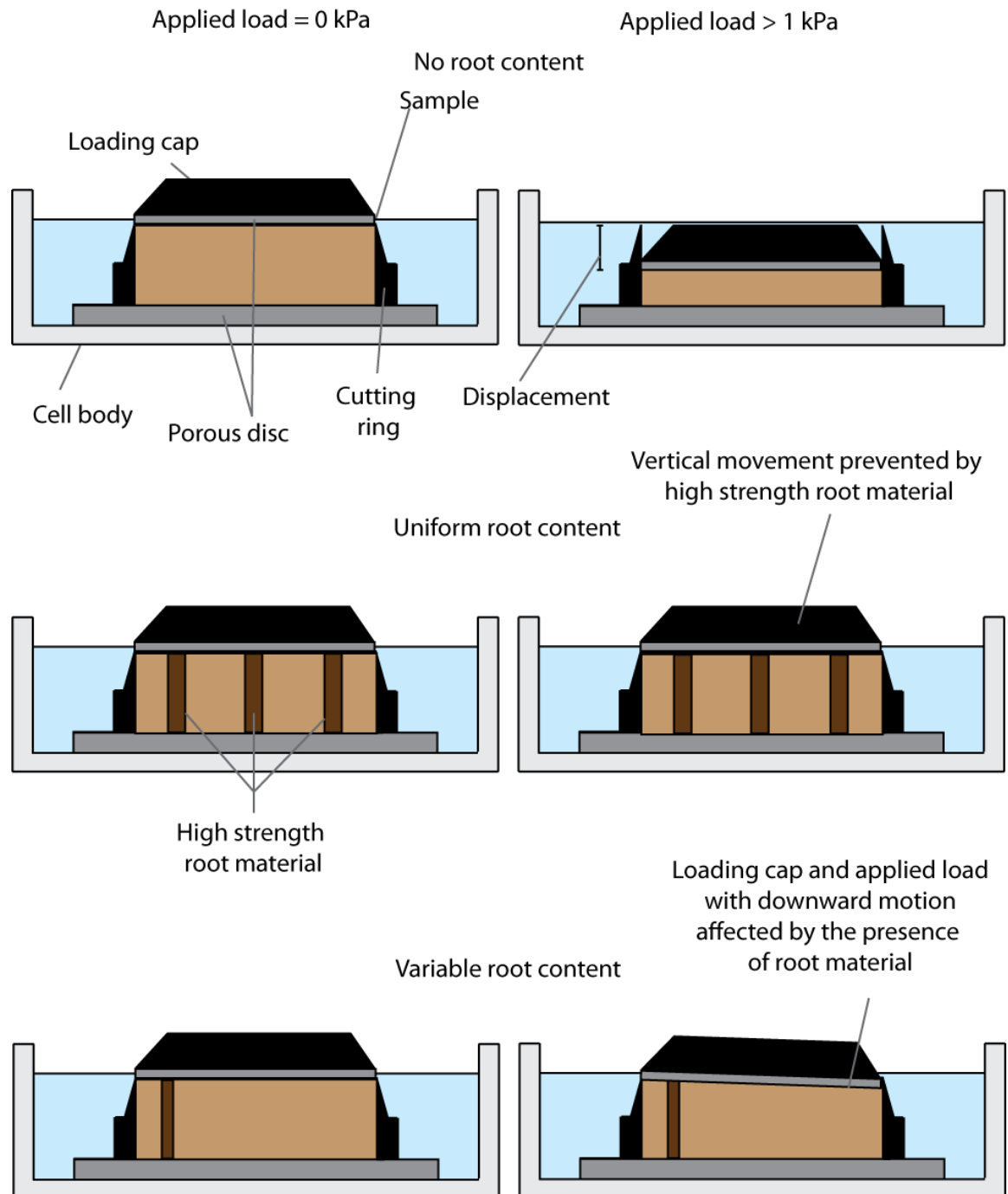


**Figure 3.16** The potential effects of oedometer loading with and without root content. The first scenario shows an oedometer sample with no root material which upon loading shows vertical displacement in a linear manner. The second scenario shows the potential impacts of having root content across the whole sample by preventing the downward motion of the oedometer. The third scenario shows the potential non-linear displacement if root content strengthens one side of an oedometer sample.

If the *in situ* compression behaviour of intertidal sediment is considered in relation to laboratory testing then removing root material is justified (Figure 3.17).

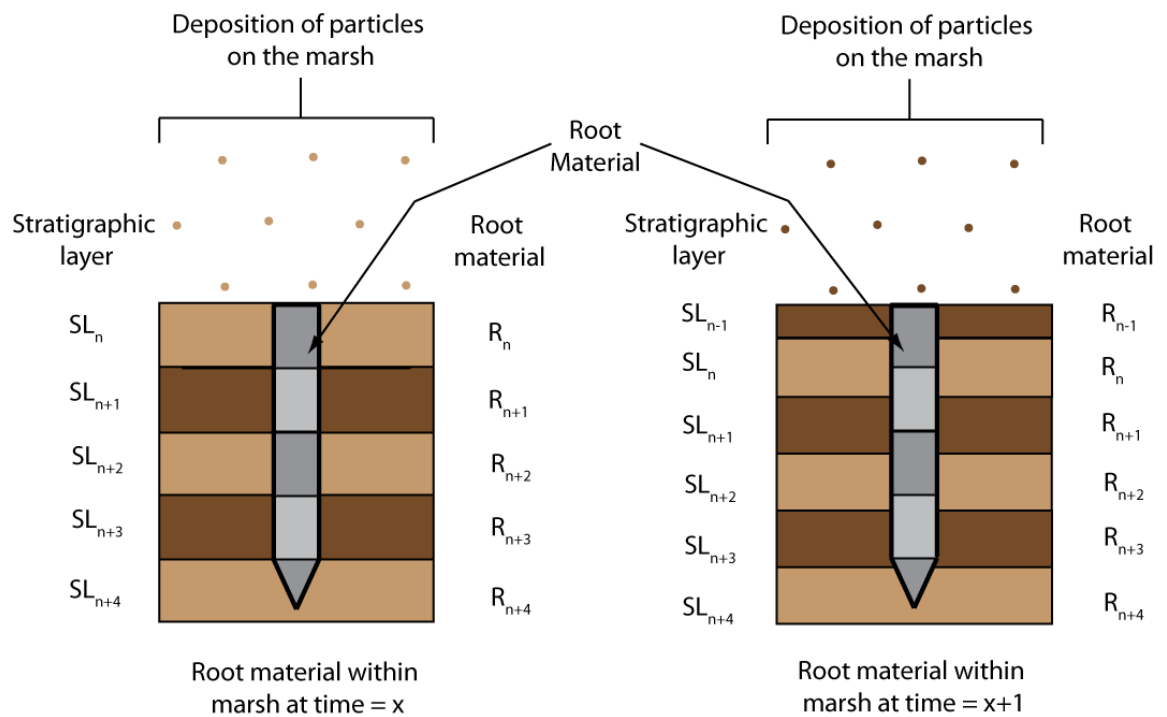


**Figure 3.17** Presence of root material within the marsh environment. Loading occurs with the deposition of individual particles upon the marsh causing an increase in effective stress and thus sediment compression. Root material is potentially stronger than the surrounding marsh sediment and thus does not compress with the small loading of particles, however, the surrounding sediment material does compress. It is considered that the difference in compression behaviour between oedometer and field loading with root content is sufficiently different to justify the removal of root material.

Loading within the marsh does not occur with the application of a loading cap but rather with the deposition of small particles or organic growth. Thus PDL is unlikely to be hindered by the presence of root material. As a result, leaving roots within oedometer samples prevents laboratory testing from replicating the volumetric reduction observed within the field. Therefore it has been deemed appropriate to remove root material from oedometer samples by slowly pulling them out of the sample with tweezers (Head, 1988). The implications of root removal and their subsequent repair is shown in Figure 3.18. Following the removal of roots any holes were filled with surrounding materials as per Hobbs (1986).

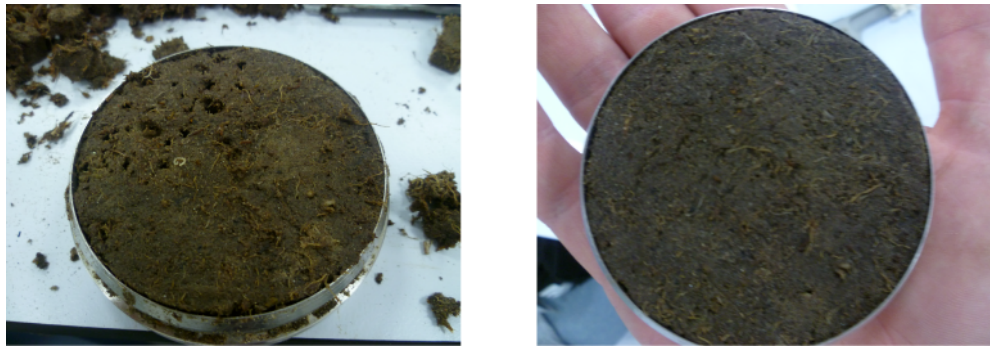


**Figure 3.18:** Root removal and then subsequent 'repair' is shown for oedometer samples.

Conventional oedometer testing uses a 2:1 loading approach whereby loads are doubled with each subsequent stage (Head, 1988). Each loading increment is applied for 24 hours (Head, 1988); however, due to the potential for organic materials to display significant secondary compression with such testing this may not be suitable for highly organic samples (MacFarlane, 1969; Hobbs, 1986; Head, 1988). Therefore, a testing strategy is required which can suitably quantify the compression behaviour of organic intertidal sediments by reducing the creep component during laboratory testing. Identification of the end of primary consolidation using graphical constructions (Casagrande, 1936; Taylor, 1942) is difficult due to the compressibility of the skeletal structure of organic materials, which results in continuously curved time-displacement curves (Figure 3.19) (MacFarlane, 1969; Hobbs, 1986; Head, 1988; Brain, 2006).

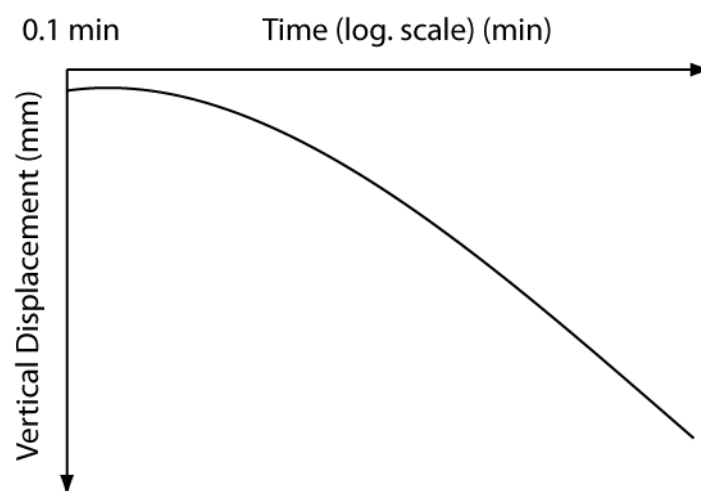


**Figure 3.19** A continuously curved time-displacement curve. These are common with highly organic materials (Hobbs, 1986; Head, 1988; Brain, 2006).

The measurement of pore water pressure can facilitate a method to identify the end of primary consolidation. Triaxial cells are available within the laboratory, though cannot fully replicate  $K_0$  conditions and therefore are not appropriate for

assessing the compression behaviour of intertidal sediments. As a result, a method was required that prevented the occurrence of secondary compression without identification of the end of primary consolidation.

Prior to exploring the options available to prevent creep during testing there were two prerequisites that were desired for testing: loading to begin at ~1 kPa to better understand compression behaviour at very low effective stresses (Brain *et al.*, 2012), and a high resolution of data at low effective stresses, to constrain the yield stress with greater accuracy and statistical confidence. A high resolution understanding of time-settlement behaviour allows more data to be collected in the stress range observed within the marsh environment (~3 kPa assuming hydrostatic conditions (see section 4.8.1)).

With these factors in mind, and the requirement to prevent secondary compression during laboratory loading, the loading approach below was undertaken. Loading increments initially began at ~0.5 kPa, however, this was very time consuming and following the testing of one sample (LA-11-GC18-1) it was increased to ~1 kPa. Reduced loading increments were continued to ~25kPa. Using very small loading increments ensures that the pore water dissipation is rapid (Leonards and Girault, 1961). Various loading periods were used; initial testing began with a period of 45 minutes and samples were later loaded for between 3 - 10 minutes. Ng and Eischens (1983) report that primary consolidation can occur within 1 minute for applied loads of 23.9 kPa on highly organic sediments (LOI = ~70 – 85%). Therefore with the low loading ratios used, 1 minute loading was deemed appropriate to ensure the dissipation of pore water pressure. During the exploratory approach various loading approaches were used before 25 kPa these are outlined in Table 3.4.

**Table 3.4** Pre-25 kPa stress loading strategies used for each sample.

Loading Strategy Pre-Yield Stress	Samples	
	LA-11-GC	LA-12-GC
One minute loading	4-1, 5-1, 6-1, 7-1, 8-1, 9-1, 10-1, 11-1, 14-2, 15-1	1-1, 3-1, 4-1, 6-1, 7-1
Short term loading (3-10 mins)	12-1, 13-1, 14-1, 13-2	-
45 minute loading	9-1, 16-1, 17-1, 18-1, 9-2 16-2, 16-3, 17-2, 17-3	-
24 hour loading	15-2	-

At stresses greater than 25 kPa the loading ratio was increased. Initially the loading duration was kept at 1 minute for the increased loading stages, however, it was found that this did not enable full pore water dissipation and as a result changes were made to the loading strategy. It was decided that fewer loads would be applied for later stages (as such a high-resolution of data is not required), but would be applied for greater lengths of time. Loading at effective stresses greater than 25 kPa, used a loading pattern of 49, 196 and 784 kPa. Loads of 49 and 196 kPa were left for approximately 1 hour and 3 hours, respectively before the final load being applied for a minimum of 24 hours.

### 3.2.4 Change point Regression Modelling

Following laboratory testing  $e \log \sigma'$  curves were analysed using the change point regression modelling software used by Brain *et al.* (2012) (Carlin *et al.*, 1992; Lunn *et al.*, 2000; Parnell, 2005). This enabled values of  $C_r$ ,  $C_c$ ,  $e_1$  and  $\sigma'_y$  to be calculated.

### 3.3 Summary

These two chapter sections (3.1 and 3.2) have looked at the field site and methods used within this thesis. Loch Laxford is located in northwest Scotland and is used as part of the 'North Atlantic sea-level change and climate in the last 500 years' project. The protected inlet Tràigh Bad na Bàighe contains an embayment marsh within which two sediment successions have been used to provide a



reconstruction of relative sea level over the last 2000 years. The site offers a location where surface materials can be gathered which can potentially help to develop the regression models used within BR1. The core materials used in the Barlow and Long (unpublished data) offer the potential to decompact a sea-level reconstruction. The model developed is then considered in reference to the middle marsh (LA-10-2C) and lower marsh (LA-11-03) cores collected (Figure 3.1) in Chapters 5 and 6.

The methods used within this thesis are derived from different fields, many of which are common to sea-level studies but also from geotechnical soil mechanics. Many of the tests undertaken use conventional methods, however, adaptations have had to be made to oedometer testing in order to account for the compressibility of peat. The data collected with these methods are presented and discussed in the following chapters.

## **Chapter 4 Results**

### **4.1 Introduction**

This chapter presents the results (all data in Appendix 2) collected using the methods described in Section 3.2.3.3. Physical and geotechnical properties of surface materials are described against elevation (m OD) and key compression variables are described in relation to the controlling variable as outlined by Brain *et al.* (2012) (compression variables are plotted and described against elevation in Appendix 2). Fossil materials are described against their depth below ground level (m bgl). The sample naming convention is explained in Table 3.3.

### **4.2 Contemporary Surface**

#### **4.2.1 LOI**

LOI variations for surface materials from this research and Barlow *et al.* (unpublished data pers. comm.) are displayed against elevation (Figure 4.1). A repeat measurement (4 times) of LOI for samples used for oedometer testing allows calculation of the standard deviation (S.D.) for these materials. Both datasets exhibit increased organic content up marsh. LOI values are lowest (<20%) in sand flat environments and the cliff at the lowest extent of the salt marsh (<1.50 m OD). LOI increases abruptly from 20 to 50% between 1.50 and 1.60 m OD, where the cliff levels out to the salt marsh. Above 1.60 m OD LOI values increase to a peak value of ~90% at 3.00 m OD. Variability is small (~1% S.D.) in the high and low marsh and greatest in the middle marsh. Average S.D. values for all measurements are ~3.13%.

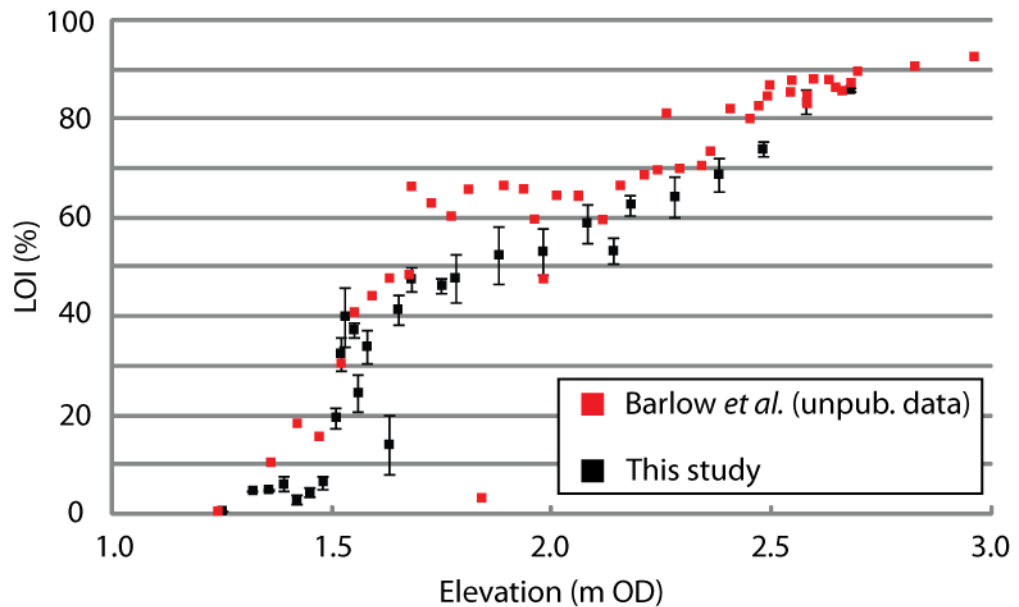


**Figure 4.1** Variations in LOI against elevation (m OD) are displayed from both this thesis and Barlow *et al.* (unpublished data pers. com.). Repeat measurements of surrounding material from the oedometer samples collected allow the calculation of the standard deviation of results.

#### 4.2.2 Moisture Content

Surface moisture content is plotted against elevation in Figure 4.2.

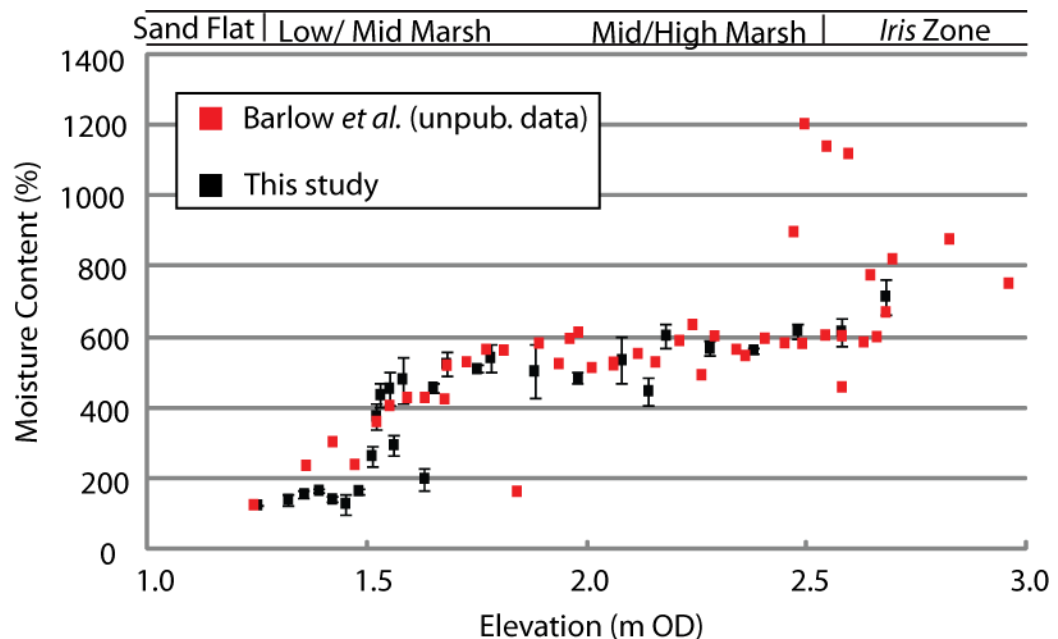


**Figure 4.2** Variations in moisture content against elevation (m OD) from both this thesis and Barlow *et al.* (unpublished data pers. comm.). Repeat measurements of surrounding material from the oedometer samples collected allow the calculation of the standard deviation of results.

Moisture contents are lowest (<300%) below 1.50 m OD (mean = 154% S.D. = 8%). Between 1.50 to 1.60 m OD, values and variability increase (150 to 600%). As elevation increases (1.57 to 2.54 m OD) moisture contents display no obvious trend, and values of moisture constants lie within the range 350 to 700%. Values

at highest elevations within the marsh between ~2.50 to 2.60 m OD have very high (> 850%) moisture contents. These samples were collected from ponded locations where micro-topography prevents drainage of surface water. Values of moisture content within the freshwater zone are higher than within the salt marsh and vary between 600 - 900 %.

#### 4.2.3 Particle Size

The particle size fractions of 15 materials from the upper marsh to sand flat are displayed in Figure 4.3.

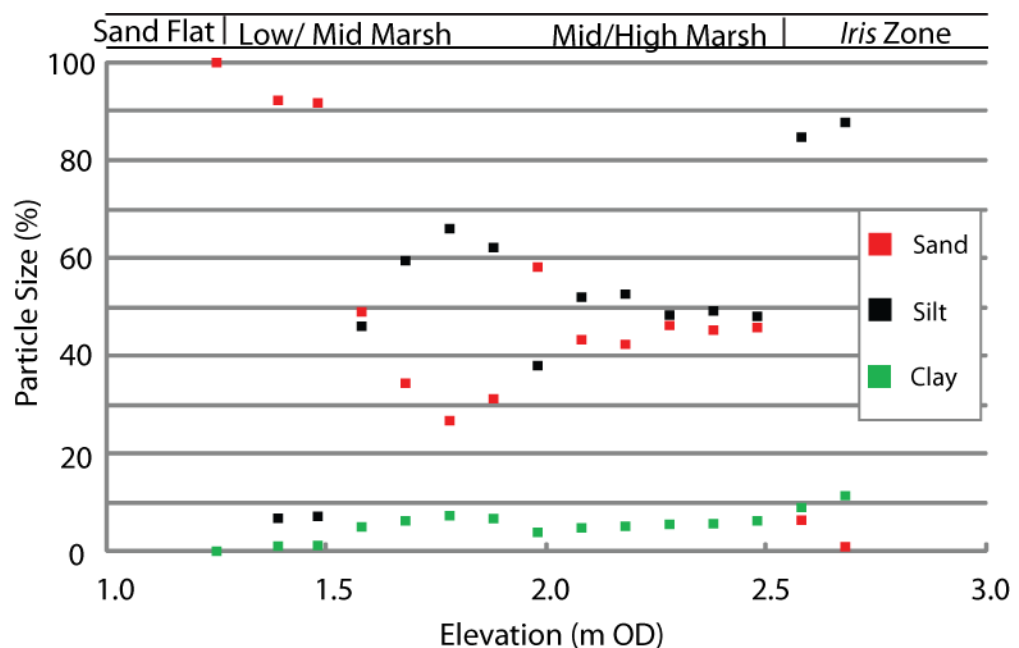


**Figure 4.3** Variations in particle size against elevation (m OD).

One sand flat sample (1.25 m OD) consists of 100% sand and the two samples from below 1.50 m OD contain >90% sand content. Sand content falls to a minima (30%) at 1.80 m OD before stabilising (50%) above 2.10 m OD and falling to a minimum (<1%) in the highest marsh. Silt content rises from 10 to 60% between 1.50 to 1.80 m OD, remains constant (~50%) between 2.10 to 2.50 m OD and increases to ~90% above 2.50 m OD. Clay content changes little throughout the marsh and reaches a maximum (11%) in the highest marsh.

### 4.3 Contemporary Physical Properties

#### 4.3.1 Description of Lithology of Surface Samples

A description of each surface sample is given in accordance with British Standards Institute (2002) (Table 4.1).

**Table 4.1** Descriptions of sample lithology.

<b>Sample</b>	<b>Lithological Description</b>
LA-11-GC4-1	Soft to firm, wet, dark brown, heterogeneous, silty fibrous PEAT
LA-11-GC5-1	Soft to firm, wet, dark brown, heterogeneous, silty fibrous PEAT
LA-11-GC6-1	Soft to firm, moist, brown, heterogeneous, silty fibrous PEAT
LA-11-GC7-1	Soft to firm, wet, dark brown with slightly orange mottling, heterogeneous, silty fibrous PEAT
LA-11-GC8-1	Soft to firm, wet, heterogeneous, brown silty fibrous PEAT
LA-11-GC9-1	Soft to firm, moist, heterogeneous, brown, silty fibrous PEAT
LA-11-GC9-2	Soft to firm, moist heterogeneous, brown, silty fibrous PEAT
LA-11-GC10-1	Soft to firm, moist, heterogeneous, dark brown, sandy fibrous PEAT
LA-11-GC11-1	Soft to firm, moist, heterogeneous, dark brown, sandy fibrous PEAT
LA-11-GC12-1	Soft to firm, wet, heterogeneous, dark brown, silty fibrous PEAT
LA-11-GC13-1	Soft, very wet, heterogeneous, brown spongy very organic sandy, coarse SILT
LA-11-GC13-2	Soft, wet, heterogeneous, brown, very organic sandy coarse SILT
LA-11-GC14-1	Soft, wet, heterogeneous, brown, very organic, sandy, coarse SILT
LA-11-GC14-2	Soft, wet, heterogeneous, brown very organic sandy very coarse SILT
LA-11-GC15-1	Very soft, wet, heterogeneous, brown, organic silty fine SAND
LA-11-GC15-2	Very soft, wet, heterogeneous, brown very organic sandy coarse SILT
LA-11-GC16-1	Soft, moist, heterogeneous, brown, slightly organic, medium to fine SAND
LA-11-GC16-2	Soft to firm, moist, heterogeneous, light brown, slightly organic, medium to fine SAND
LA-11-GC16-3	Soft to firm, moist, heterogeneous, light brown slightly organic, medium to fine SAND
LA-11-GC17-1	Soft, moist, heterogeneous, brown, slightly organic, silty, fine SAND
LA-11-GC17-2	Soft to firm, heterogeneous, light brown, slightly organic, very fine to fine SAND
LA-11-GC17-3	Soft to firm, heterogeneous, grey, slightly organic, very fine to fine SAND
LA-11-GC18-1	Loose, wet, homogenous, grey fine to medium SAND
LA-12-GC1-1	Soft to firm, moist, dark brown, silty fine SAND
LA-12-GC3-1	Soft, moist, heterogeneous, dark brown silty PEAT
LA-12-GC4-1	Soft, moist, heterogeneous, dark brown silty PEAT
LA-12-GC6-1	Soft to firm, moist homogeneous, dark brown silty fine SAND
LA-12-GC7-1	Soft to firm, moist, dark brown silty fine SAND

### 4.3.2 Bulk Density

Bulk densities decrease as elevation increases (Figure 4.4). Bulk densities are highest within the sand flat at  $\sim 2 \text{ g/cm}^3$  and decrease to  $\sim 1 \text{ g/cm}^3$  by 1.60 m OD. Above 1.60 m OD bulk densities display little variability.

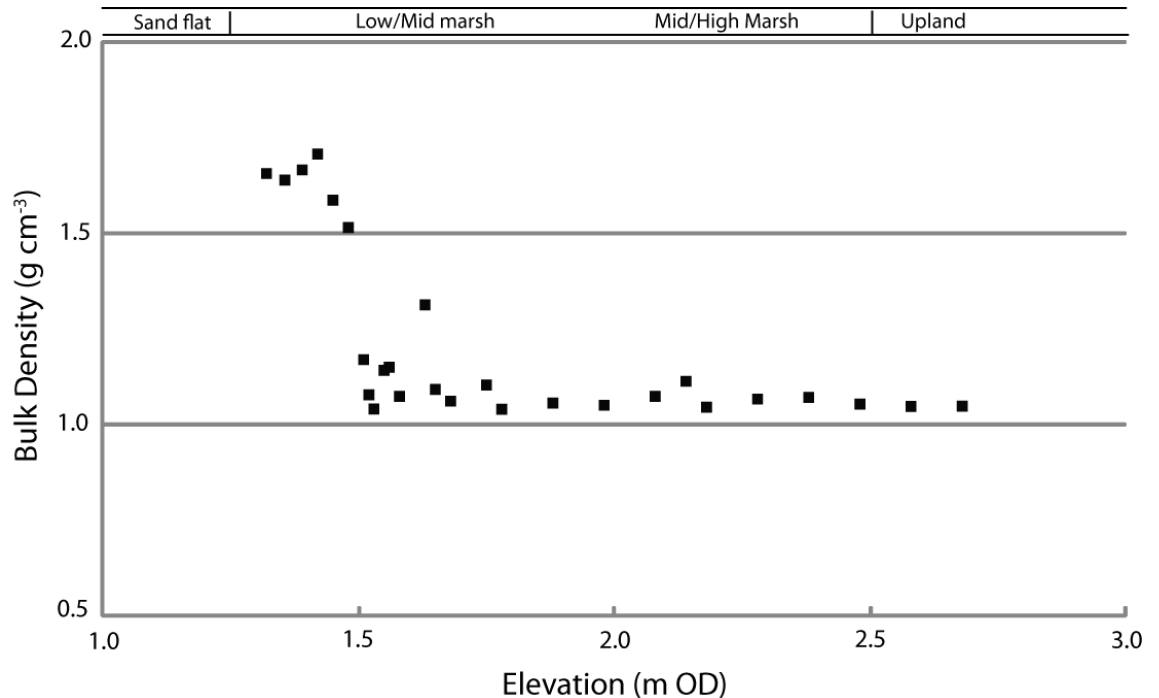


**Figure 4.4** Variations in bulk density against elevation (m OD).

### 4.3.3 Initial Void Ratio ( $e_i$ )

$e_i$  increases with increased elevation (Figure 4.5). Values are lowest in the sand flat (LA-11-GC18-1,  $e_i = 0.69$ ) and highest in the highest marsh (LA-11-GC4-1,  $e_i = 11.34$ ).  $e_i$  increases abruptly between  $\sim 1.50$  and  $1.80$  m OD from  $\sim 2$  to  $10$ . Above  $\sim 1.60$  m OD  $e_i$  varies between  $\sim 7$  and  $12$ .

## 4.4 Contemporary Geotechnical Properties

### 4.4.1 Shear Vane

Hand shear vane shear strengths of the marsh-forming sediments (Figure 4.6) vary between  $\sim 20$  and  $100 \text{ kPa}$  and generally increase up-marsh. The small dataset prevents any clear relationships being identified. However, a reduction from  $\sim 100$ - $60 \text{ kPa}$  occurs above  $2.50 \text{ m OD}$ . Values at low elevations ( $< 2.00 \text{ m OD}$ ) are largely consistent (range c.  $30$ - $50 \text{ kPa}$ ).

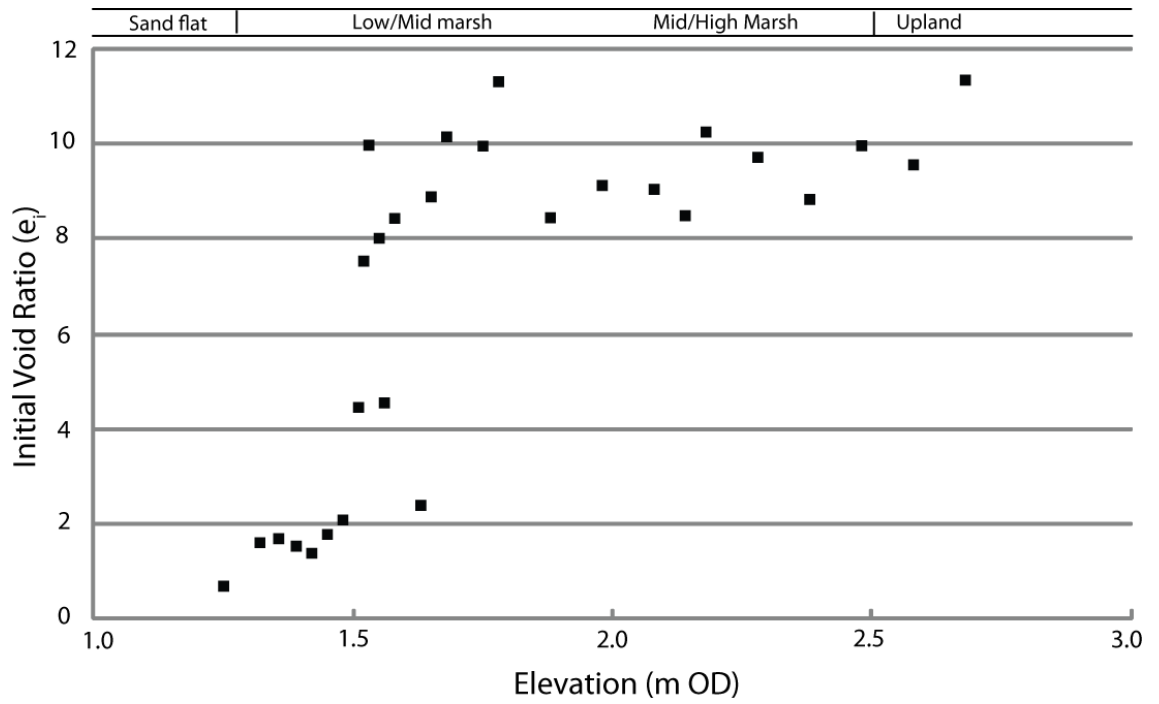


**Figure 4.5** Variations in initial void ratio against elevation (m OD).

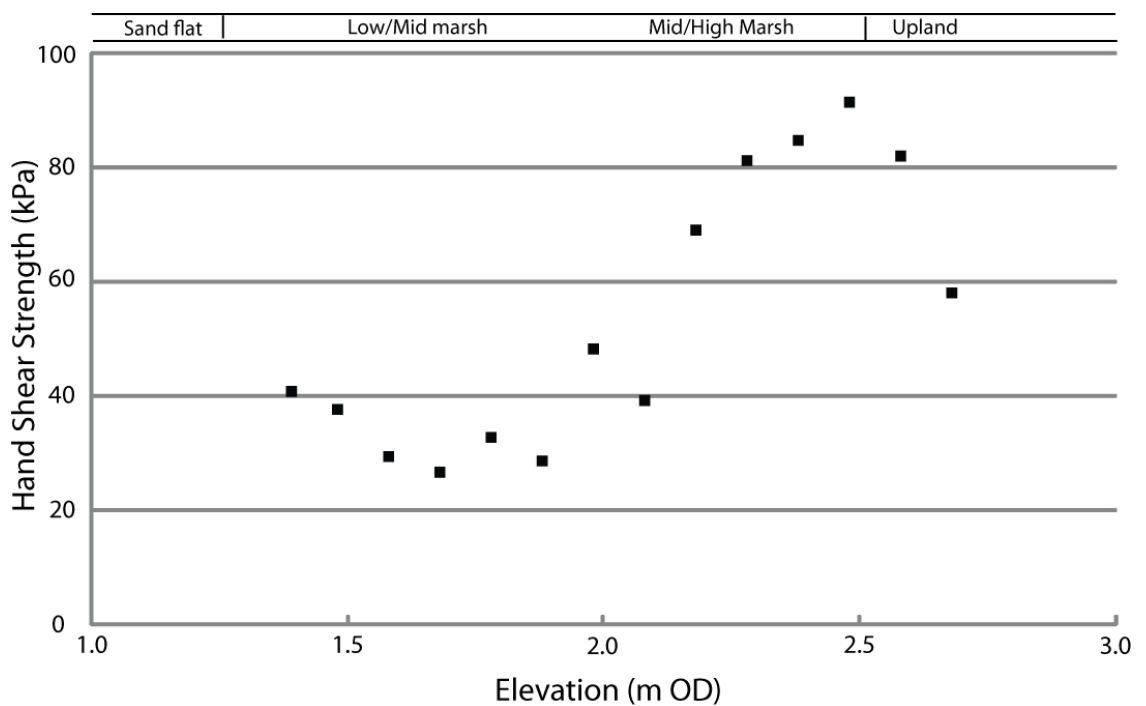


**Figure 4.6** Variations in hand shear strength (kPa) against elevation (m OD).

#### 4.4.2 Oedometer Testing Strategy

Section 3.2.3.3 outlined the oedometer testing strategy in terms of the removal of roots and loading strategy used. The results from tests investigating the effects of these factors are outlined below.

##### 4.4.2.1 Root Material

The compression behaviour of samples from the mid (LA-11-GC9-1+2, 2.18m OD) and low (LA-11-GC16-1+2, 1.48m OD) marsh with roots retained (LA-11-GC9-2 and LA-11-GC16-2) and removed (LA-11-GC9-1 and LA-11-GC16-1+3) were investigated. The compression behaviour of samples with roots removed and retained are shown in Figure 4.7 and 4.8, LA-11-GC9+16 respectively. There appears to be no clear deviation in compression behaviour between the different loading scenarios when the variability in sediment compression behaviour described by Brain *et al.* (2011; 2012) is considered.

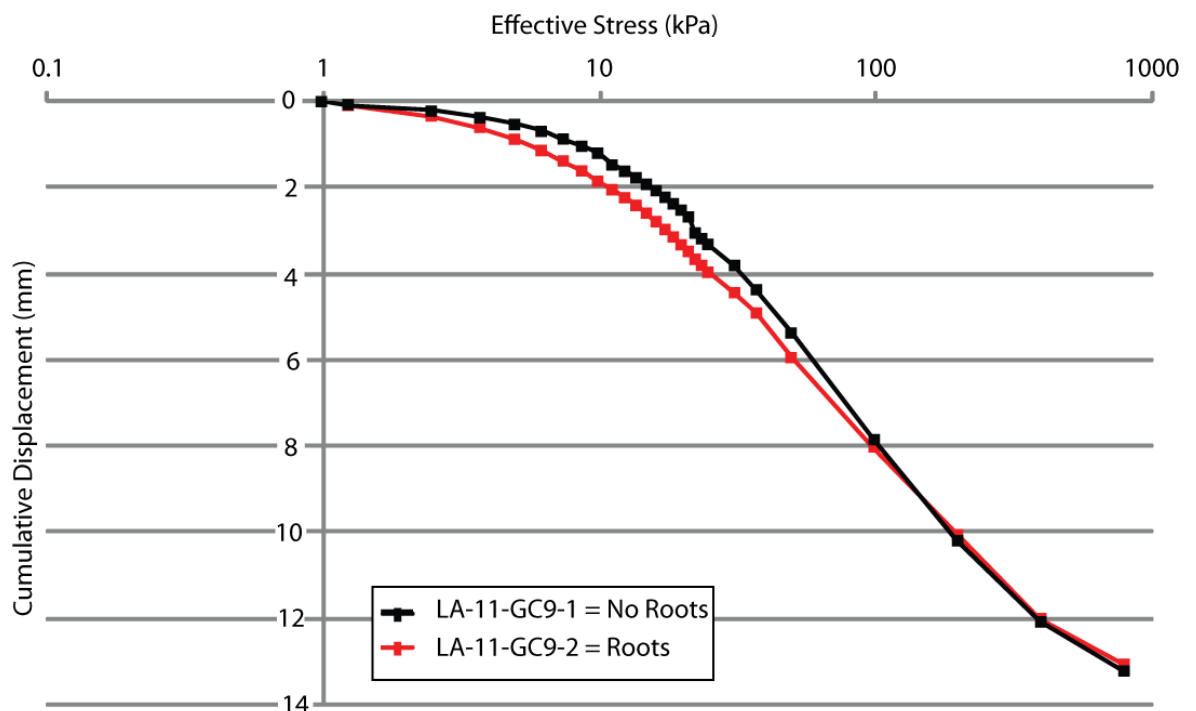


**Figure 4.7** Cumulative displacement of LA-11-GC9-1+2 following the application of various loads. There is no clear deviation in compression behaviour between the two samples.



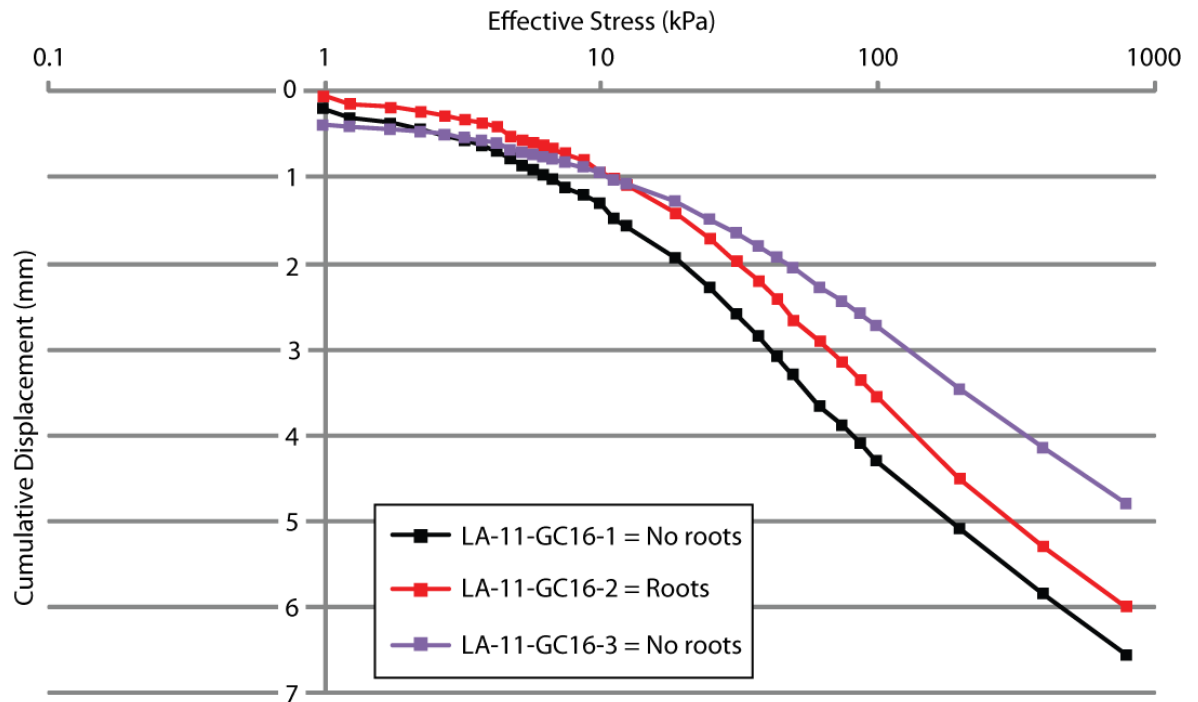


**Figure 4.8** Cumulative displacement of LA-11-GC16-1,2+3 following the application of various loads. Variability in compression curves can be explained by the variability in compression behaviour observed by Brain *et al.* (2011).

#### 4.4.2.2 Loading Strategy

The loading strategy undertaken has previously been discussed in Section 3.2.3.3. Examples of the results are displayed here. Initial testing of 45 minutes displayed time-displacement curves as displayed in Figure 4.9.

The shape of the curve suggests that pore water dissipation occurred within the first minute due to the rapid vertical displacement observed, and so shorter loading periods were used. Figure 4.10 shows the typical compression behaviour observed with subsequent 1 minute loading tests. It appears that primary consolidation takes place within the first 10 – 20 seconds, and is followed by a reduced period of secondary compression compared to 45 minute loading.

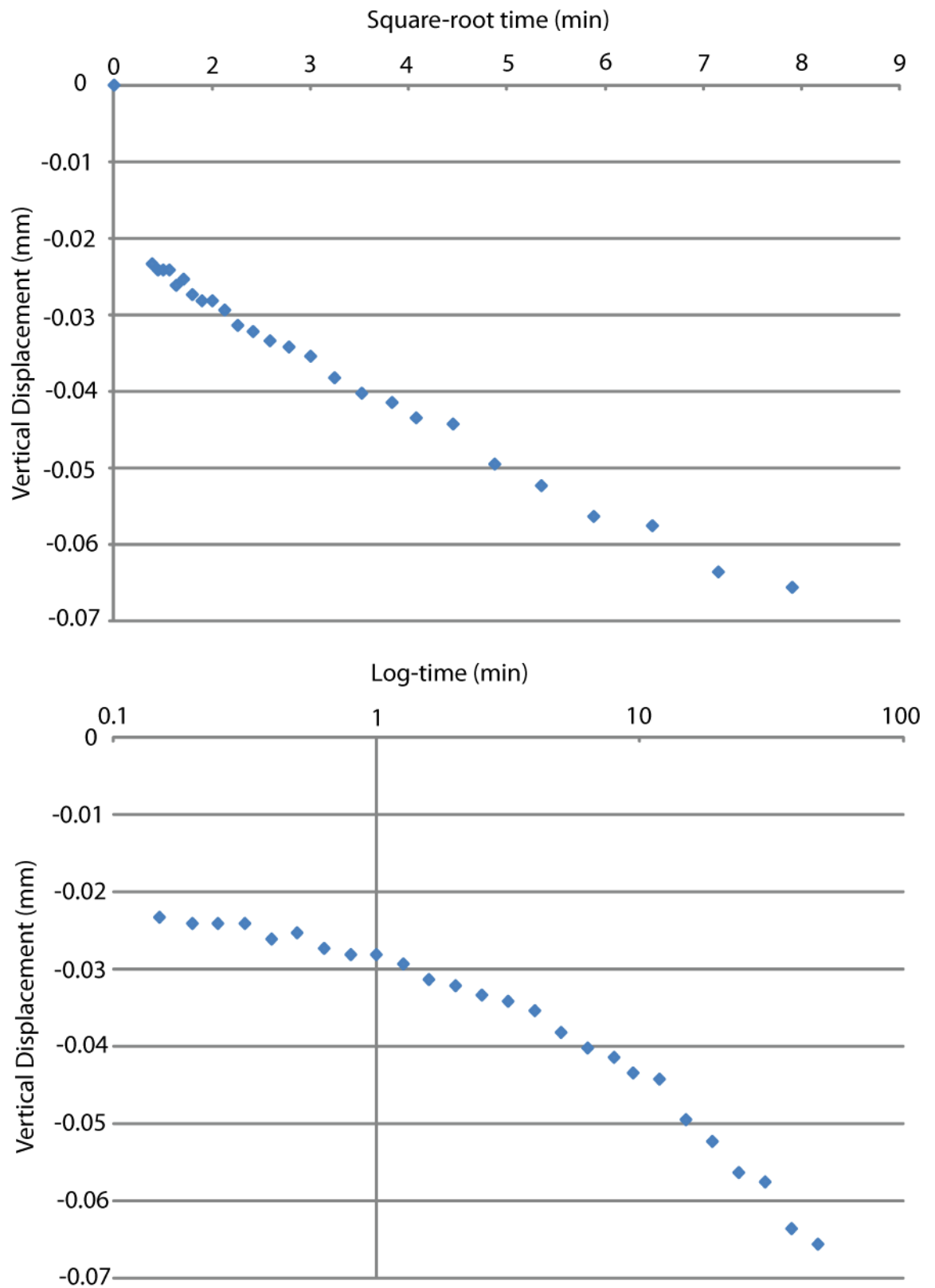


**Figure 4.9** Time-displacement curve of LA-11-GC16-1. 45 min loading of 2.7 kPa load.

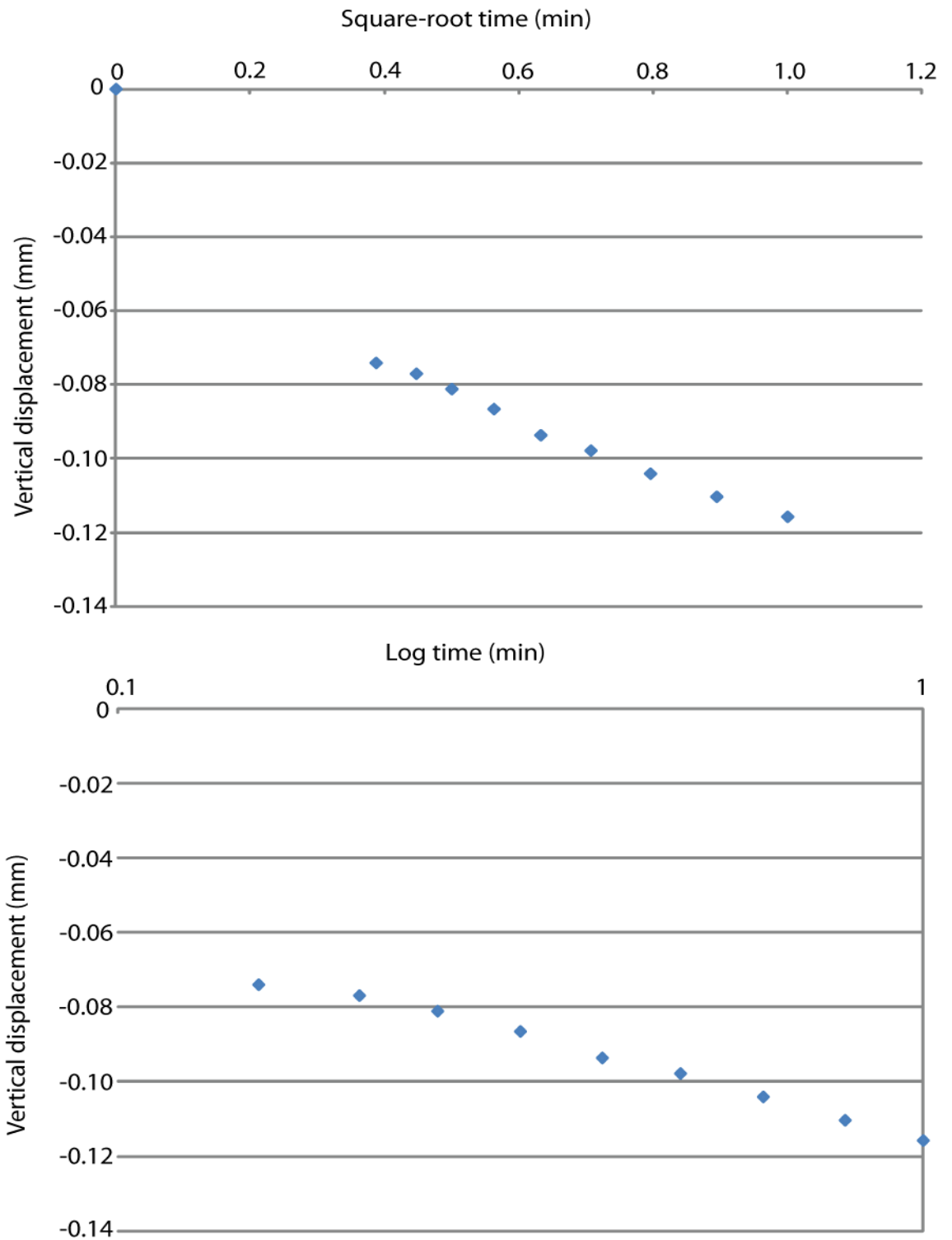


**Figure 4.10** Time displacement curve of LA-11-GC5-1. 1 min loading of 3.7 kPa load.

#### 4.4.3 Compression Behaviour

The e-log $\sigma'$  plots of all samples from Loch Laxford are shown in Figure 4.11. Materials all demonstrate both overconsolidated and normally consolidated sections. Yield stresses vary between ~5 and 30 kPa.

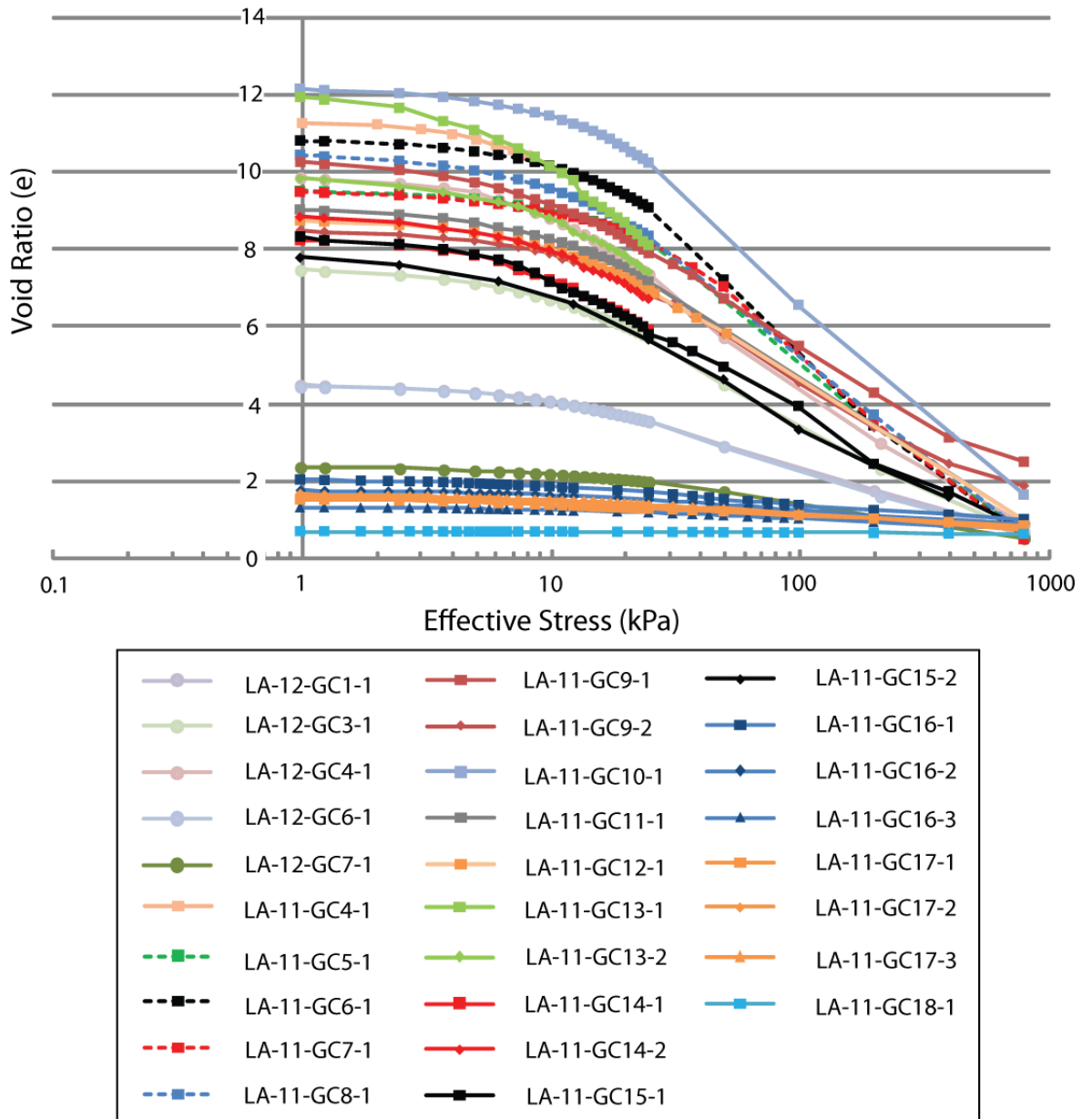


**Figure 4.11** Compression behaviour of all samples. Surface samples are followed by the suffix -1 and sub-surface samples are followed by -2 or -3 depending on the depth of the sample. Repeat measurements allowed materials with similar properties to be compared directly with compression testing. For more detail on the naming of samples see Table 3.3.

#### 4.5 Key Compression Properties of Surface Materials

The key compression variables are here described in terms of their relationship with their controlling variables ( $e_1$ ,  $C_c$ ,  $C_r$  and  $G_s$  with LOI and  $\sigma'_y$  with SWLI after Brain *et al.*, 2012) (Figure 4.12). Data from Loch Laxford are plotted with data from

Brain *et al.* (2012). It is considered that elevation and variable loading strategies exert a minimal control upon the compression behaviour (Appendix 3 and 4).

#### **4.5.1 Specific Gravity ( $G_s$ )**

Between LOI of 0 – 80%  $G_s$  reduces from a maximum of 2.65 to a minimum of 1.60 at Loch Laxford. The data collected from Loch Laxford visually shows good agreement with sites used by Brain *et al.* (2012).

#### **4.5.2 Void ratio at 1 kPa ( $e_1$ )**

$e_1$  increases from ~0 to 10 at 40% LOI. At LOI greater than 40%  $e_1$  varies between 8 to 10. Data collected from Loch Laxford within the same LOI (0 – 40%) range from Brain *et al.* (2012) shows good agreement, however, this trend does not continue at values greater than 40%.

#### **4.5.3 Compression Index ( $C_c$ )**

$C_c$  increases from 0 to 6 at ~85% LOI. Data from Brain *et al.* (2012) shows a similar relationship to that collected from Loch Laxford.

#### **4.5.4 Recompression Index ( $C_r$ )**

$C_r$  increases from 0 to 1.2 at ~85% with considerable variability. Variability increases with greater LOI.  $C_r$  does not show good agreement with data collected by Brain *et al.* (2012). The two samples collected by Brain *et al.* (2012) (from Cowpen Marsh) with increased organic content (~40% LOI) display increased  $C_r$  which show better agreement with data from Loch Laxford.

#### **4.5.5 Yield Stress ( $\sigma'_y$ )**

Maximum  $\sigma'_y$  (34.5 kPa) at Loch Laxford is observed in the sand flat (SWLI value of 73). All other values of  $\sigma'_y$  vary between 5 – 25 kPa between a SWLI range of ~75 – 105. No clear trend is observed within the Loch Laxford data. The unimodal relationship between  $\sigma'_y$  and SWLI found by Brain *et al.* (2012) is not identified within the data from Loch Laxford.

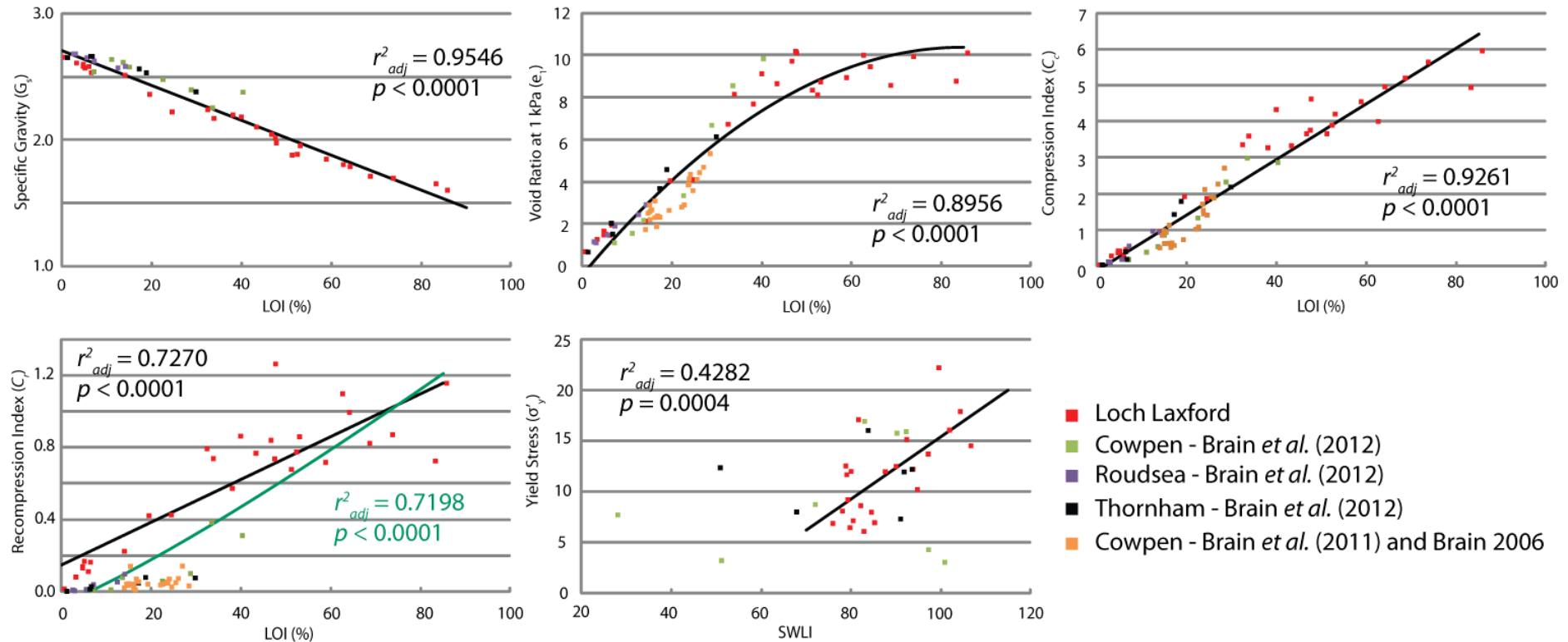


**Figure 4.12** The key compression variables against their primary controlling variables, or proxies thereof. Data from this thesis is plotted with that from Brain *et al.* (2012). Trend lines and statistical significance of each model is referred to in Chapter 5. For plots of data against elevation see Appendix 3.

## LA-10-2C

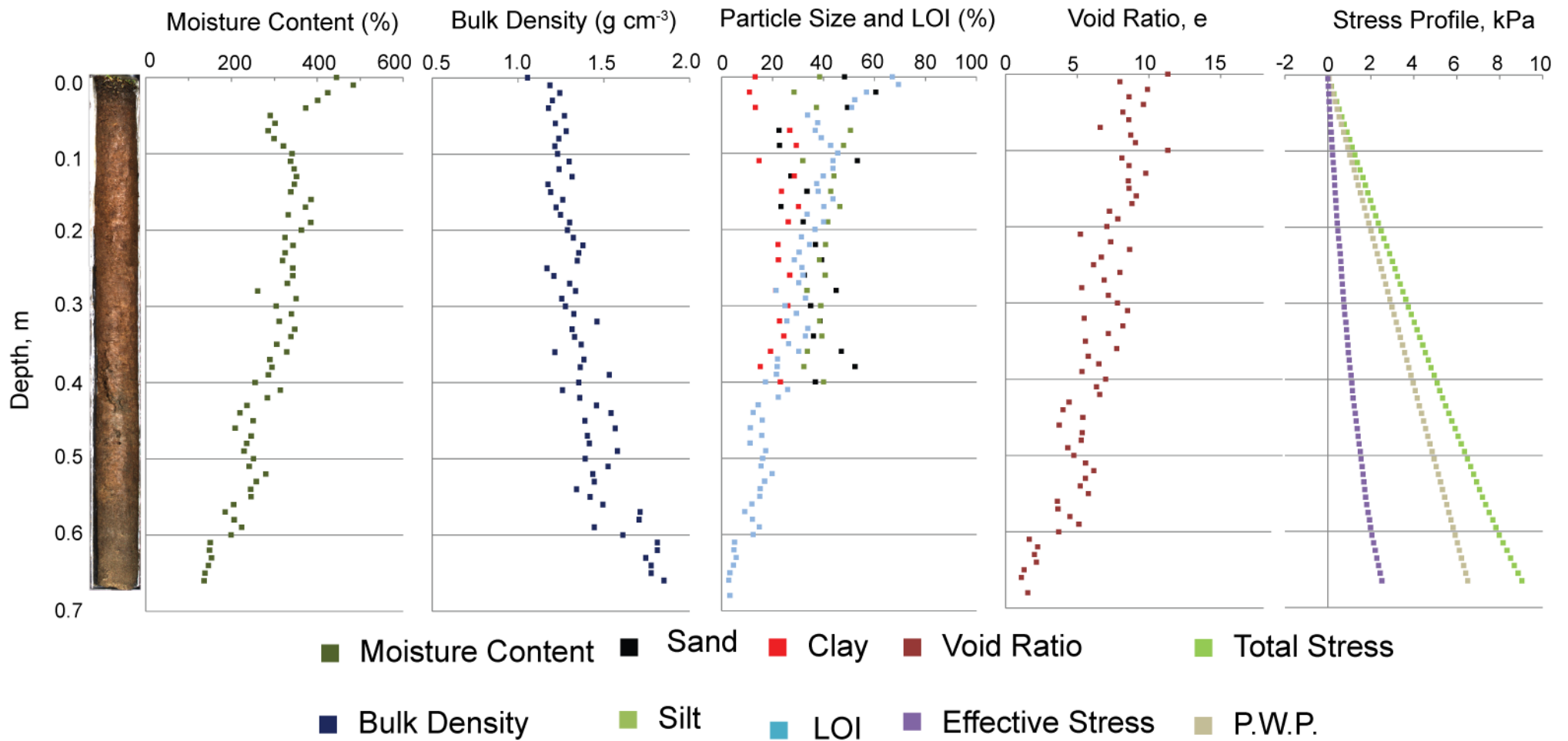


**Figure 4.13** Summary of physical and geotechnical properties from the middle marsh core (LA-10-2C).

## LA-11-03

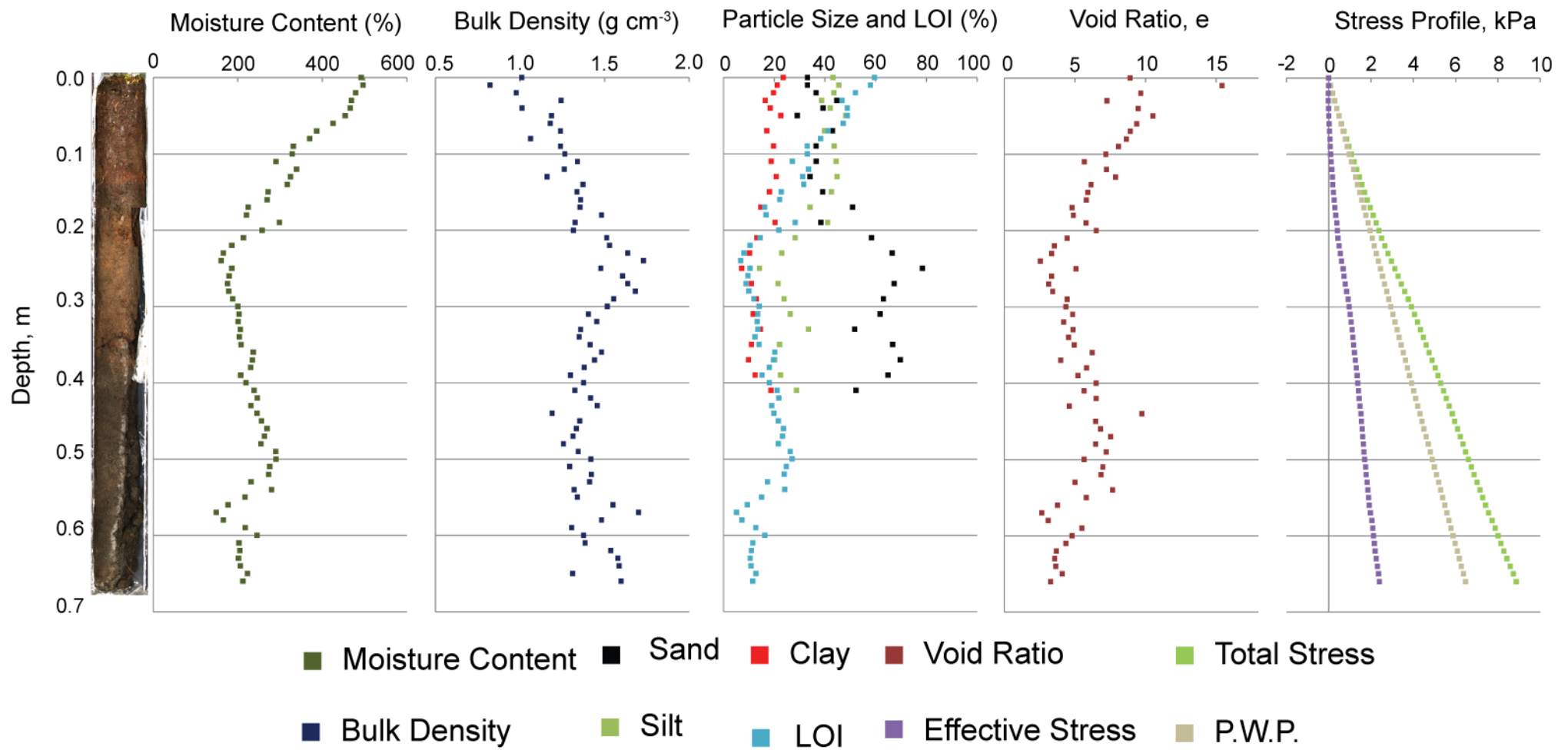


**Figure 4.14** Summary of physical and geotechnical properties from the lower marsh core (LA-11-03).



## 4.6 Core Sediments

The stratigraphy of the marsh has previously been referred to in Section 3.2 (Figure 3.5). Here the two cores used for this study and the sea-level reconstructions (LA-10-2C (middle-marsh), 2.11 m OD Figure 4.13 and LA-11-03 (low-marsh), 1.81 m OD Figure 4.14) are resampled. The middle marsh core is from 0 - 0.67 m bgl long and low marsh core is between 0 - 0.68 m bgl.

### 4.6.1 Lithological Description

A description of the lithology of the two stratigraphic successions is outlined in Table 4.2 following the convention of British Standards Institute (2002):

**Table 4.2** Description of core lithology.

Depth (m bgl)	Lithological Description – LA-10-2C Middle marsh core
0.00-0.07	Soft, wet, dark brown, silty fibrous PEAT
0.07-0.43	Soft, moist, light brown, very organic SILT
0.43-0.58	Soft, moist, brown, organic SAND
0.58-0.68	Soft to firm, grey, slightly organic silty SAND

Depth (m bgl)	Lithological Description – LA-11-03 Lower marsh core
0.00-0.11	Soft, wet, dark brown, silty fibrous PEAT
0.11-0.25	Soft, moist, brown, sandy silt fibrous PEAT
0.25-0.32	Soft, moist, light brown, organic SAND
0.32-0.63	Soft, moist, dark brown, very organic silty SAND
0.63-0.67	Soft to firm, grey slightly organic SAND

## 4.7 Core Physical Properties

### 4.7.1 Organic Content (LOI)

LOI increases up core in LA-10-2C (middle marsh) from approximately 5 to 60%. Between 0.10 m bgl to the base of the core the organic content has a linear

relationship with depth. Above 0.10m bgl there is a small fall in LOI before it increases to approximately 70% at the present surface.

LOI of LA-11-03 (lower marsh) is low at the core base (~10%), increases from 10 to 30% between 0.68 m bgl to 0.50 m bgl and then falls to 10% by 0.20 m bgl. Above 0.20 m bgl organic content increases linearly to 60%.

#### **4.7.2 Moisture Content**

The moisture content of LA-10-2C (middle marsh) increases from ~200% at the base to ~500% at the surface. Moisture contents increase linearly up to ~350% at ~0.10 m bgl before appearing to reverse slightly to ~300% between 0.10 to 0.05 m bgl.

LA-11-03 (lower marsh) moisture contents is more varied in relation to LA-10-2C. At the base of the core values are ~200% and fluctuate between ~200 to 300% until approximately 0.40 m bgl with some variability observed. Between 0.20 to 0.40 m bgl values drop to below 200% and are the lowest values of moisture content observed above the base of the core. Moisture contents begin to increase above 0.20 m bgl and increase to 500%.

#### **4.7.3 Particle Size Analysis**

The sand fraction of LA-10-2C (middle marsh) has a mean value of 37.1% though shows considerable variability (S.D. = 10.0%). Sand content reduces from ~50% at 0.40 m bgl to ~30% at 0.15 m. Between 0.05 to 0.15 m values fluctuate significantly between ~25 to 55%. The silt fraction is also broadly constant (mean = 39.0%, S.D. = 5.3%) and increased variability within the top 0.05 m. The clay fraction is largely constant between 0.05 to 0.40 m bgl (mean = 23.0%) with limited variability (S.D. = 5.0%) and falls above 0.05 m bgl (mean = 12.9%, S.D. = 1.3%).

The sand fraction of LA-11-03 (lower marsh) is considerably less variable above 0.20 m bgl (mean = 38.1%, S.D. = 5.7%) than it is below (mean = 63.8%, S.D. = 3.0%). The silt fractions are greater in the top 0.20 m bgl (mean = 42.5%, S.D. = 3.5%) than below (mean = 24.1%, S.D. = 3.0%). The clay fraction in the top 0.20 m bgl (mean = 19.4%, S.D. = 2.5%) is greater than below (mean = 12.1%, S.D. = 3.0%).

#### **4.7.4 Bulk Density**

The bulk density of LA-10-2C (middle marsh) increases with depth, increasing from  $\sim 1.20 \text{ g/cm}^3$  at the present surface to  $\sim 1.80 \text{ g/cm}^3$  at the base.

Bulk density of LA-11-03 (lower marsh) is more variable and remains constant at  $\sim 1.50 \text{ g/cm}^3$  below  $\sim 0.20 \text{ m bgl}$  and increase to  $\sim 1.00 \text{ g/cm}^3$  at the present surface.

### **4.8 Core Geotechnical Properties**

#### **4.8.1 *In Situ* Hydrostatic Stress Profile**

For the middle marsh core (LA-10-2C) all three curves (total stress, effective stress and pore water pressure) increase with depth. Total stress increases approximately linearly reaching  $\sim 9 \text{ kPa}$  at the base. Below  $0.55 \text{ m bgl}$  there is a slight increase in the rate of change of total stress with depth, which is linked to the increased bulk density of those materials.

Assuming the groundwater table is at the ground surface and hydrostatic conditions (no movement of groundwater and no seepage pressures resulting from the frictional drag of water on soil particles (Terzaghi and Peck, 1948) and no overpressuring resulting from retarded drainage (Gutierrez and Wangen, 2005)) then pore water pressure increases at a rate of  $9.81 \text{ kPa/m}$  below the piezometric surface. Effective stress increases slowly, reaching  $1 \text{ kPa}$  at  $\sim 0.40 \text{ m bgl}$  and are greatest at the base of the core ( $\sim 2.5 \text{ kPa}$ ).

The increase in total stress of the lower marsh (LA-11-03) is not linear and increases rapidly between  $0.20 \text{ m bgl}$  to  $0.30 \text{ m bgl}$ . This is linked to the increase in bulk density referred to in section 4.5.4. This causes a shift in the value of effective stresses from  $\sim 0 \text{ kPa}$  above  $0.20 \text{ m bgl}$  to suddenly increase to  $\sim 1 \text{ kPa}$  by  $0.30 \text{ m bgl}$ , before continuing to increase to  $\sim 2 \text{ kPa}$  at the base of the core.

#### **4.8.2 Void Ratio**

The void ratio profile of middle marsh core (LA-10-2C) shows a linear increasing pattern. Void ratios at the base of the core are low ( $\sim 1$ ) and increase linearly to the present surface ( $\sim 10$ ).

The void ratio profile of the lower marsh core (LA-11-03) has a lowest value of  $\sim 3$  at the base and increases to  $\sim 10$  with a maximum of  $15.4$  found at  $0.02 \text{ m bgl}$  depth. The profile does not follow the same linear pattern observed in LA-10-2C.

Void ratio increases from ~4 at the base to ~7 at 0.50 m bgl depth before falling to ~3 at 0.25 m bgl depth.

#### **4.9 Summary**

The key compression properties from Loch Laxford are plotted against their controlling variables. It is found that a similar relationship between  $e_1$ ,  $C_r$ ,  $C_c$  and  $G_s$  is identified within the same LOI range as Brain *et al.* (2012) though  $\sigma'_y$  and SWLI display a different relationship. The relationships identified are considered further in Chapter 5. Trends in the properties of the two cores are also considered. It is found that variables in LA-10-2C (middle marsh) are largely linear with increased depth with a slight deviation at ~0.05 m bgl. In LA-11-03 (lower marsh) there is a clear deviation in trends at ~0.20 – 0.30 m bgl.

## Chapter 5 Model Development & Compression Modelling

### 5.1 Model Development

#### 5.1.1 Introduction

The aim of using BR1 is to predict PDL within intertidal sediment successions. In order to do this there is a requirement to account for the variability in sediment structure and compressibility by using appropriate error terms to model the compression behaviour of materials (Brain *et al.*, 2011; 2012). BR1 uses predictive relationships that have been shown to exist between the key model parameters ( $e_1$ ,  $C_r$ ,  $C_c$ ,  $\sigma'_y$  and  $G_s$ ) and physical parameters in a probabilistic, Monte Carlo approach to account for the errors observed. These relationships are outlined in Section 2.5.4. In order to apply such an approach a detailed understanding of the errors, in terms of their magnitude and distribution, is required. Below, physical reasons are given for statistical relationships identified and their error terms are considered in order to form regression models for application in BR1. These relationships provide an alternative to time consuming geotechnical compression testing of materials from the whole stratigraphic succession.

#### 5.1.2 Regression Models

##### 5.1.2.1 Specific Gravity ( $G_s$ )

The linear relationship between LOI and  $G_s$  is statistically significant ( $r^2_{adj} = 0.96$ ,  $p < 0.0001$ ). The standard error of the regression model is small (Standard error of estimate (SE) = 0.0719) and, having passed the Shapiro-Wilk test ( $P = 0.0707$ ), the residuals display a normal distribution.

A similar negative relationship between  $G_s$  and LOI exists in freshwater bog environments (MacFarlane, 1969; Skempton and Petley, 1970; Hobbs, 1986). The  $G_s$  of inorganic material is approximately 2.7 whilst the  $G_s$  of pure peat (cellulose) is 1.4 (Hobbs, 1986; Skempton and Petley, 1970). Therefore, the relative proportions of inorganic and organic materials, as described by LOI, can give an approximation of  $G_s$  in freshwater environments.

### 5.1.2.2 Yield Stress ( $\sigma'_y$ )

The same relationship between  $\sigma'_y$  and SWLI found by Brain *et al.* (2012) is not observed at Loch Laxford. Instead  $\sigma'_y$  displays no clear trend with SWLI but large variability.

Brain *et al.* (2012) note that sand flat samples are not assessed for modelling as they are not investigated within the modelling approach. As a result samples LA-11-GC18-1, LA-11-GC16-2+3 and LA-11-GC17-2+3 have been removed from the dataset as these are either sand flat samples or sub-surface samples on the cliff at Loch Laxford which are most comparable to the sand flat. When using marsh materials only the relationship between SWLI and  $\sigma'_y$  is stronger and statistically significant ( $r^2_{adj} = 0.43$ ,  $p = 0.0004$ ). Regression model residuals passed a Shapiro-Wilk test, and so conform to a normally distributed error term (SE = 3.1949).

Even with removal of the samples described above there is a clear difference between the dataset from Loch Laxford and that of Brain *et al.* (2012).

There are two main controls upon  $\sigma'_y$ : the desiccation of surface materials due to reduced flooding of materials at greater elevations and the presence of surface biomass which retains moisture thus preventing desiccation of samples (Brain *et al.*, 2012).

The linear relationship between  $\sigma'_y$  and SWLI at Loch Laxford is identified by Brain *et al.* (2012) at lower elevations due to increased exposure. However, at Loch Laxford  $\sigma'_y$  continues to increase. At Loch Laxford, there is a limited cover of biomass on the salt marsh surface and no clear high marsh environment at higher elevations suggesting that materials could become increasingly desiccated due to increased sub-aerial exposure.

This suggests that whilst at the Brain *et al.* (2012) sites the same relationship is found between elevation and  $\sigma'_y$  this is not consistent across all marshes. Brain *et al.* (2011) have previously highlighted that changes in  $\sigma'_y$  are site specific, however, whilst this may be the case the physical reasons for changes in  $\sigma'_y$  are consistent across the four marshes. This suggests that  $\sigma'_y$  cannot be predicted within the intertidal zone without an understanding of site specific conditions, particularly an understanding of the surface biomass of the marsh, the energy of the marsh for transport of biomass and thus the tidal regime of the marsh.

### 5.1.2.3 Void ratio at 1 kPa ( $e_1$ )

$e_1$  can be predicted from LOI using a second order polynomial equation ( $r^2_{adj} = 0.90$ ,  $p < 0.0001$ ). Using a normal error distribution is a valid assumption with the data passing the Shapiro-Wilk test ( $p = 0.0553$ ,  $SE = 1.0006$ ).

Void ratios can be predicted from LOI (Brain *et al.*, 2012). It has previously been reported that freshwater peats can exhibit void ratios in excess of 20 (Hobbs, 1986; MacFarlane, 1969; Mesri and Ajlouni, 2007) which is substantially higher than those observed in Loch Laxford. Specific gravities observed are comparable to those of freshwater peats and thus suggest that moisture contents are the controlling factor preventing such high void ratios within the intertidal zone (Appendix 1). Moisture contents of freshwater peats commonly reach values of 1000% and can exceed 2000% (Hobbs, 1986) which are considerably larger than those observed within the intertidal zone (max = 795%). Freshwater peats with comparable moisture contents are found to exhibit similar void ratios to samples within the intertidal zone. However, as moisture is expelled during sediment compression it cannot be used for prediction of *in situ* variables.

It is possible that with increased  $\sigma'_y$  materials are denser and thus cause the observed reduced values of  $e_1$ . Reduced values of  $e_1$  are likely a result of site-specific conditions within the Loch Laxford intertidal zone. If  $\sigma'_y$  shows reduced values at higher elevations, as observed by Brain *et al.* (2012), then values of  $e_1$  may not reduce due to the increased presence of moisture and a reduced density due to lower  $\sigma'_y$ .

### 5.1.2.4 Recompression Index ( $C_r$ )

$C_r$  from Loch Laxford shows a linear relationship with increased LOI whilst data from Brain *et al.* (2012) shows reduced values of  $C_r$ . This is particularly evident with lower LOI (< 30%) where values of  $C_r$  increase at a much slower rate with LOI than that observed at Loch Laxford. However, Brain *et al.* (2012) do demonstrate that at increased organic contents  $C_r$  can increase to greater values which are comparable to those from Loch Laxford. Due to the different behaviour of  $C_r$  at low organic contents an inter-site relationship with organic content is difficult to determine. As a result, two regression models have been developed allowing the testing of the implications of the different  $C_r$  behaviour. This is deemed necessary as values of  $C_r$  are crucial for modelling within the intertidal zone as the majority of

intertidal stratigraphic successions will be within the stress range observed (i.e.  $< \sigma'_y$ ).

If the data from Brain *et al.* (2012) is ignored and just Loch Laxford data is considered then a linear relationship ( $r^2_{adj} = 0.73$ ,  $p < 0.0001$ ) is observed. This dataset passes the Shapiro-Wilk test ( $p = 0.1472$ ,  $SE = 0.1851$ ) and thus a normal error distribution can be used to describe the  $C_r$  errors.

A power law relationship ( $r^2_{adj} = 0.72$ ,  $p < 0.0001$ ) could be used to describe the data from both Loch Laxford and Brain *et al.* (2012), however, the equation identified does not appear to visually fit the data set and seems to over-predict  $C_r$  with lower LOI and under-predict at higher LOI. The dataset fails the Shapiro-Wilk test ( $p = 0.0084$ ) and thus residuals cannot be described by a normal distribution. Instead, a uniform error distribution is used to account for the residuals  $\pm$  half the range of observed error (0.5629).

Materials with increased LOI display increased  $C_r$  which agrees with the findings of Brain *et al.* (2011; 2012). Materials with increased organic content are likely to display more open structures which are more compressible (Brain *et al.*, 2011; 2012).

Materials do, however, display a different relationship to that found by Brain *et al.* (2012). There are two reasons which are most likely for this difference: the potential influence of secondary compression upon organic materials within the testing methods used or the difference in materials that are used in Loch Laxford compared to those used by Brain *et al.* (2012) – specifically the increased organic content, and particularly the increased fibrosity, of samples used at Loch Laxford.

Leonards and Girault (1961) report, following testing upon Mexico City clays, that by using lower loading ratios ( $\sigma/\Delta\sigma$ ) for oedometer testing the amount of secondary compression could increase as a percentage compared to the amount of primary consolidation observed. The implications of this could potentially cause increased  $C_r$  values. However, with such a short loading period used for each stage, the effects of this have been minimised as much as feasibly possible with the testing equipment available.

The organic nature of samples collected from Loch Laxford could be a potential reason for the increased values of  $C_r$  observed. Materials, even at relatively low organic contents had a significant organic matrix, which due to its compressible



nature could increase the compressibility of these lower organic content samples. High marsh samples from Cowpen Marsh (Brain *et al.*, 2012) display comparable values of  $C_r$  to those observed within Loch Laxford perhaps suggesting that increased fibrosity of marsh materials can cause increased values of  $C_r$ .

To develop a greater understanding of the controls upon  $C_r$  further work is required upon samples with similarly high organic contents, to investigate whether the compression behaviour observed at Loch Laxford is consistent across other locations.

#### **5.1.2.5 Compression Index ( $C_c$ )**

$C_c$  can be described statistically significantly ( $p < 0.00001$ ) by a linear ( $r^2_{adj} = 0.93$ ) relationship with LOI. The model fails the Shapiro-Wilk test and thus variability cannot be modelled with a normal distribution. In order to account for variability in the model a uniform error distribution is used  $\pm$  half the range of observed residuals (1.23).

A relationship between LOI and  $C_c$  is observed which is likely caused by the compressibility and open structure of organic materials (Brain *et al.*, 2012). Hobbs (1986) and Mesri *et al.* (1997) suggest that  $C_c$  of highly organic materials can be as high as 10-12. The maximum value of  $C_c$  observed within Loch Laxford is 5.95 (LA-11-GC4-1). The reason for these values being lower is most likely linked to the reduction of void ratios at higher organic contents.

#### **5.1.3 Summary of Compression Properties**

The compression properties required for the Brain *et al.* (2011) framework are predictable with simple laboratory tests from Loch Laxford; however they do display some site specific characteristics.  $e_1$ ,  $C_r$ ,  $C_c$  and  $G_s$  can be predicted with LOI whilst  $\sigma'_y$  can be predicted with elevation in the intertidal zone (SWLI). The relationships of LOI with  $C_c$  and  $G_s$  appear to be predictable across all sites using linear relationships.  $e_1$  and  $\sigma'_y$  appear to display more site specific behaviour. At Loch Laxford materials are more overconsolidated up marsh and it is likely that this causes reduced  $e_1$  values within the upper marsh. This has not been observed within the Brain *et al.* (2012) sites and thus, for future modelling work a relationship between how overconsolidated materials are and their void ratios may be required with reference to their site specific conditions. This does not affect modelling the compression behaviour of materials from Loch Laxford as

contemporary materials have been tested from the site.  $C_r$  displays a more complex relationship albeit one which is controlled by LOI; further testing may be required to gather a greater understanding of the relationship.

## **5.2 Compression Modelling**

### **5.2.1 Introduction**

Decompaction of the middle marsh succession is now undertaken using the regression models described and explained in Section 5.1. The lower marsh core is not considered in this chapter owing to the erosive event identified in the radiocarbon dating described in Section 3.3 (Figures 3.6 and 3.7). Subsequently, the impact of decompacting the middle marsh core is considered in context with the sea-level record collected from the core (Figure 3.10).

### **5.2.2 Middle Marsh Core Decompaction**

Decompaction modelling uses the same approach as BR1 (see Figure 2.6) with the regression models developed (Figure 4.12); PMSE error is also considered to account for the range of elevations identified by the sea-level reconstruction for prediction of  $\sigma'_y$ .

Firstly, the impact of using two different  $C_r$  regression models is considered by looking at the two PDL curves (Figure 5.1).

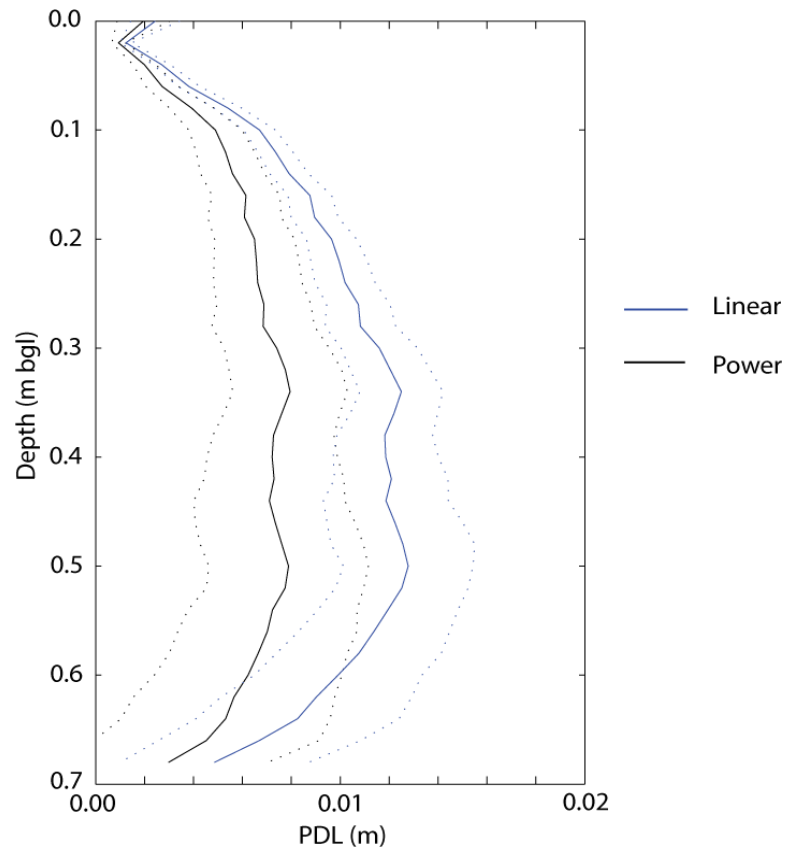


**Figure 5.1** PDL curve of using the linear and power regression model for  $C_r$ .

Both curves display the same shape though the linear model used has a greater magnitude of PDL which is expected due to greater values of predicted  $C_r$ . The differences in PDL are minimal. At their maxima  $\sim 0.35 - 0.50$  m bgl the difference is approximately 0.005 m. If the bulk densities and effective stresses (Figure 5.2) of each model run are considered then they are very similar, suggesting that the differences between the two model runs are minimal. As a result, all further model runs use the linear regression, the most parsimonious relationship, which uses only data from Loch Laxford and is thus most applicable to these sediment successions.

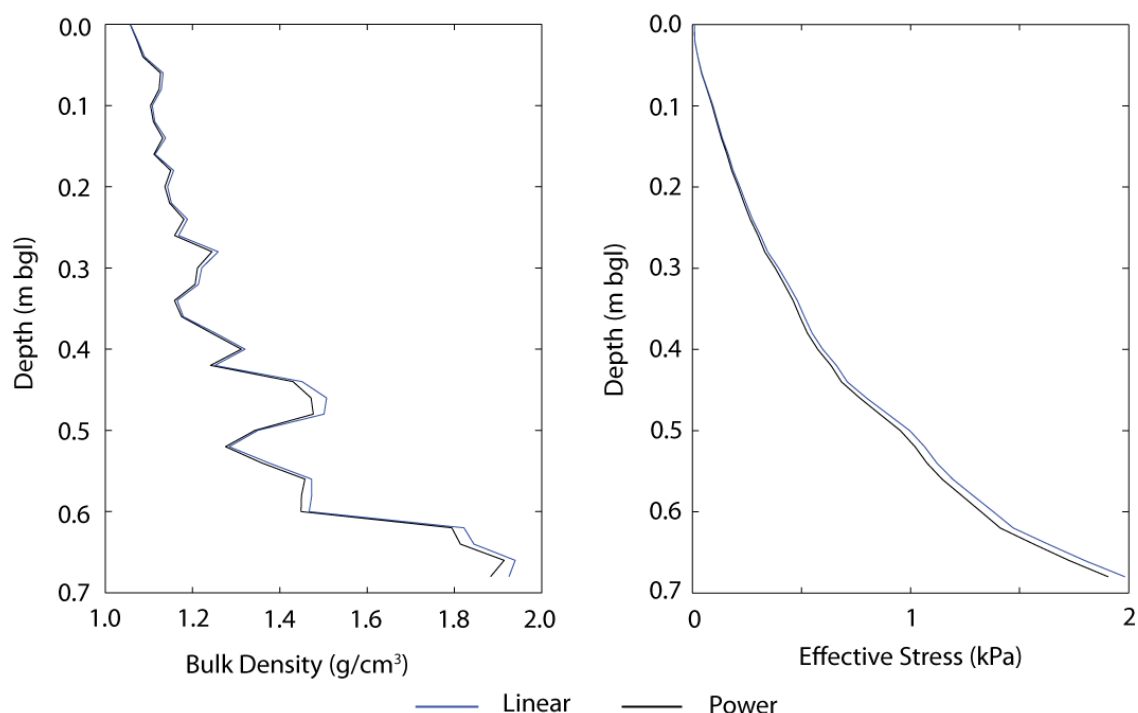


**Figure 5.2** Bulk density and effective stress profiles from the linear and power regression models for  $C_r$ .

Outputs from the linear regression model runs (bulk density, effective stress and PDL) are considered in more detail (Figure 5.3). Modelled bulk density displays an increasing trend with depth and follows an inverse relationship with LOI. Effective stresses increase to a maximum of  $\sim 2$  kPa at the base of the core. The stratigraphic succession under consideration is gradually regressive and shows a gradual reduction in LOI with increased depth (m bgl). Therefore as changes in LOI are gradual there are no sudden changes in PDL with depth. Maximum PDL is observed at just below the middle of the core and is approximately  $0.013 \pm 0.005$  m ( $2\sigma$ ) between 0.35 – 0.50 m bgl. PDL curves calculated by Brain *et al.* (2012) show that lowering is 0 m at the top of the core, this is not identified for the PDL curve calculated for the middle marsh core. An inflection is identified at 0.02 m bgl whereby PDL increases for the top layer.

At the top of the core it is likely that the inflection in the PDL curve is caused by using 0.01 kPa as a largely arbitrary value for the top layer. A value of zero cannot be used with the logarithmic modelling approach. It is applicable to use a value of 0.01 kPa for the modelling approach of minerogenic sediments (Brain *et al.*, 2012) where sediments are much denser and thus result in effective stresses being greater than 0.01 kPa in the surface layer. However, with organic materials having such open structures at the top of the core (LOI > 50%) it is possible that selecting

0.01 kPa could provide an effective stress which is larger than present in the stratigraphic succession. This is investigated within the modelling approach by varying the initial effective stress between 0.1 – 0.0001 kPa (Figure 5.4). Changing the value of the initial effective stress has a negligible effect upon layers below the top 0.02 m bgl. It is seen that with a greater initial effective stress the top layer displays a greater inflection and the lowest value (0.0001 kPa) shows a reduction in PDL. A value between 0.01 and 0.001 kPa appears to be most appropriate for the modelling of this particular succession. Whilst it is possible to identify the 'correct' initial effective stress via trial and error this would be a site specific value and would yield little information for other studies. As the impact of having such an inflection has a minimal effect upon the rest of the core the modelling approach continues to use an initial effective stress of 0.01 kPa, as in BR1.

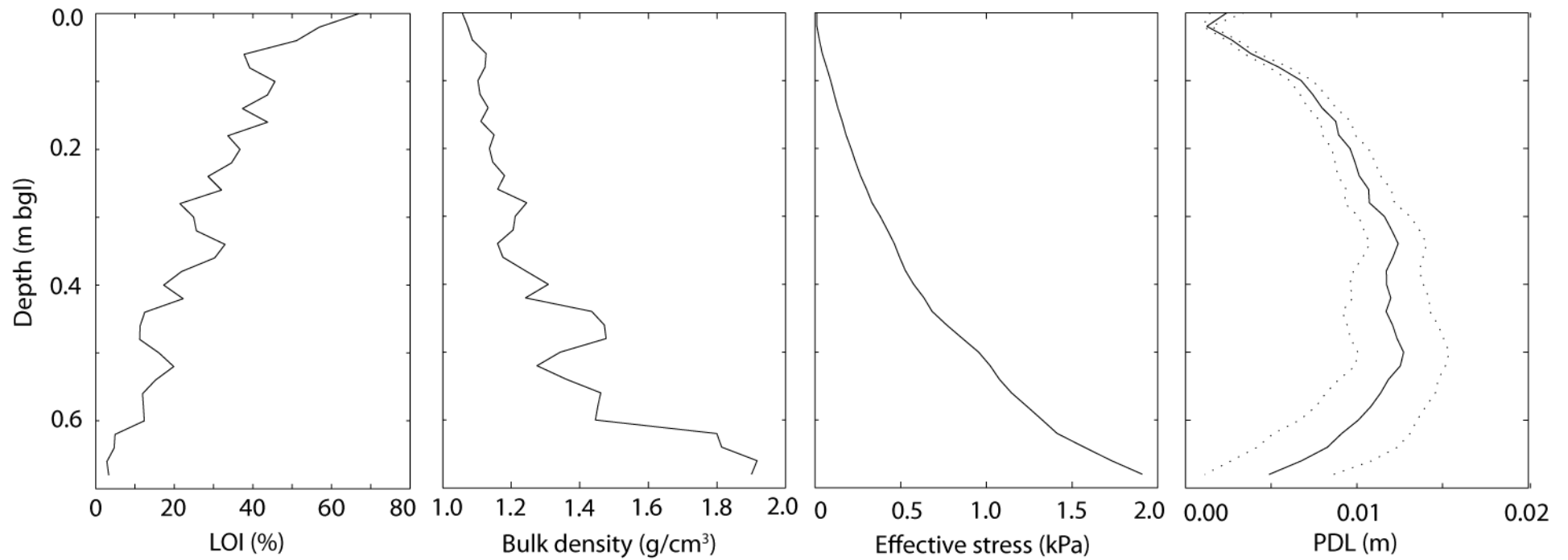


**Figure 5.3** Modelled outputs using the linear regression models.

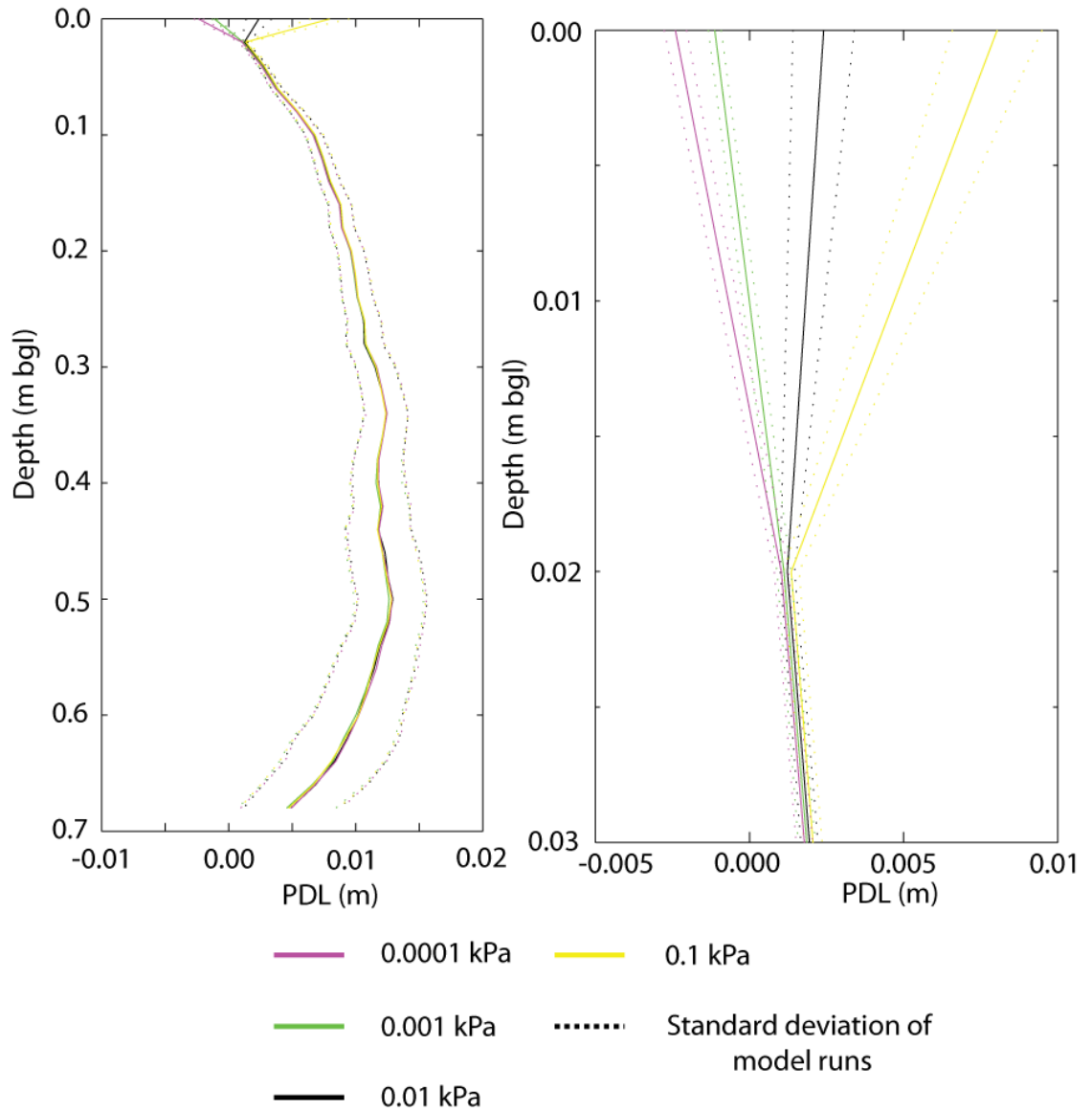


**Figure 5.4** The effects of a variable initial load is demonstrated by applying a range of values between 0.0001 – 0.1 kPa.

### 5.2.3 Middle Marsh Core Model Validation

In order to validate modelled results, modelled void ratio, bulk density and effective stress profiles are compared to observed *in situ* values (Figures 5.5, 5.6, 5.7, 5.8, 5.9 and 5.10). Residuals are calculated by subtracting the measured geotechnical and physical properties from their modelled values.

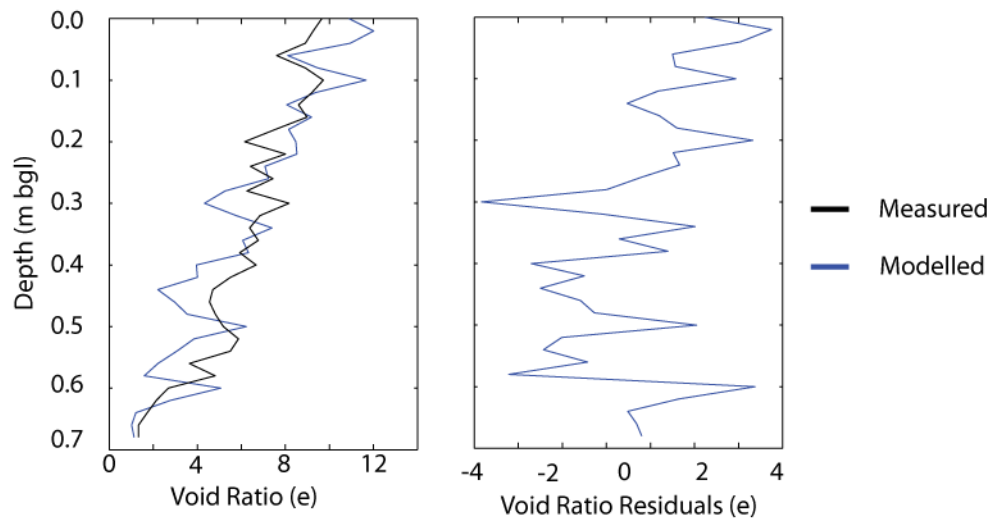


**Figure 5.5** Void ratio from modelled and measured data and their residuals.

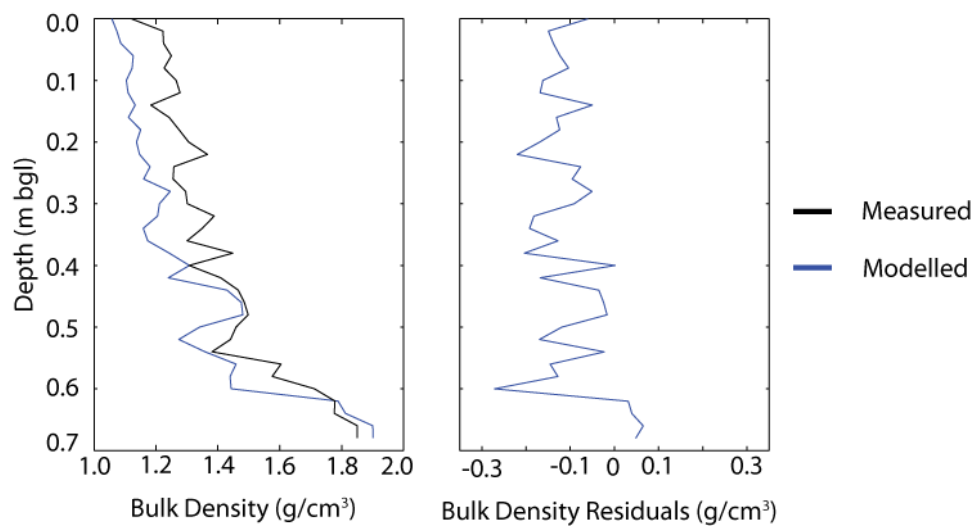


**Figure 5.6** Bulk density from modelled and measured data and the residuals.

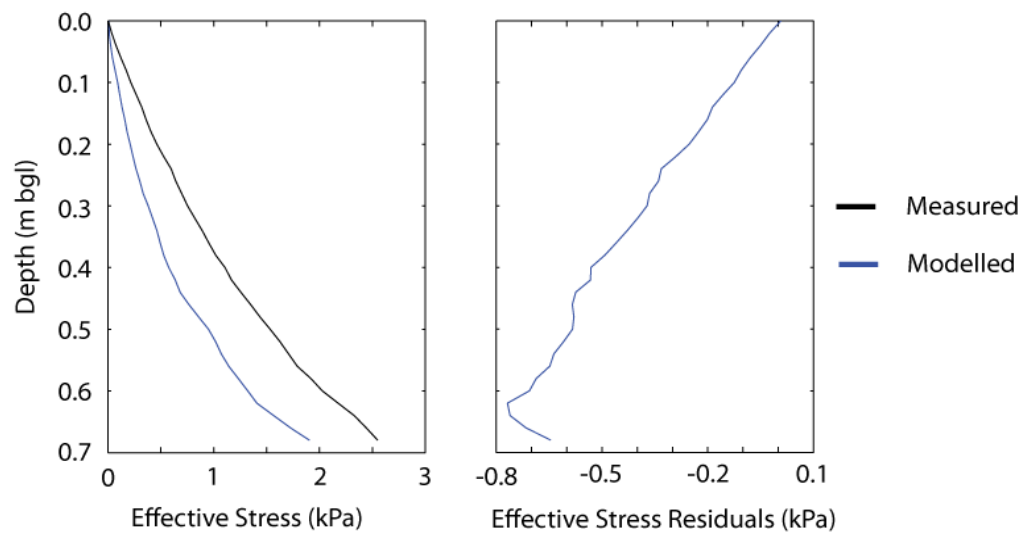


**Figure 5.7** Effective stress from modelled and measured data and their residuals.



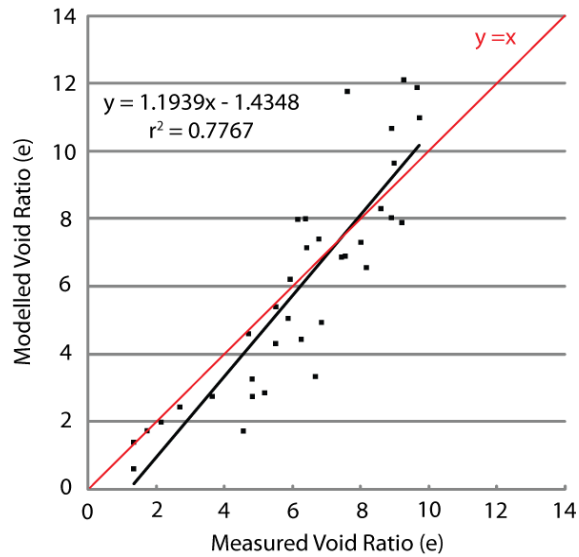


**Figure 5.8** Modelled void ratio against measured data.

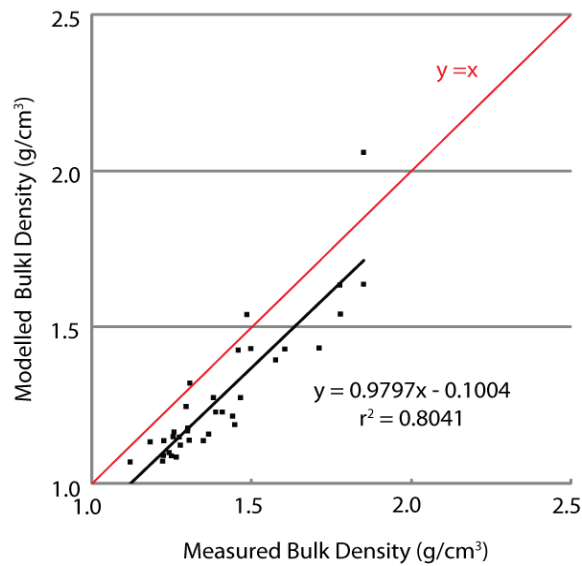


**Figure 5.9** Modelled bulk density against measured data.

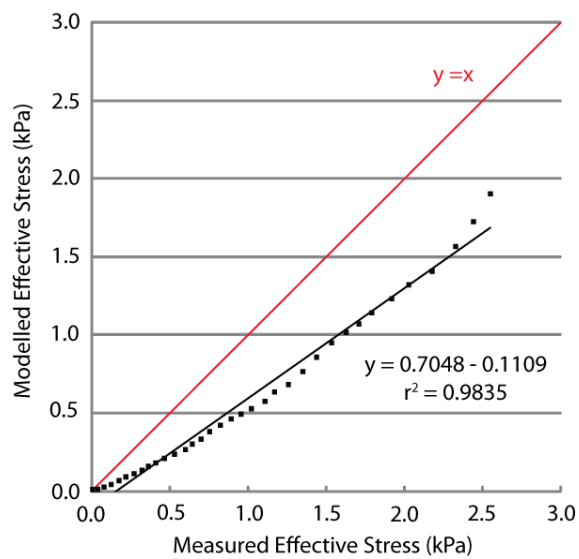


**Figure 5.10** Modelled effective stress against measured data.

Firstly the void ratio residuals are considered (Figure 5.5). There is good agreement between the modelled and measured void ratios. There is an offset between data whereby measured values are greater by an average of 0.23. When modelled void ratio is regressed against measured data (Figure 5.8) there is a strong agreement between the two datasets ( $r^2 = 0.7767$ ). Furthermore, if the equation of the line of best fit ( $y = 1.1939x - 1.4348$ ) is considered the line is very close to  $y = x$  with an offset of under 20%. It is considered that despite the minor offset in data that void ratio is predicted well by the modelled data and provides good predictions of the measured data.

Measured bulk density (Figure 5.6) shows increased variability compared to modelled values which show a gradual decreasing trend. Despite the increased variability measured values plot close to the modelled values; this is particularly true at lower depths (<0.25 m bgl). Above 0.25 m bgl measured bulk densities are consistently  $\sim 0.1 \text{ g/cm}^3$  greater than their modelled equivalents. Whilst this may appear considerable it is less than 10% of the measured values. If the modelled and measured bulk densities are regressed (Figure 5.9) then it is observed that there is a strong correlation between the two datasets ( $r^2 = 0.8041$ ). Furthermore, if the line of best fit is considered ( $y = 0.9797x - 0.1004$ ) then there is a small offset from  $y = x$ , showing there is a strong predictive capacity which, coupled with the high  $r^2$  value, indicates that the model provides good predictive power for values of bulk density.

Measured effective stresses increase with depth more quickly than modelled values (Figure 5.7). This is linked to the increased measured bulk densities described previously. Residuals increase between  $\sim 0.00 - 0.40 \text{ m bgl}$  before remaining approximately constant at elevations below 0.40 m bgl. This is quite a considerable offset between measured and modelled effective stresses (mean offset = 0.43 kPa) in the context of this core (i.e. nearly 17 % of the max value). If the modelled and measured effective stresses are regressed (Figure 5.10) then a strong correlation ( $r^2 = 0.9835$ ) is found. However, the line of best fit ( $y = 0.7048x - 0.1109$ ) does not closely follow the desired  $y = x$  relationship and suggests that modelled data is approximately 70% of the measured data. However, the probabilistic nature of BR1 enables this variability to be accounted for and thus allows a range of effective stresses to be predicted within the modelling approach.

#### 5.2.4 Middle Marsh Core Sea-Level Record

The decompacted relative sea-level record (add PDL to *in situ* RSL) from the middle marsh core at Loch Laxford is displayed alongside the compacted relative sea-level record (Figure 5.11). With a maximum PDL of  $0.013 \pm 0.005$  m there is very little impact upon the relative sea-level record and an  $r^2_{adj} = 0.9990$  is calculated between the decompacted and uncompacted records. When the errors in the sea-level record are considered then the effect of sediment compression is negligible. This corroborates the findings of Brain *et al.* (2012), who suggest that short regressive sediment successions are most conducive for preventing sediment compression in sea-level reconstructions, owing to their small downcore effective stresses.

#### 5.2.5 Summary

This chapter utilises the regression models between key compression parameters and *in situ* properties developed in Section 5.1. PDL curves are calculated for the two  $C_r$  regression models and with very little difference found it is deemed suitable to use data from just Loch Laxford as these materials are most comparable to the core. The modelled results are displayed and validated with measured data before decompacting the sea-level record from Barlow *et al.* (unpublished data pers. comm.). It is found that sediment compression has a minimal effect upon the short, regressive succession.

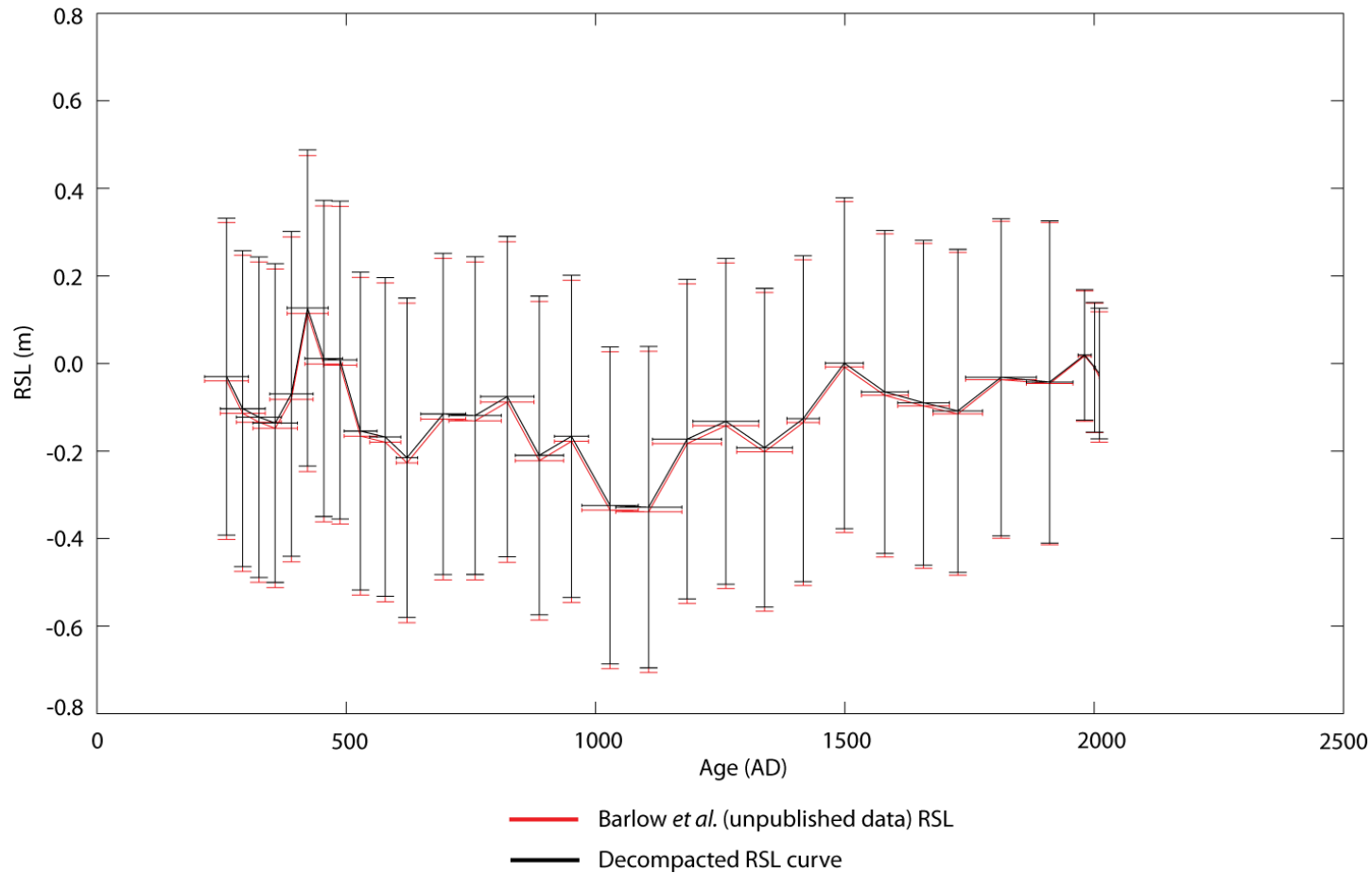


**Figure 5.11** RSL record from Barlow *et al.* (unpublished data pers. comm.) and the decompacted RSL curve. Vertical error bars represent the error in RSL whilst horizontal bars represent dating errors. Vertical errors arise from transfer function, levelling, borehole uncertainty etc. (see section 2.2). Errors from the Barlow *et al.* (unpublished data) reconstruction which are older than 1900 AD have an error of  $\sim\pm 0.37$  m. Samples younger than 1900 AD have an error of  $\sim\pm 0.15$  m. The decompacted sea-level record accounts for the amount of PDL and has a larger error term of  $\pm 0.005$  m to account for the error in predicted PDL.

## **Chapter 6 Lower Marsh Erosion and Compression**

### **6.1 Introduction**

An erosive event has been identified in the radiometric dating undertaken at Loch Laxford, in a stratigraphic succession that displayed no clear evidence of such in the bio- or litho-stratigraphy (Section 3.2 and 3.3, Figure 3.5). This chapter uses the data described in Sections 4.6, 4.7 and 4.8 to highlight the results gathered as a potential method for finding erosive events that are not easily identifiable without the use of expensive radiometric dating or detailed laboratory analysis. Finally this chapter considers the compression behaviour of the lower marsh core schematically, due to the complexities and unknowns associated with the erosive contact preventing a modelled approach.

### **6.2 Evidence of an erosive event**

An understanding of the development of a salt marsh is crucial for applying BR1 to intertidal sediments in order to ascertain whether deposition has been continuous or not. It is also an important assumption for sea-level studies where continuous records of sea-level change are desired to develop both age-models and predictions of PMSE. An erosive event only identified by high-resolution radiometric dating is an expensive problem for sea-level studies. A simple, easy and cost-effective method to identify such an erosive event would be of great benefit for future work.

It is found that geotechnical and physical laboratory tests of the core material display similar relationships with depth as the age-models (Figures 3.6, 3.7, 4.13 and 4.14). Whilst physical properties (moisture content and LOI) do deviate where the erosive event is identified, they do not do so significantly, or in a way that could clearly be a sign of an erosive event. Sudden changes in void ratio and bulk density show a more pronounced effect, and appear to be sensitive to increases in sand content in the lower marsh core. The trends of bulk density and void ratio in the middle marsh core are linear, and thus display the same trend as the radiometric dating.

An erosive event and change in deposition conditions would be expected to be picked up by measurement of the *in situ* void ratio. Materials from the sand flat or lower marsh display decreased void ratios in relation to those from the mid or

higher marsh (Brain *et al.*, 2011; 2012; Section 4.4 and 4.5). Measurements of void ratio can therefore offer an approximation of the deposition environment of a material, with greater values indicating a higher marsh deposit and lower values indicating materials of greater density from the lower marsh (Brain *et al.*, 2011; 2012). This is particularly evident in Figure 6.1 where it is shown that elevation in the marsh is predicted by void ratio statistically significantly.

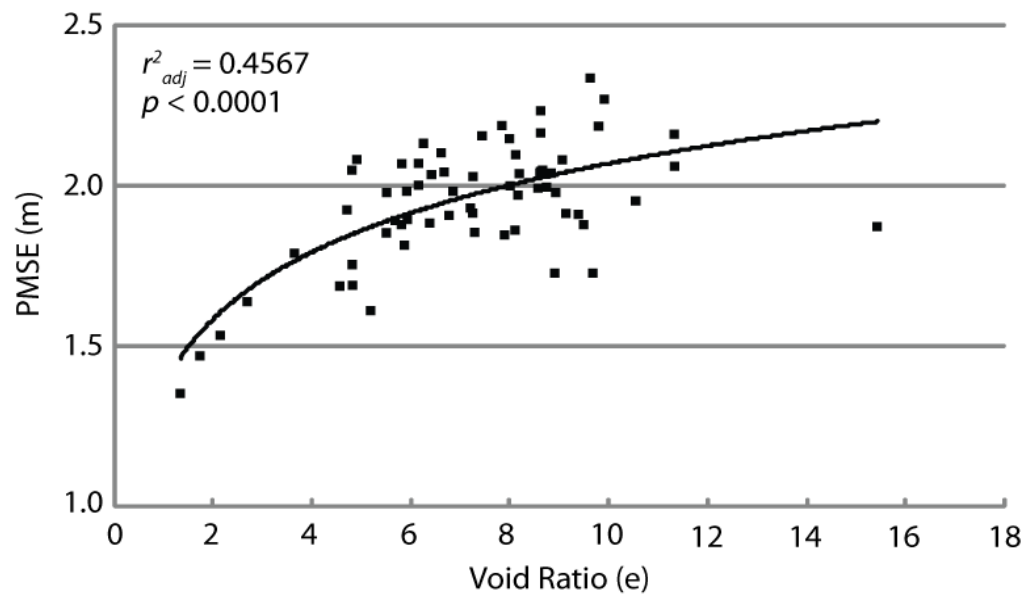


**Figure 6.1** Variations in PMSE (measured by Barlow *et al.* (unpublished data pers. comm.)) against void ratio from both the middle (LA-10-2C) and lower (LA-11-03) marsh core.

Brain *et al.* (2012) have previously suggested that LOI and bulk density data should be presented in order to address the potential for sediment compaction. These properties are useful and important properties for sediment compression but can also yield information regarding erosive events. Furthermore, calculation of the *in situ* void ratio (within the overconsolidated section of the stratigraphy where effects of sediment compression are reduced) can offer a simple, cost-effective method to identify suitable sediment successions for radiometric dating, sea-level studies and subsequent compression modelling, despite an ostensibly uniform lithostratigraphic unit.

### 6.3 Sediment Compaction

It is also pertinent to consider the implications of an erosive break in context with the compression behaviour of the succession. In the lower marsh core the erosive event means that material has been removed from the succession before being subsequently loaded again (Figure 6.2). This creates several problems within the BR1 framework. Firstly, the potential for other processes to occur during an

erosive event such as excessive desiccation of materials, results in a potential unknown in the compression behaviour. Secondly, the amount of material removed during the erosive event is also unknown. A separate approach is thus required to address the amount of material removed during the erosive event. A modelling approach has not been attempted and sediment compression is instead considered conceptually.

If it is assumed that excessive desiccation is not an issue, then PDL can likely be considered as follows (Figure 6.2). In Figure 6.2a, the sediment succession is assumed to be a continuous deposit of the material found in the bottom 0.25 m bgl of the present day lower marsh core. As these materials have a constant density a uniform PDL curve will likely be displayed. It is also likely that with these materials having a greater density than the highly organic surface materials observed at present then *in situ* effective stresses are greater than those measured at present. Subsequently material is removed due to the erosive event (Figure 6.2b). The implication for PDL is that materials will likely swell slightly (hence negative PDL), but will not return to their initial conditions due to the plastic nature of soils (Powrie, 2004). As a result these materials will become overconsolidated due to a removed sediment overburden (Head, 1988). With the deposition of present day materials (Figure 6.2c) above 0.25 m bgl effective stresses will again increase. Due to the organic nature and low densities of the materials effective stresses are unlikely to increase to the level observed prior to the erosion. Thus it is likely that with the gradual regressive succession observed then the PDL curve will be uniform in shape in the newly deposited surface materials whilst the lower, denser materials will display a reduced PDL curve as a result of their increased stability. This increased stability is a result of previous loading causing these materials to become increasingly overconsolidated.

If deposition prior to the erosive event did not occur with a continuous density but instead displayed a similarly regressive succession to present, then a similar effect to that described above will occur. Whilst materials may not be denser, they will still expose the lower materials (<0.25 m bgl) to increased effective stresses which will result in them becoming more stable compared to deposition occurring in a continuous manner (as in the middle marsh (LA-10-2C) core). Thus their PDL potential during the second loading period is reduced due to their increased stability. Furthermore, if it is considered that materials did desiccate during the

erosive event then these lower materials would become increasingly overconsolidated due to capillary suction stresses (Powrie, 2004) and thus become increasingly stable.

Of interest for the Loch Laxford sea-level reconstruction is the top 0.25 m bgl of the low marsh core above the erosive event. It is considered that materials below this, those retained during the erosive event, have likely been subjected to effective stresses due to prior loading or desiccation and have thus undergone PDL, so are more stable than materials observed in a continuous deposit. Thus it is likely that with the portion of the succession of interest being so short (0.25 m) and regressive that PDL is minimal and thus compaction effects the sediment succession minimally.

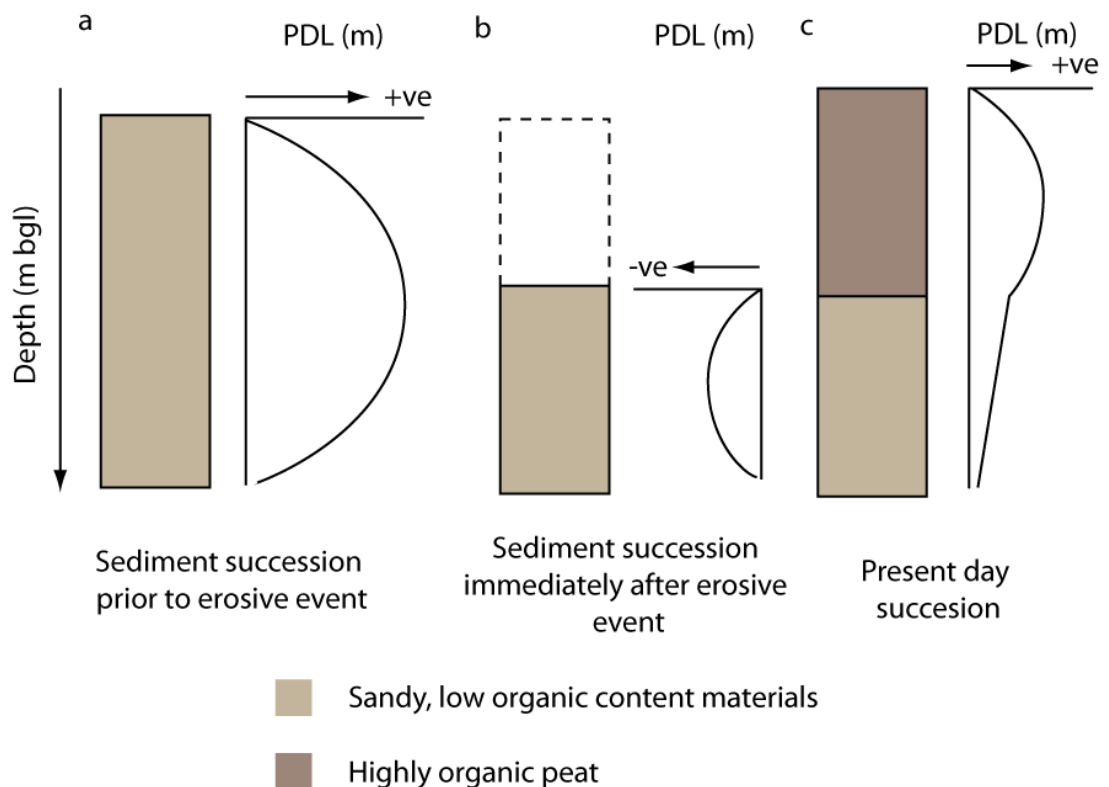


**Figure 6.2** Hypothetical PDL curves based upon the assumed lower marsh erosive event considered in Figure 3.8.

In order to model sediment compression within this succession BR1 could be used with the assumption that other processes are not an issue. However, this would require a separate model to incorporate the deposition of material prior to the erosion, the erosion of the material and subsequent deposition. This is information which is not available within the dataset collected.



## 6.5 Summary

This chapter has outlined a potential new method for identifying erosive events in a stratigraphic succession, that using regular sea-level science methods may not be easily identified until the expensive collection of radiometric dates. This could be a useful and important method for identification of such events for future sea-level studies. Furthermore, this chapter concludes by considering the compression behaviour of the lower marsh core schematically as the required precise history of the erosive event cannot be ascertained with the data collected. It is considered that the Barlow *et al.* (unpublished data, pers. comm.) record in the top 0.25 m bgl is affected minimally by sediment compression. The underlying materials will have already been compressed and potentially desiccated prior to the post-erosive deposition causing them to become increasingly overconsolidated and resistant to further compression. Thus these layers will compress minimally with the subsequent deposition of the surface layers causing very small PDL.

## Chapter 7 Discussion: Implications and Future Research

### 7.1 Introduction

The broader implications of this research, as well as areas where future research is required, are now considered.

### 7.2 New Regression Models

The regression models developed for use within BR1 are all statistically significant (Section 5.1) and by accounting for the errors, either as normal or uniform distributions, it is possible to account for the variability in compression properties. It is apparent that there are site specific variations between several properties ( $\sigma'_y$ ,  $e_1$  and  $C_r$ ) which require further testing to expand and investigate their controls.

At present, as there is no clear high marsh environment at Loch Laxford, the retention of moisture is restricted within the higher marsh which can cause increased desiccation and overconsolidation and subsequently effect  $e_1$ . This is different to the relationship identified with the marshes used by Brain *et al.* (2012) and thus a different regression model to predict  $\sigma'_y$  may be required within the intertidal zone at sites with limited AGB. Measurement of the hand shear strength of a material can potentially offer a method to predict  $\sigma'_y$  within the intertidal zone (Figure 7.1).

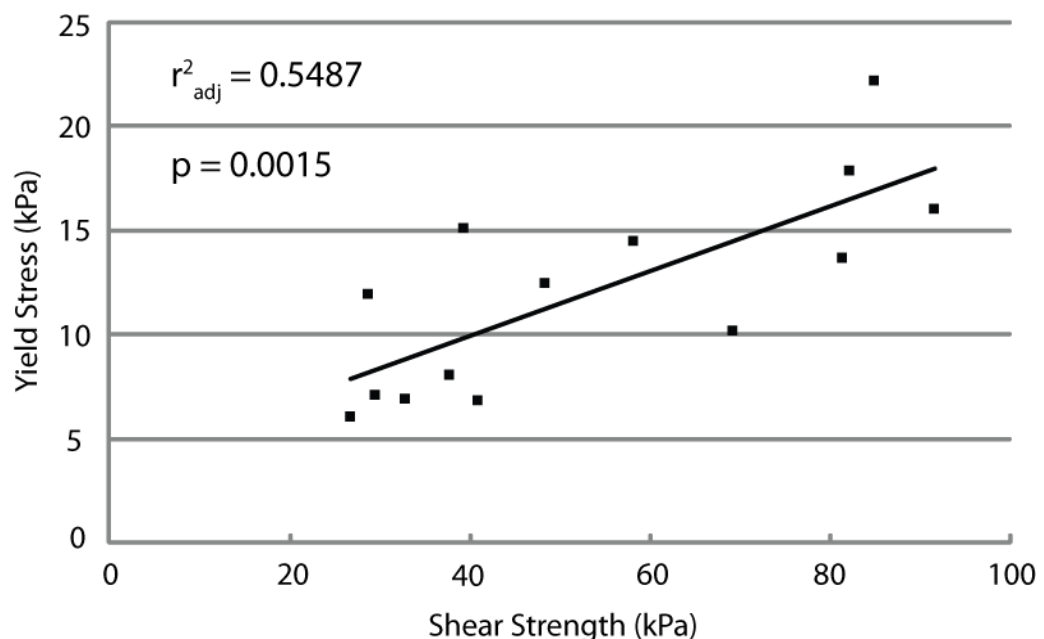


**Figure 7.1** Variations in yield stress against shear strength.

A relationship between yield stress and shear strength is expected as drier materials have greater inter-particle friction and higher  $\sigma'_y$ . Whilst a statistically significant relationship has been identified between yield stress and shear strength

at Loch Laxford, further work is required in order to test if this is consistent across other marsh environments. It is hypothesised that, as the physical reasoning for changes in  $\sigma'_y$  remain consistent across the different marsh environments, measurements of hand shear strength could predict  $\sigma'_y$  across different marsh environments. The hand shear vane method is easy to apply and offers the potential to develop a non-invasive and non-time consuming method to predict  $\sigma'_y$  in the intertidal zone.

Further work is required for prediction of  $C_r$ . It is found, at Loch Laxford, that greater values of  $C_r$  are observed compared to the values of Brain *et al.* (2012). It is considered (Section 5.2.4) that this is either a result of the testing strategy undertaken or a result of the fibrosity of the samples collected. Further work into the compressibility of highly organic intertidal materials would be greatly enhanced by using Rowe consolidation cells (Head, 1988) which can measure the pore water pressure of samples and thus remove creep processes as a potential control.

### **7.3 Sediment Compression Modelling**

This study has enabled the first use of BR1 upon an empirical relative-sea-level record from the Late Holocene and has found that sediment compression has a minimal effect upon the reconstruction at Loch Laxford. Maximum PDL of  $0.013 \pm 0.005$  m does not displace the RSL record significantly and the two reconstructions display the same trends (Figure 5.11). This conclusion is in accordance with the findings of Brain *et al.* (2012) who suggest that short, regressive sediment successions will be affected minimally by sediment compression due to low downcore effective stresses.

By modelling the effects of sediment compression it is found that the errors induced by this process are accounted for and thus the future findings of Barlow *et al.* (unpublished data pers. comm.) are a result of the interaction between the atmosphere, ocean and cryosphere system. Therefore, RSL records from Loch Laxford can be considered against other sea-level records with the knowledge that sediment compression has affected the reconstruction minimally. Whilst the effects of sediment compression at Loch Laxford are negligible this does not mean that sediment compression does not affect other reconstructions to a greater degree. It is found that highly organic materials display much greater values of  $C_r$  than those observed by Brain *et al.* (2011; 2012) due to their increased compressibility. As such, the presence of highly organic material could cause a greater distortion to

RSL records than those modelled by Brain *et al.* (2012). However, as noted by Brain *et al.* (2012), organic materials display much reduced bulk densities and so, reduced downcore effective stresses. Despite this, in favourable conditions there is potential for the significant distortion of records. If long (~3 m), transgressive successions are identified, such as Sand Point, North Carolina (Kemp *et al.*, 2009; 2011), then there is a potential for increased PDL due to the large downcore effective stresses within highly compressible materials.

This thesis has developed a greater understanding of sediment compression in materials with high LOI. To further develop the understanding of sediment compaction work is required to assess volumetric reduction caused by chemical effects and creep processes. Initial work into the effects of chemical process by Brain (2006) have suggested that the effects of non-mechanical diagenetic processes do not alter compression behaviour or *in situ* void ratio enough to increase model complexity at Cowpen Marsh. Whilst this may be true for materials at Cowpen Marsh, these are minerogenic materials with limited organic content. This could reduce the impact that creep and diagenetic processes have upon materials in this marsh. It is possible that in organogenic marshes such as Loch Laxford, and those in North America, that the impact these processes have upon sea-level reconstructions is greater, and perhaps even dominant. It is also possible that the effect of creep and chemical processes such as humification could alter the compression behaviour of sediments from the Brain *et al.* (2011) framework. Further work into the longer term compression behaviour, and factors other than an increase in effective stress, are crucial to better understand the volumetric reduction of intertidal sediments. This is particularly true when sea-level reconstructions (Kemp *et al.* 2009, 2011) are being undertaken in locations where these process are shown to be significant in similarly organic materials in freshwater (Hobbs, 1986) and delta (Van Asselen *et al.*, 2011) environments.

#### **7.4 Identification of Erosive Events**

The site at Loch Laxford has been affected by an erosive event which has removed a considerable portion of the lower marsh environment. This thesis has identified a potential method, measurement of the void ratio, to recognise such events that may not be evident in the bio- or litho-stratigraphy. The implication of erosive events that may not be easily observed within the intertidal zone is considerable for sea-level science. Gehrels *et al.* (2005) identify what they refer to

as a 'blind spot' in the radiocarbon calibration curve at ~1700 AD, which can cause fluctuations in sea-level records during this period. This 'blind spot' coincides approximately with the age of the erosive event identified at Loch Laxford. Whilst these two events are not linked, it does suggest that jumps in an age model may not solely be a result of the calibration curve. Instead erosive events could cause similar jumps that could mistakenly be identified as calibration curve effects. This is not to say that studies that find jumps in their radiocarbon dating during this period (e.g. Gehrels *et al.*, 2002; 2005; van de Plassche *et al.*, 1998; van de Plassche, 2000) are affected by erosive events; variations in deposition rates can occur for a multitude of reasons, but there is clearly a need to remove erosion as a potential effect within intertidal successions being used for sea-level studies. The findings of this thesis suggest a potential method to identify such erosive hiatuses by using geotechnical and physical analyses of sediment cores. This potentially offers a cost-effective method to identify appropriate sediment successions for radiometric dating. Brain *et al.* (2012) have previously suggested that LOI and bulk density data should be presented in order to address sediment compaction. These properties are useful and important properties for sediment compression, but can also yield information regarding erosive events. Furthermore, calculation of the *in situ* void ratio can, within the overconsolidated section of the stratigraphy, offer information pertaining to sediment deposition conditions and whether sudden changes in deposition rate have occurred, despite an ostensibly uniform lithostratigraphic unit.

In addition to measurement of the void ratio for future sea-level research higher marsh sediment successions should be deemed more appropriate due to their increased stability in the intertidal zone (Tambroni and Seminara, 2012). This would reduce the likelihood of erosive events being included within sediment successions used for sea-level studies.

The effects of sediment compression have been considered schematically within an eroded succession (Chapter 6). It has been considered that sediment compression would have a minimal effect in the surface layers used for the RSL record. However, if studies use a sediment succession which has had material eroded and then compare SLIPs from both the undereroded surface and eroded bottom layers, then the effects of sediment compression could distort the sea-level record. The potential for desiccation during erosive events or compression owing

to the loading of eroded materials could cause these bottom materials to have compressed significantly. Furthermore, without knowing the amount of material removed and the history of desiccation then this cannot be modelled. Studies such as Gehrels *et al.* (2012) use a sediment succession where materials were temporarily desiccated for a period of ~400 years before deposition occurred on top. SLIPs from this desiccated part of the succession are used to place the Late Holocene RSL record (~200 years) measured in context with the longer term Holocene pattern of RSL change (~4000 years). It is likely that these desiccated materials have reduced in volume since their initial deposition and thus could distort the longer term Holocene record. Whilst in comparison, the surface materials are short (~0.4 m) and thus are likely to generate limited downcore increases in effective stresses, and thus be affected minimally by PDL.

### **7.5 Summary**

It is found that the physical controls upon compression behaviour within the intertidal zone are likely universal, though site-specific factors observed by Brain *et al.* (2011; 2012) and at Loch Laxford may complicate the prediction of certain variables for a universal model at present. Extra testing to develop the regression models could greatly enhance the understanding of compression behaviour in the intertidal zone.

It is found that sediment compression affects the sea-level reconstruction minimally. Though further work is required to better understand the potential effects of chemical and creep processes within the intertidal zone.

Finally, it is found that a geotechnical assessment of sediment successions used for sea-level reconstructions can yield pertinent information for understanding the development of a marsh environment. Future sea-level reconstructions would likely be enhanced by encompassing such geotechnical methods and techniques.

## Chapter 8 Conclusions

The main aim of this project, as set out in Section 1.2, was to decompact a Late Holocene sea-level record from salt marsh data using geotechnical methods and theory. This aim has been addressed by using a modified version of BR1. The outcomes of this research can be considered by referring to the objectives referred to in Section 1.2:

- Develop a sampling and laboratory strategy to quantify the compression behaviour of intertidal sediments of highly organic sediments.

A sampling and laboratory testing strategy was developed in order to assess the compressibility of materials at low stresses (<3 kPa) and attempt to remove creep from testing. The testing strategy developed is deemed the most appropriate possible to yield both a high-resolution dataset at low effective stresses and limit creep as much as feasibly possible.

- Develop regression models for the compression properties required for BR1.

Statistically significant relationships were found with physical properties for all five of the compression properties used by Brain *et al.* (2012) for use within BR1. Relationships were consistent across all sites for  $G_s$  and  $C_c$  which is explained by the increased presence of low density and porous vascular plant material. Changes in  $e_1$  and  $\sigma'_y$  display a different relationship than those observed by Brain *et al.* (2012), however, it is considered that the physical mechanisms involved remain the same. A method for future prediction of  $\sigma'_y$  is given in the form of hand shear strengths which show a statistically significant relationship. Values of  $C_r$  increase with LOI though are greater than those measured by Brain *et al.* (2012). Further testing is required of highly organic and fibrous materials in a modified oedometer to measure pore water pressures and thus remove creep as a potential effect.

- Assess the effect of sediment compaction upon a sea-level record from the last 2000 years.

A relative-sea-level reconstruction from the last 2000 years was decompacted using BR1 and the regression models developed in Section 5.1. The gradual regressive sediment succession under consideration was ~0.7 m long and had a maximum PDL of  $0.013 \pm 0.005$  m. The effect that this had upon the sea-level

record from Loch Laxford is negligible and nearly unnoticeable in context with the errors of the reconstruction. The findings corroborate with the evidence of Brain *et al.* (2012) who suggest that short, regressive successions are likely to be affected minimally by sediment compaction.

When assessing the applicability of BR1 to the two sediment successions it was found that the erosive break in the lower marsh (LA-11-03) core meant a regular decompaction procedure could not be attempted. The compression behaviour of the eroded core was investigated schematically. The top 0.25 m bgl used for the reconstruction was considered to be affected minimally by sediment compression. This is due to the low effective stresses applied by the low density surface layers and potential for previous loading and desiccation to overconsolidate underlying sediments creating a stable and relatively incompressible base layer.

An interesting outcome of the research into the erosive event was the measurement of void ratio as a potential predictor for erosive layers in sediment successions. It was found that the void ratio can predict the PMSE of samples statistically significantly and thus provide a quick and simple method for assessing the deposition history of a marsh environment.

- Address the implications that findings could have for future sea-level research.

In terms of sediment compression the main outcomes of the research are similar to those of Brain *et al.* (2012), short regressive sediment successions are preferred for sea-level reconstructions as these minimise downcore effective stresses.

A further outcome of the research has been the use of geotechnical methods to identify an erosive break in the lower marsh core. This can provide a cost-effective method for the future identification of such events without expensive radiometric dating. It is also considered that use of a high marsh succession for sea-level reconstructions is favourable in comparison to a lower marsh core due to the increased stability in higher marsh locations.

Finally, by schematically exploring the compression behaviour of the lower marsh core it is considered that comparing SLIPs from materials both below and above erosive events could potentially cause significant distortion between the two layers.



## References

- Adger, W.N., Hughes, T.P., Folke, C., Carpenter, S.R. and Rockstrom, J., 2005. Social-ecological resilience to coastal disasters. *Science*, 309: 1036-1039.
- Admiralty Tide Tables, 2001. Hydrographer of the Navy. Taunton, Somerset.
- Allen, J.R.L., 1999. Geological impacts on coastal wetland landscapes: Some general effects of sediment autocompaction in the Holocene of northwest Europe. *Holocene*, 9(1): 1-12.
- Allen, J.R.L., 2000. Morphodynamics of Holocene salt marshes: A review sketch from the Atlantic and Southern North Sea coasts of Europe. *Quaternary Science Reviews*, 19(12): 1155-1231.
- Barlow, N.L. and Long, A.J., (unpublished data). Results of a sea-level reconstruction have been made accessible for use within this thesis by the authors. This work formed part of the 'North Atlantic sea-level changes and climate in the last 500 years' project (PIs Profs. Antony Long and Roland Gehrels) project and has provided a large amount of data to complement the work undertaken.
- Bates, C.R., Moore, C.G., Harries, D.B., Austin, W. and Mair, J., 2004. Broad scale mapping of sublittoral habitats in Loch Laxford, Scotland. Scottish Natural Heritage Comissioned Report NO. 004 (ROAME No. F01AA401A).
- Been, K. and Sills, G.C., 1981. Self-weight consolidation of soft soils: an experimental and theoretical study. *Geotechnique*, 31(4): 519-535.
- Berry, P.L. and Poskitt, T.J., 1972. The consolidation of peat. *Geotechnique*, 22(1): 27-52.
- Bindoff, N.L., Willebrand, J., Artale, V., Cazenave, A., Gregory, J., Gulev, S., Hanawa, K., LeQuéré, C., Levitus, S., Nojiri, Y., Shum, C.K., Talley, L.D. and Unnikrishnan, A., 2007. Observations: oceanic climate change and sea level. In: Solomon, S., Qin, D., Manning, M., Chen, Z., Marquis, M., Averyt, K.B., Tignor, M. and Miller, H.L. (Eds.) *Climate Change 2007: The Physical Science Basis: Contribution of Working Group 1 to the Fourth Assessment report of the Intergovernmental Panel on Climate Change*. Cambridge University Press, Cambridge, United Kingdom; New York, NY, USA, pp. 385-432.
- Bjerrum, L., 1967. Engineering geology of Norwegian normally consolidated marine clays as related to settlements of buildings. *Geotechnique*, 17: 81-118.
- Bloom, A.L., 1964. Peat accumulation and compaction in a Connecticut salt marsh. *Journal of Sedimentary Petrology*, 34: 599-603.
- Blott, S.J. and Pye, K., 2001. Gradistat: A grain size distribution and statistics package for the analysis of unconsolidated sediments. *Earth Surface Processes and Landforms*, 26(11): 1237-1248.
- Bradley, S.L., Milne, G.A., Shennan, I. and Edwards, R., 2011. An improved Glacial Isostatic Adjustment model for the British Isles. *Journal of Quaternary Science*. 26(5): 541-552.
- Brain, M.J., 2006. Autocompaction of mineralogenic intertidal sediments. Unpublished D.Phil Thesis. University of Durham.
- Brain, M.J., Long, A.J., Petley, D.N., Horton, B.P. and Allison, R.J., 2011. Compression behaviour of mineralogenic low energy intertidal sediments. *Sedimentary Geology*. 233: 28-41.

- Brain, M.J., Long, A.J., Woodroffe, S.A., Petley, D.N., Milledge, D.G. and Parnell, A.C., 2012. Modelling the effects of sediment compaction on salt marsh reconstructions of recent sea-level rise. *Earth and Planetary Science Letters*. 345-348: 180-193.
- British Standards Institute, 1990. BS 1377 methods of test for soils for civil engineering purposes. British Standards Institute, Milton Keynes.
- British Standards Institute, 1999. BS 5930 Code of Practice for Site Investigations. British Standards Institute, London.
- British Standards Institute, 2002. BS EN ISO 14688-1:2002: Eurocode 7 – Geotechnical investigation and testing – identification and classification of soils – Part1: Identification and Description. British Standards Institute, London.
- Bronk Ramsey, C., 2009. Bayesian analysis of radiocarbon dates. *Radiocarbon*, 51(1): 337-360.
- Brooks, A.J., Bradley, S.L., Edwards, R.J., Milne, G.A., Horton, B. and Shennan, I., 2008. Postglacial and relative sea-level observation from Ireland and their role in glacial rebound modelling. *Journal of Quaternary Science*. 23(2): 175-192.
- Burland, J.B., 1990. On the compressibility and shear strength of natural clays. *Geotechnique*, 40(3): 329-378.
- Cahoon, D.R., Reed, D.J. and Day Jr, J.W., 1995. Estimating shallow subsidence in microtidal salt marshes of the southeastern US: Kaye and Barghoorn revisited. *Marine Geology*, 128(1-2): 1-9.
- Callard, S.L., Gehrels, W.R., Morrison, B.V., Grenfell, H.R., 2011. Suitability of salt-marsh foraminifera as proxy indicators of sea level in Tasmania. *Marine Micropaleontology*. 79, 121–131.
- Carlin, B.P., Gelfand, A.E. and Smith, A.F.M., 1992. Hierarchical Bayesian analysis of changepoint problems. *Applied Statistics*, 41(2): 389-405.
- Casagrande, A., 1936. Determination of the preconsolidation load and its practical significance. *Proceedings of the First International Conference on Soil Mechanics and Foundation Engineering*, Cambridge, Massachusetts. 3: 60-64.
- Cazenave, A. and Nerem, R.S., 2004. Present-day sea level changes: observations and causes. *Reviews of Geophysics*, 42(RG3001): DOI:10.1029/2003RG000139.
- Chang, M.F., Moh, Z.C., Liu, H.H. and Viranuvut, S., 1997. A method for determining the in situ  $k_0$  coefficient. *Proceedings of the Ninth International Conference on Soil Mechanics and Foundation Engineering*, Tokyo, Japan. 1: 61-64.
- Church, J.A. and White, N.J., 2006. A 20th century acceleration in global sea-level rise. *Geophysical Research Letters*, 33(LO1602): DOI: 10.1029/2005GL024826.
- Davis, E.H. and Poulos, H.G. 1965 The analysis of settlement under three-dimensional conditions. *Symposium on Soft Ground Engineering*. Brisbane.
- Delaune, R.D., Nyman, J.A. and Patrick J, W.H., 1994. Peat collapse, ponding and wetland loss in a rapidly submerging coastal marsh. *Journal of Coastal Research*, 10(4): 1021-1030.
- Den Haan, E.J., 1996. A compression model for non-brittle soft clays and peat. *Geotechnique*. 1: 1-16.

- Devoy, R.J.N. 1979. Flandrian sea-level changes and vegetational history of the lower Thames Estuary. *Philosophical Transactions of The Royal Society of London. Series B, Biological Science*. 285(1010): 355-407.
- Donnelly, J.P., Cleary, P., Newby and Ettinger, R., 2004. Coupling instrumental and geological records of sea-level change: Evidence from southern New England of an increase in the rate of sea-level rise in the late 19<sup>th</sup> Century. *Geophysical Research Letters*, 31(5): L05203 1-4.
- Douglas, B.C., 1992. Global sea level acceleration. *Journal of Geophysical Research*, 97(C8), 12699–12706.
- Edwards, R.J., 2006. Mid to late Holocene sea-level change in southwest Britain and the influence of sediment compaction: The Holocene. 16, 575–587.
- Edwards, R.J. and Horton, B.P., 2000. High resolution records of relative sea-level change from UK salt-marsh foraminifera. *Marine Geology*, 169: 41-56.
- Engelhart, S.E. and Horton, B.P., in press. Holocene sea level database for the Atlantic coast of the United States. *Quaternary Science Review*. 1-14.
- Garlanger, J.E., 1972. The consolidation of soils exhibiting creep under constant effective stress. *Geotechnique*, 22(1): 71-78.
- Gehrels, W.R., 1999. Middle and late Holocene sea-level changes in eastern Maine reconstructed from foraminiferal saltmarsh stratigraphy and AMS <sup>14</sup>C dates on basal peat. *Quaternary Research*, 52(3): 350-359.
- Gehrels, W.R., 2000. Using foraminiferal transfer functions to produce high-resolution sea-level records from salt-marsh deposits, Maine, USA. *The Holocene*, 10(3): 367-376.
- Gehrels, W.R., and Long, A.J., 2008. Sea level is not level: the case for a new approach to predicting UK sea-level rise. *Geography*. 93(1): 11-16.
- Gehrels, W.R., Roe, H.M. and Charman, D.J., 2001. Foraminifera, testate amoebae and diatoms as sea-level indicators in UK saltmarshes: A quantitative multiproxy approach. *Journal of Quaternary Science*, 16(3): 201-220.
- Gehrels, W.R., Kirby, J.R., Prokoph, A., Newnham, R.M., Achterberg, E.P., Evans, H., Black, S. and Scott, D.B., 2005. Onset of rapid sea-level rise in the western Atlantic Ocean. *Quaternary Science Reviews*, 24: 2083-2100.
- Gehrels, W.R., Marshall, W.A., Gehrels, M.J., Larsen, G., Kirby, J.R., Eiriksson, J., Heinemeier, J. and Shimmield, T., 2006. Rapid sea-level rise in the North Atlantic Ocean since the first half of the nineteenth century. *The Holocene*, 16(7): 949-965.
- Gehrels, W.R., Hayward, B.W., Newnham, R.M. and Southall, K.E., 2008. A 20th Century acceleration of sea-level rise in New Zealand. *Geophysical Research Letters*. 35 L02717, doi:10.1029/2007GL032632.
- Gehrels, W.R., Horton, B.P., Kemp, A.C. and Sivan, D., 2011. Two millennia of sea-level data the key to predicting change. *Eos, Transactions, American Geophysical Union*, 92(35): 289-296.
- Gehrels, W.R., Callard, S.C., Moss, P.T., Marshall, W.A., Blaauw, M., Hunter, J., Milton, J.A. and Garnett, M.H., 2012. Nineteenth and twentieth century sea-level changes in Tasmania and New Zealand. *Earth and Planetary Science Letters*. 315-316: 94-102.
- Gibson, R.E., 1958. The progress of consolidation in a clay layer increasing in thickness with time. *Geotechnique*, 3(1): 171-182.

- Gibson, R.E., England, G.L. and Hussey, M.J.L., 1967. The theory of one-dimensional consolidation of saturated clays I: Finite non-linear consolidation of thin homogeneous layers. *Geotechnique*, 17: 261-273.
- Gibson, R.E., Schiffman, R.L. and Cargill, K.W., 1981. The theory of one-dimensional consolidation of saturated clays II. Finite nonlinear consolidation of thick homogeneous clays. *Canadian Geotechnical Journal*, 18: 280-293.
- Godwin, H. And Willis, E.H., 1961. Cambridge University natural radiocarbon measurements III. *Radiocarbon*, 3, 60-76.
- Greensmith, J.T. and Tucker, M.V., 1971. The effects of Late Pleistocene and Holocene sea-level changes in the vicinity of the River Crouch, East Essex. *Proceedings of the Geologists' Association*. 82: 301-321.
- Greensmith, J.T. and Tucker, E.V., 1986. Compaction and consolidation. In: O. Van De Plassche (Editor), *Sea-level research*. Geo Books, Norwich, pp. 591-603.
- Gregory, J.M., J.A. Church, G.J. Boer, K.W. Dixon, G.M. Flato, D.R. Jackett, J.A. Lowe, S.P. O'Farrell, E. Roeckner, G.L. Russell, R.J. Stoufer, and M. Winton, 2001: Comparison of results from several AOGCMs for global and regional sea-level change 1900-2100. *Climate Dynamics*. 18, 225-240, doi:10.1007/s003820100180.
- Gutierrez, M. and Wangen, M., 2005. Modeling of compaction and overpressuring in sedimentary basins. *Marine and Petroleum Geology*, 22: 351-363.
- Haslett, S.K., Davies, P., Curr, R.H.F., Davies, C.F.C., Kennington, K., King, C.P. and Margetts, A.J., 1998. Evaluating late-Holocene relative sea-level change in the Somerset Levels, southwest Britain. *The Holocene*, 8: 197-207.
- Haslett, S.K., Howard, K.L., Margetts, A.J., and Davies, P., 2001. Holocene stratigraphy and evolution of the northern coastal plain of the Somerset Levels, UK. *Proceedings of the Cotteswold Naturalists' Field Club*. XLII: 42-52.
- Hawkins, A.B., 1984. Depositional characteristics of estuarine alluvium: some engineering implications. *Quarterly Journal of Engineering Geology*, 17: 219-324.
- Head, K.H., 1980. *Manual of Soil Laboratory Testing: Soil Classification and Compaction Tests*. Pentech Press, 416 pp.
- Head, K.H., 1988. *Manual of Soil Laboratory Testing: Permeability, Shear Strength and Compressibility Tests*. Pentech Press, 420 pp.
- Heiri, O., Lotter, A.F., Lemcke, G., 2001. Loss on ignition as a method for estimating organic and carbonate content in sediments: reproducibility and comparability of results. *Journal of Paleolimnology* 25, 101–110.
- Heyworth, A. and Kidson, C., 1982. Sea-level changes in southwest England and Wales. *Proceedings of the Geologists Association*. 93: 91-112.
- Hobbs, N.B., 1986. Mire morphology and the properties and behaviour of some British and foreign peats. *Quarterly Journal of Engineering Geology*, London. 19, 7-80.
- Holgate, S.J., 2007. On the decadal rates of sea level change during the twentieth century. *Geophysical Research Letters*, 34, DOI: 10.1029/2006GL028492.
- Horton, B.P. and Edwards, R.J., 2006. Quantifying Holocene sea-level change using intertidal foraminifera: lessons from the British Isles. *Journal of Foraminiferal Research*, Special Publication 40.

- Horton, B.P. and Shennan, I. 2009. Compaction of Holocene strata and the implications for relative sea-level change on the east coast of England. *Geology*, 37: 1083-1086.
- Horton, B.P., Corbett, R., Culver, S.J., Edwards, R.J. and Hillier, C., 2006. Modern saltmarsh diatom distributions of the Outer Banks, North Carolina, and the development of a transfer function for high resolution reconstructions of sea level. *Estuarine, Coastal and Shelf Science*. 69, 381-394.
- Horton, B.P., Peltier, W.R., Culver, S.J., Drummond, R., Engelhart, S.E., Kemp, A.C., Mallinson, D., Thieler, E.R., Riggs, S.R., Ames, D.V. and Thomson, K.H., 2009. Holocene sea-level changes along the North Carolina Coastline and their implications for glacial isostatic adjustment models. *Quaternary Science Reviews*. 28, 1725-1736.
- Housley, R.A., 1988. The environmental context of Glastonbury Lake Village. *Somerset Levels Papers*. 14, 63-82.
- Juggins, S., 2003. C2: A Microsoft Windows program for developing and applying palaeoecological transfer functions and for visualising multi-proxy stratigraphic datasets. 1.4.2 ed. Univeristy of Newcastle, Newcastle Upon Tyne.
- Jelgersma, S., 1961. Holocene Sea Level changes in the Netherlands. Van Aelst, Maastricht, pp101.
- Kaye, C.A. and Barghoorn, E.S., 1964. Quaternary sea-level change and crustal rise at Boston, Massachussetts, with notes on the autocompaction of peat. *Geological Society of American Bulletin*, 75: 63-80.
- Kemp, A.C., Horton, B.P., Culver, S.J., Corbett, D.R., van de Plassche, O., Gehrels, W.R., Douglas, B.C. and Parnell, A.C. 2009. Timing and magnitude of recent accelerated sea-level rise (North Carolina, United States). *Geology*. 37(11): 1035-1038.
- Kemp, A.C., Horton, B.P., Donnelly, J.P., Mann, M.E., Vermeer, M. and Rahmstorf, S. 2011. Climate related sea-level variations over the past two millennia. *Proceedings of the National Academy of Sciences of the United States of America*. 108(27): 11017-11022.
- Kidson, C., 1986. Sea-level changes in the Holocene. In: O. Van De Plassche (Editor), *Sea-level research*. Geo Books, Norwich, pp. 27-64.
- Kopp, R.E., Mitrovica, J.X., Griffies, S.M., Yin, J., Hay, C.C. and Stouffer, R.J., 2010. The impact of Greenland melt on local sea-levels: A partially coupled analysis of dynamic and static equilibrium effects in idealised water-hosing experiments. *Climatic Change*, 103: 619-625.
- Leonards, G.A. and Girault, P., 1961. A study of the one-dimensional consolidation test. *Proceedings of the 5<sup>th</sup> Conference on Soil Mechanics and Foundation Engineering*. 1: 213-218.
- Leorri, E., Horton, B.P. and Cearreta, A., 2008. Development of a foraminifera-based transfer function in the Basque marshes, N. Spain: Implications for sea-level studies in the Bay of Biscay. *Marine Geology*. 251: 60-74.
- Long, A.J., Woodroffe, S.A., Milne, G.A., Bryant, C.L. & Wake, L.M. (2010) Relative sea-level change in west Greenland during the last millennium. *Quaternary Science Reviews*, 29(3-4): 367-383.
- Lunn, D.J., Thomas, A., Best, N. And Spiegelhalter, D., 2000. WinBUGS – a Bayesian modelling framework: concepts, structure, and extensibility. *Statistics and Computing*. 10: 325-337.

- MacFarlane, I.C., 1969. Engineering Characteristics of Peat. In: MacFarlane I.C. (Ed), *Muskeg Engineering Handbook*. University of Toronto Press. pp78-126.
- Mann, M.E., Bradley, R.S. and Hughes, M.K., 1998. Global-scale temperature patterns and climate forcing over the past six centuries. *Nature*. 392: 799-787.
- Mann, M.E. and Jones, P.D., 2003. Global surface temperatures over the past two millennia. *Geophysical Research Letters*. 30(15): 1820. doi: 10.1029/2003GL017814, 2003.
- Massey, A.C., Paul, M.A., Gehrels, W.R. and Charman, D.J., 2006. Autocompaction in Holocene coastal back-barrier sediments from south Devon, southwest England, UK. *Marine Geology*, 226: 225-241.
- Mesri, G. and Ajlouni, M.A., 2007. Engineering Properties of Fibrous Peats. *Journal of Geotechnical and Geoenvironmental Engineering*. 133(7): 850-866.
- Mesri, G., Stark, T.D., Ajlouni, M.A. and Chen, C.S., 1997. Secondary compression of peat with or without surcharging. *Journal of Geotechnical and Geoenvironmental Engineering*, 123(5): 411-421.
- Ng, S.Y. and Eischens, G.R., 1983. Repeated Short-Term Consolidation of Peats. In: Jarrett, P.M. (Eds), *Testing of Peats and Organic Soils*, ASTM STP 820. Society for Testing and Materials. pp. 192-206.
- Nygard, R., Gutierrez, M., Gautam, R. and Hoeg, K., 2004. Compaction behaviour of argillaceous sediments as a function of diagenesis. *Marine and Petroleum Geology*, 21: 349-362.
- Palmer, A.J. and Abbott, W.H., 1986. Diatoms as indicators of sea-level change. In: van de Plassche, O. (Eds). *Sea-level research: A manual for the collection and evaluations of data*. Geobooks, Norwich, pp. 457-488.
- Parnell, A.C., 2005. The statistical analysis of former sea level. Unpublished PhD Thesis, University of Sheffield.
- Paul, M.A. and Barras, B.F., 1998. A geotechnical correction for post-depositional sediment compression: examples from the Forth Valley, Scotland. *Journal of Quaternary Science*, 13(2): 171-176.
- Peltier, W.R., Shannan, I., Drummond, R. and Horton, B., 2002. On the postglacial isostatic adjustment of the British Isles and the shallow viscoelastic structure of the Earth. *Geophysical Journal International*, 148(3): 443-475.
- Pizzuto, J.E. and Schwendt, A.E., 1997. Mathematical modeling of autocompaction of a Holocene transgressive valley-fill deposit, Wolfe Glade, Delaware. *Geology*, 25(1): 57-60.
- Powrie, W., 2004. *Soil Mechanics: Concepts and Applications*. Spon Press/Taylor and Francis Group, London and New York., 675 pp.
- Price, J.S., Cagampan, J. and Kellner, E., 2005. Assessment of peat compressibility: is there an easy way? *Hydrological Processes*. 19: 3469-3475 <http://dx.doi.org/10.1002/hyp.6068>.
- Rahmstorf, S., 2007. A semi-empirical approach to projecting future sea-level rise. *Science*, 315: 368-370.
- Reed, D.J. (1995) The response of coastal marshes to sea-level rise: survival or submergence? *Earth Surface Processes and Landforms*, 20: 39-48.
- Sallenger Jr, A.H., Doran, K.S. and Howd, P.A., 2012. Hotspot of accelerated sea-level rise on the Atlantic coast of North America. *Nature Climate Change*, doi:10.1038/nature.2012.10880.

- Scott, D.B. and Medioli, F.S. 1978. Vertical zonations of marsh foraminifera as accurate indicators of former sea-levels. *Nature*, 272: 528-531.
- Shennan, I., 1980. Flandrian sea-level changes in the Fenland. Department of Geography, University of Durham.
- Shennan, I., 1982. Interpretation of Flandrian sea-level data from the Fenland, England. *Proceedings Geologists' Association*, 93(1): 53-63.
- Shennan, I., 1986. Flandrian sea-level changes in the Fenland II: Tendencies of sea-level movement, altitudinal changes, and local and regional factors. *Journal of Quaternary Science*, 1: 155-179.
- Shennan, I., 1989. Holocene crustal movements and sea-level changes in Great Britain. *Journal of Quaternary Science*. 4(1): 77-89.
- Shennan, I. and Andrews, J., 2000. Holocene land-ocean interaction and environmental change around the North Sea. Geological Society Special Publication, London.
- Shennan, I. and Horton, B., 2002. Holocene land- and sea-level changes in Great Britain. *Journal of Quaternary Science*, 17(5-6): 511-526.
- Shennan, I., Lloyd, J., McArthur, J., Rutherford, M., Horton, B., Innes, J. and Gehrels, R., 2000a. Late Quaternary sea-level changes, crustal movements and coastal evolution in Northumberland, UK. *Journal of Quaternary Science*, 15(3): 215-237.
- Shennan, I., McArthur, J., Innes, J., Lloyd, J., Rutherford, M., Wingfield, R., Lambeck, K., Flather, R. and Horton, B., 2000b. Modelling western North Sea palaeogeographies and tidal changes during the Holocene. Geological Society Special Publication(166): 299-319.
- Shennan, I., Peltier, W.R., Drummond, R. and Horton, B.P., 2002. Global to local scale parameters determining relative sea-level changes and the post-glacial isostatic adjustment of Great Britain. *Quaternary Science Reviews*. 21(1-3): 397-408.
- Shennan, I., Bradley, S., Milne, G., Brooks, A., Bassett, S. and Hamilton, S., 2006. Relative sea-level changes, glacial isostatic modelling and ice sheet reconstructions from the British Isles since the Last Glacial Maximum. *Journal of Quaternary Science*, 21(6): 585-599.
- Shennan, I., Milne, G. and Bradley, S., 2011. Late Holocene vertical land motion and relative sea-level changes: lessons from the British Isles. *Journal of Quaternary Science*. 27(1): 64-70.
- Sills, G., 1998. Development of structure in sedimenting soils. *Philosophical Transactions of the Royal Society of London*, 356: 2515-2534.
- Skempton, A.W., 1944. Notes on the compressibility of clays. *Quarterly Journal of the Geological Society of London*, 100: 119-135.
- Skempton, A.W., 1970. The consolidation of clays by gravitational compaction. *Quarterly Journal of the Geological Society of London*, 125: 373-411.
- Skempton, A.W. and Petley, J., 1970. Ignition loss and other properties of peats and clays from Avonmouth, King's Lynn and Cranberry Moss. *Geotechnique*. 20(4): 343-356.
- Smith, M.V., 1985. The compressibility of sediments and its importance on Flandrian Fenland deposits. *Boreas*, 14(1): 1-18.
- Smith, A.G. and Morgan, L.A., 1989. A succession to ombrotrophic bog in the Gwent Levels and its demise: a Welsh parallel to the peats of the Somerset Level. *New Phytologist*. 112: 145-167.

- Somerset County Council, 1992. A palaeoenvironmental investigation of a field off White's Drove, Godney Moor, Near Wells, Somerset. Unpublished Interim Report. Cited in: Edwards, R.J., 2006, Mid to late Holocene sea-level change in southwest Britain and the influence of sediment compaction: The Holocene. 16, 575–587.
- Southall, K.E., Gehrels, W.R. and Hayward, B.W. 2006. Foraminifera in a New Zealand salt marsh and their suitability as sea-level indicators. *Marine Micropaleontology*, 60: 167-179.
- Tambroni, N. And Seminara, G., 2012. A one-dimensional eco-geomorphic model of marsh response to sea level rise: Wind effects, dynamics of the marsh border and equilibrium. *Journal of Geophysical Research*, 117, F03026, doi:10.1029/2012JF002363.
- Taylor, D.W., 1942. Research on consolidation of clays. Massachusetts Institute of Technology, Department of Civil Engineering, Cambridge.
- Terzaghi, K., 1936. The shearing resistance of saturated soils. *Proceedings of the First International Conference on Soil Mechanics*. 1:54-56.
- Terzaghi, K. and Peck, R.B., 1948. *Soil mechanics in engineering practice*. Wiley, New York.
- Törnqvist, T.E., Wallace, D.J., Storms, J.E.A., Wallinga, J., van Dam, R.L., Blaauw, M., Derksen, M.S., Klerks, C.J.W., Meijneken, C. and Snijders, E.M.A. 2008. Mississippi Delta subsidence primarily caused by compaction of Holocene strata. *Nature Geoscience*, 1: 173-176.
- Tooley, M.J., 1978. UNESCO-IGCP Project on Holocene sea-level changes. *International Journal of Nautical archaeology and Underwater Exploration*, 7(1): 75-76.
- Tooley, M.J., 1982. Introduction - I.G.C.P. Project 61, sea-level movements during the last deglacial hemicycle (about 15 000 years). *Proceedings Geologists' Association*, 93(1): 3-6.
- Tooley, M.J., 1985. Sea levels. *Progress in Physical Geography*, 9(1): 113-120.
- Tovey, N.K. and Paul, M.A., 2002. Modelling self-weight consolidation in Holocene sediments. *Bulletin of Engineering Geology and the Environment*, 61(1): 21-33.
- van Asselen, S., Stouthamer, E. and van Asch, Th.W.J. 2009. Effects of peat compaction on delta evolution: a review on process, responses, measuring and modelling. *Earth-Science Reviews*. 92: 35-51.
- van de Plassche, O., van der Borg, K. and de Jong, A.F.M, 1998. Sea level-climate correlation during the past 1400 yr. *Geology*, 26: 319-322.
- van de Plassche, O., 2000. North Atlantic climate-ocean variations and sea level in Long Island Sound, Connecticut, since 500 cal. Yr. A.D.. *Quaternary Research*, 53: 89-97.
- Woodworth, P.L., White, N.J., Jevrejeva, J., Holgate, S.J., Church, J.A. and Gehrels, W.R. 2009. Evidence for the accelerations of sea-level on multi-decade and century timescales. *International Journal of Climatology*. 29: 777-789.



## Appendix 1 Methods

### 1.1 Moisture Content and LOI

Moisture content and LOI testing requires drying a material of known mass in a container of known mass,  $m_1$ , to a constant mass,  $m_2$ , which generally takes 24 hours at 105°C as shown in equation (1.1):

$$w = \frac{m_1 - m_2}{m_2} \times 100\% \quad (1.1)$$

where  $w$  is the moisture content (the percentage of water to solid in a material) (BS 1377, 1990). When the moisture content is calculated the dry mass,  $m_2$ , can be used for the calculation of LOI. LOI calculations use the method of Heiri *et al.* (2001) where samples are heated to a temperature of 550°C for four hours. If  $m_3$  = mass of container and dry soil heated to 550°C then:

$$LOI = \frac{m_2 - m_3}{m_2} \times 100\% \quad (1.2)$$

Sample weights were measured to 0.0001g for both moisture content and LOI tests. Samples were stored in desiccators to prevent the uptake of moisture between stages.

### 1.2 Specific Gravity

The specific gravity of surface samples was calculated using the small pycnometer method (BS 1377, 1990; Head, 1980). Each density bottle was first washed with water then dried by rinsing with acetone and blowing warm air onto them before being weighed. The sample was dried and ball-milled to fit through a 2mm sieve. Material was placed into the density bottles and weighed to 0.0001g. Enough de-aired water was added to the sample to cover it and was subsequently stirred to ensure all material was saturated. The bottles were placed in a water bath and sonicated for approximately 5 minutes to remove any loose air bubbles. Samples were placed in a vacuum and the pressure reduced to 2kPa and returned to normal pressure repeatedly to encourage the removal of air before being left at 2kPa overnight. The samples were then filled with de-aired water and returned to the vacuum to ensure no air entered the sample. Samples were placed into a bath of a constant temperature for an hour before weighing the samples to 0.0001g. To calculate the specific gravity,  $G_s$  ( $\text{Mg m}^{-3}$ ), of a sample then:

$$G_s = \frac{p_w (m_2 - m_1) + 4 - m_1 - (m_3 - m_2)}{m_2 - m_1} \quad (1.3)$$

Where  $\rho_L$  is the density of the liquid at a constant temperature,  $m_1$  is the mass of the density bottle,  $m_2$  is the mass of the bottle and dry soil,  $m_3$  is the mass of the bottle, soil and liquid and  $m_4$  is the mass of the bottle and liquid. The average of a minimum of three values was calculated. If any value of each test differs from the average by more than  $0.03 \text{ Mg/m}^3$  then the test was repeated.

### 1.3 Void Ratio

The voids ratio of a sample was calculated by the Height of Solids method (Head, 1980). Where the Height of Solids (HoS) are calculated by:

$$H_s = \frac{m_1}{G_s \times A} \quad (1.4)$$

Where  $m_1$  is the dry mass of material,  $G_s$  is specific gravity of material and  $A$  is the area of the sample.  $G_s$  was predicted for core material by the regression equation in Section 5.2.2.1. To calculate the void ratio,  $e$ :

$$e = \frac{(H - H_s) \times G_s}{H_s} \quad (1.5)$$

where  $H$  is the height of the sample.

## Appendix 2 Results Summary

**Table A2.1** Summary of physical properties of contemporay samples.

	Sample code	Altitude (m OD)	SWLI	Moisture content (%)	LOI (%)	Bulk density (g/cm <sup>3</sup> )	Sand (%)	Silt (%)	Clay (%)	G <sub>s</sub>
Surface Samples	LA-11-GC4-1	2.68	106.67	715%	85.86	0.92	0.9	87.7	11.4	1.60
	LA-11-GC5-1	2.58	104.29	615%	83.33	0.96	6.4	84.7	8.9	1.65
	LA-11-GC6-1	2.48	101.90	618%	73.80	0.99	45.8	48.0	6.2	1.70
	LA-11-GC7-1	2.38	99.52	563%	68.72	0.97	45.2	49.2	5.6	1.71
	LA-11-GC8-1	2.28	97.14	568%	64.19	0.99	46.2	48.3	5.5	1.79
	LA-11-GC9-1	2.18	94.76	604%	62.68	0.97	42.3	52.6	5.1	1.80
	LA-11-GC10-1	2.08	92.38	535%	58.90	1.00	43.3	52.0	4.8	1.85
	LA-11-GC11-1	1.98	90.00	485%	53.11	1.00	58.2	38.0	3.9	1.95
	LA-11-GC12-1	1.88	87.62	503%	52.45	1.00	31.2	62.2	6.7	1.89
	LA-11-GC13-1	1.78	85.24	542%	47.78	1.01	26.7	66.0	7.3	1.98
	LA-11-GC14-1	1.68	82.86	524%	47.56	0.98	34.4	59.5	6.2	2.02
	LA-12-GC7	1.63	81.67	200%	14.13	1.31	X	X	X	2.51
	LA-11-GC15-1	1.58	80.48	480%	33.91	1.07	49.0	46.0	5.0	2.17
	LA-12-GC1	1.56	80.00	295%	24.59	1.15	X	X	X	2.22
	LA-12-GC4	1.53	79.29	436%	40.00	1.04	X	X	X	2.18
	LA-12-GC3	1.52	79.05	375%	32.52	1.08	X	X	X	2.24
	LA-12-GC6	1.51	78.81	264%	19.60	1.17	X	X	X	2.36
	LA-11-GC16-1	1.48	78.10	165%	6.60	1.42	91.8	7.1	1.1	2.53
	LA-11-GC17-1	1.39	75.95	166%	6.11	1.57	92.3	6.7	1.0	2.58
	LA-11-GC18	1.25	72.62	124%	0.73	1.95	100.0	0.0	0.0	2.65
Sub-Surface Samples	LA-11-GC9-2	2.14	93.81	478%	51.29	1.04	37.5	44.8	17.7	1.88
	LA-11-GC13-2	1.75	84.52	517%	46.75	1.07	27.9	51.2	21.0	2.04
	LA-11-GC14-2	1.65	82.14	467%	43.39	0.97	29.5	49.6	21.0	2.10
	LA-11-GC15-2	1.55	79.76	481%	38.14	1.09	31.7	44.0	24.3	2.20
	LA-11-GC16-2	1.45	77.38	154%	4.85	1.53	94.5	3.9	1.7	2.60
	LA-11-GC16-3	1.42	76.67	145%	3.33	1.63	95.3	3.2	1.6	2.61
	LA-11-GC17-2	1.36	75.14	158%	5.23	1.55	89.9	7.1	3.1	2.57
	LA-11-GC17-3	1.32	74.29	153%	4.82	1.56	91.6	6.1	2.3	2.58

**Table A2.2** Summary of geotechnical properties of contemporary samples.

	Sample Name	Altitude (m OD)	SWLI	$e_i$	$C_r$	$C_c$	$e_1$	$\sigma'_y$ (kPa)	Hand Vane Shear Strength (kPa)
Surface Samples	LA-11-GC4-1	2.68	106.67	11.34	1.16	5.95	10.11	14.49	58.08
	LA-11-GC5-1	2.58	104.29	9.56	0.72	4.93	8.76	17.86	82.01
	LA-11-GC6-1	2.48	101.90	9.96	0.87	5.64	9.93	16.03	91.43
	LA-11-GC7-1	2.38	99.52	8.83	0.82	5.20	8.57	22.18	84.76
	LA-11-GC8-1	2.28	97.14	9.71	0.99	4.96	9.45	13.68	81.23
	LA-11-GC9-1	2.18	94.76	10.25	1.10	4.00	10.00	10.19	69.06
	LA-11-GC10-1	2.08	92.38	9.04	0.72	4.54	8.94	15.10	39.24
	LA-11-GC11-1	1.98	90.00	9.12	0.86	4.20	8.72	12.47	48.27
	LA-11-GC12-1	1.88	87.62	8.44	0.77	3.89	8.12	11.94	28.65
	LA-11-GC13-1	1.78	85.24	11.31	1.26	4.62	10.11	6.92	32.77
	LA-11-GC14-1	1.68	82.86	10.15	0.74	3.76	10.18	6.06	26.68
	LA-12-GC7	1.63	81.67	2.39	0.22	0.96	2.13	17.06	x
	LA-11-GC15-1	1.58	80.48	8.43	0.74	3.59	8.15	7.11	29.43
	LA-12-GC1	1.56	80.00	4.54	0.43	1.87	4.09	11.97	x
	LA-12-GC4	1.53	79.29	9.97	0.86	4.33	9.12	9.17	x
	LA-12-GC3	1.52	79.05	7.53	0.79	3.36	6.72	11.64	x
	LA-12-GC6	1.51	78.81	4.45	0.42	1.92	4.05	12.50	x
	LA-11-GC16-1	1.48	78.10	2.08	0.16	0.46	1.94	8.07	37.67
	LA-11-GC17-1	1.39	75.95	1.53	0.11	0.28	1.46	6.84	40.81
	LA-11-GC18	1.25	72.62	0.69	0.02	0.04	0.68	34.51	x
Sub-Surface Samples	LA-11-GC9-2	2.15	93.81	8.49	0.68	3.66	8.34	12.19	x
	LA-11-GC13-2	1.75	84.52	9.95	0.84	3.66	9.71	7.95	x
	LA-11-GC14-2	1.65	82.14	8.89	0.77	3.33	8.65	8.60	x
	LA-11-GC15-2	1.55	79.76	8.01	0.57	3.27	7.68	6.43	x
	LA-11-GC16-2	1.45	77.38	1.77	0.13	0.42	1.66	12.88	x
	LA-11-GC16-3	1.42	76.67	1.38	0.08	0.28	1.26	16.98	x
	LA-11-GC17-2	1.36	75.14	1.68	0.17	0.41	1.51	14.06	x
	LA-11-GC17-3	1.32	74.29	1.60	0.14	0.37	1.47	16.03	x

## Appendix 3 Compression Properties against Elevation

### 3.1 Introduction

Here LOI and compression properties are displayed against elevation (m OD) (Figure A3.1) to assess whether any trends are identified.

### 3.2 Specific Gravity ( $G_s$ )

Values of specific gravity reduce with elevation. Highest values are observed within the sand flat (LA-11-GC18-1,  $G_s = 2.65$ ) and are lowest within the highest marsh (LA-11-GC4-1,  $G_s = 1.60$ ). There is an approximately linear relationship with elevation between ~1.60-2.70 m OD where specific gravities decrease from 2.00 to 1.60. A sharp reduction in specific gravity values from 2.60 - 2.00 occurs between ~1.40-1.60 m OD.

### 3.3 Void Ratio at 1 kPa ( $e_1$ )

Below elevations of 1.50 m OD  $e_1$  is <2 but increases abruptly between 1.50 to 1.60 m OD (2 to ~10). Above 1.60 m OD values fluctuate between 8 to 10.

### 3.4 Recompression Index ( $C_r$ )

$C_r$  increases up marsh from 0.02 in the sand flat (LA-11-GC18-1) to 1.26 within the salt marsh (LA-11-GC13-1). Increases in  $C_r$  are initially rapid to ~1.60 m OD before values broadly stabilise (albeit with increased variability).

### 3.5 Compression Index ( $C_c$ )

$C_c$  increases non-linearly with elevation with limited scatter. Values are lowest (LA-11-GC18-1,  $C_c = 0.04$ ) in the sand flat and are highest (LA-11-GC4-1,  $C_c = 5.95$ ) in the upper marsh. There is a clear jump in  $c_c$  between elevations ~1.50-1.60 m OD which corresponds to the cliff edge.

### 3.6 Yield Stress ( $\sigma'_y$ )

$\sigma'_y$  varies between values of ~5 – 35. The  $\sigma'_y$  of sand flat samples is required in order to model the compression behaviour of salt marsh sediments (Brain *et al.* 2012). With LA-11-GC18-1 removed there is a weak correlation between  $\sigma'_y$  and elevation ( $r^2 = 0.19$ ). Above ~2.0 m OD values  $\sigma'_y$  increase approximately linearly.

### 3.7 Summary

It appears that whilst the compression properties ( $G_s$ ,  $C_r$ ,  $C_c$  and  $e_1$ ) do increase or decrease with changes in LOI there is no clear relationship. Instead it is apparent that  $G_s$ ,  $C_r$ ,  $C_c$  and  $e_1$  covary with LOI and thus in Sections 4.5, and 5.1 these variables are plotted against LOI to develop statistically significant relationships.  $\sigma'_y$  appears to display a limited relationship with elevation – particularly at lower elevations – this is discussed further in Section 5.1.

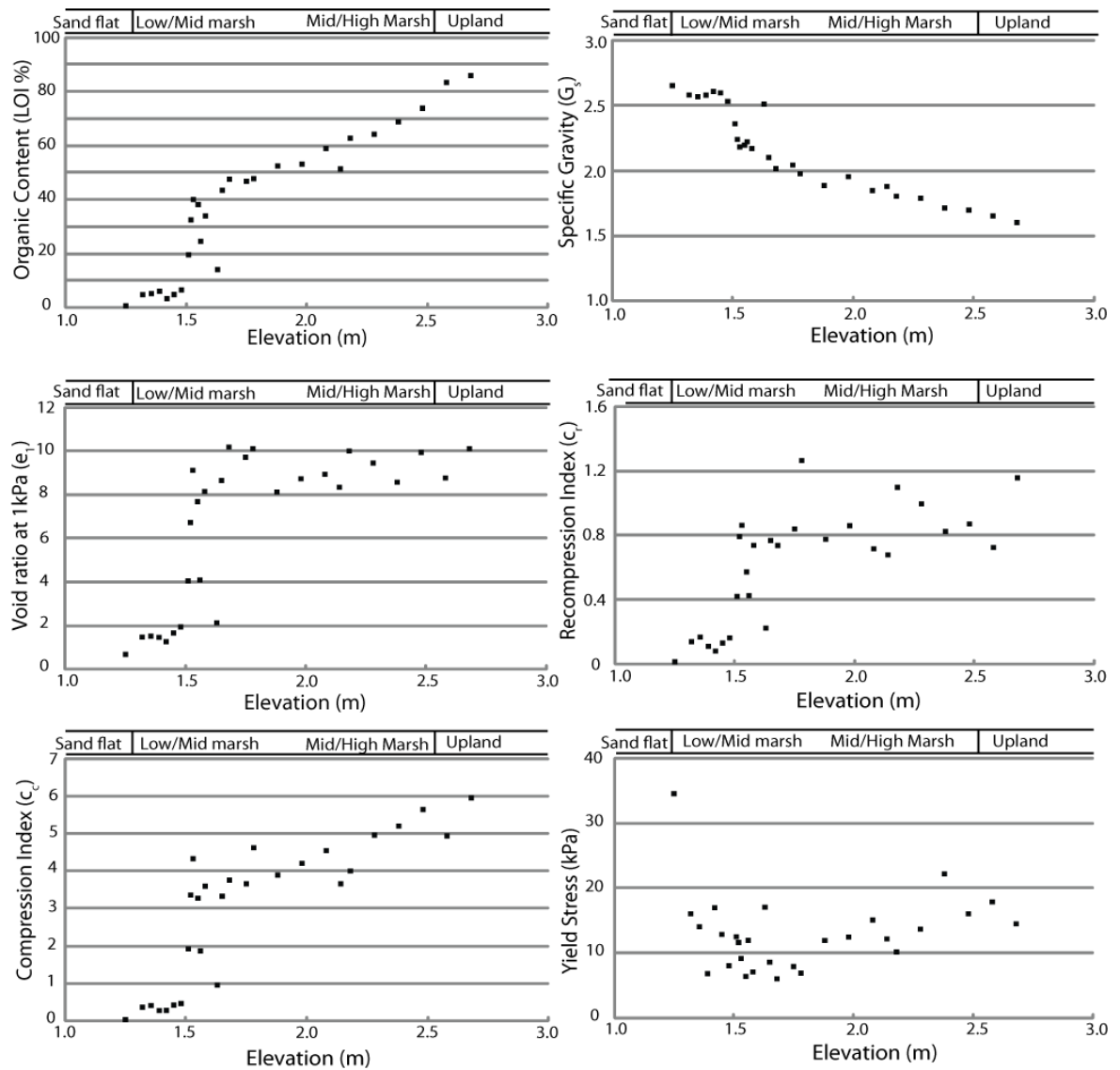


**Figure A3.1** Variations in LOI and the compression properties measured within the intertidal zone against elevation (m OD).

## Appendix 4 Effects of Variable Loading

### 4.1 Introduction

The effects of a variable loading strategy are now assessed against the four compression properties of the Brain *et al.* (2011; 2012) framework (Figure A4.1).

### 4.2 Yield Stress ( $\sigma'_y$ )

$\sigma'_y$  is split into separate loading scenarios in order to investigate the effect of variable loading increments. The different loading approaches used are described in Section 3.2.3.3. There is a cluster of samples displaying yield stresses of ~5 - 10 kPa between a SWLI range of 75 to 85 of all loading strategies. There is, however, increased variability of samples within this elevation range with samples loaded for 1 minute for each loading stage samples appearing to display greater  $\sigma'_y$ . However, this can be explained by the natural variability in  $\sigma'_y$  observed within samples from Brain *et al.* (2012) rather than being a result of the testing method used. Above SWLI values of 85, there are relatively limited data other than samples subjected to 1 minute loading stages however, a pattern of increased  $\sigma'_y$  is observed which the longer term tests appear to follow with samples at SWLI values of 90 showing increased  $\sigma'_y$  from the cluster described previously. It is considered that the observed variability of  $\sigma'_y$  is natural and such variability is not just displayed within this dataset displayed but also from the work of Brain *et al.* (2011; 2012).

### 4.3 Void Ratio at 1 kPa ( $e_1$ )

The impact of variable loading strategies upon  $e_1$  is considered to be negligible.  $e_1$  values appear to show little variability and different loading strategies show clear overlap within the same trend.

### 4.4 Recompression Index ( $C_r$ )

All data pre- $\sigma'_y$  is collected (except for LA-11-GC18-1) using shorter term loading and thus it is likely that if an effect is to be seen it will be upon  $C_r$ . Data from Loch Laxford appears to demonstrate similar behaviour with itself. All loading scenarios appear to show a strong relationship with organic content and no obvious deviation from the linear relationship observed is found from different loading strategies.

However, it is apparent that there is a significant deviation in  $C_r$  behaviour when values from Loch Laxford are compared to those collected by Brain *et al.* (2012).

#### 4.5 Compression Index ( $C_c$ )

The effect of variable loading upon  $C_c$  shows little effect. The greatest amount of scatter is observed with greater LOI where examples of all loading scenarios are observed. This could suggest that different loading methods have a different effect upon  $C_c$  but when viewed in context with data from Brain *et al.* (2012) it appears that this is more likely to be a result of structural variability than a result of the method of testing used. Furthermore with greater homogeneity of organic materials variable compression behaviour is to be expected.

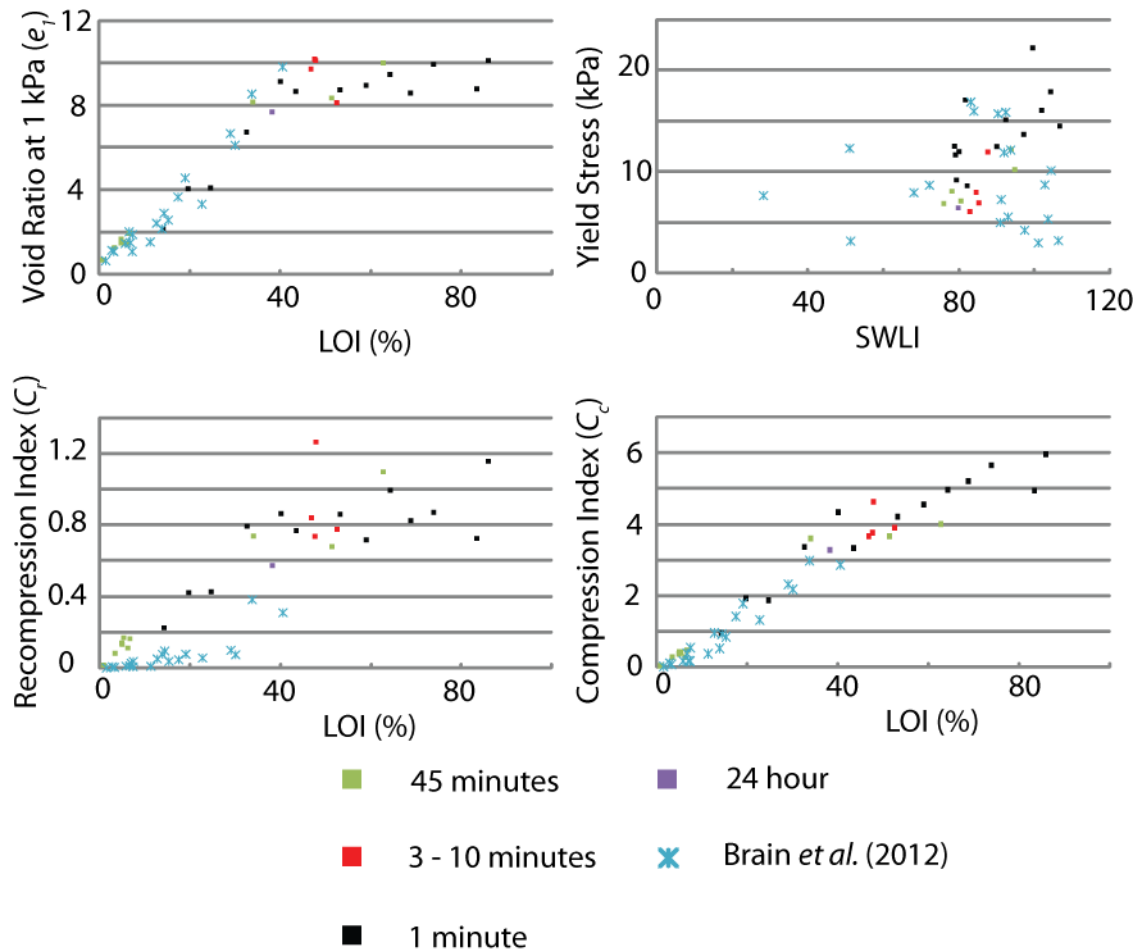


**Figure A4.1** Compression properties ( $e_1$ ,  $\sigma'_y$ ,  $C_r$  and  $C_c$ ) are plotted against their controlling variables (LOI and SWLI) to assess the effect of a variable loading approach.

#### 4.6 Summary

There appears to be a limited effect upon the compression properties by using a variable loading approach. The same trends are observed by all loading approaches in all variables at Loch Laxford. If testing is considered against that from Brain *et al.* (2012) then broadly the same relationships are observed. It appears that  $C_r$  is an exception to this when considered alongside the data of Brain *et al.* (2012). Section 5.1 considers the potential reasons for this and



attributes the difference to either the testing strategy or increased LOI and fibrosity of samples from Loch Laxford.